EVIDENCE-BASED HUMAN-CENTRIC LIGHTING ASSIST TOOL TOWARDS A HEALTHIER LIT ENVIRONMENT

by

Armin Amirazar

A dissertation submitted to the faculty of
The University of North Carolina at Charlotte
in partial fulfillment of the requirements
for the degree of Doctor of Philosophy in
Infrastructure and Environmental Systems

Charlotte

2021

Approved by:

_____
Dr. Mona Azarbayjani

_____
Dr. Mariana G. Figueiro

_____
Dr. Dimitris Papanikolaou

_____
Dr. Isaac Cho

_____
Dr. Jay Wu

ABSTRACT

ARMIN AMIRAZAR. Evidence-based human-centric lighting assist tool towards a healthier lit environment. (Under the direction of DR. MONA AZARBAYJANI)

Light is an essential element of building design that influences human health, comfort, performance, and well-being. Humans' daily rhythms in behavior and physiology, such as wake/sleep patterns, have evolved under natural light-dark cycles over millions of years. Nowadays, as we spend a large proportion of our time in the built environment, we are exposed to less light during daytime hours and more light during nighttime hours than what we would have naturally received across day and night. Thus, inappropriate and insufficient personal light exposure during the day and night can negatively affect this standard rhythm and is associated with a range of psychological, physical, and mental health issues. While most lighting design recommendations and standards have been limited to addressing the energy and visual aspects of light, this trend has been criticized, and current standards acknowledge the link between light and human health. Moreover, lack of low-cost and reliable tool to track and monitor the characteristics of light exposure as a stimulus that affects the human circadian system is evident.

This dissertation proposed a novel user-centric lighting assist tool consisting of a low-cost and wearable spectrometer to measure light spectrum and an interactive dashboard to visualize the collected data in meaningful and easy to understand quantities. Three studies covering the proposed tool are presented to 1) develop a low-cost and wearable spectrometer using Artificial Neural Networks (ANNs); 2) examine practical applicability of wearable spectrometer in the real-world environment ; and 3) develop and test the usability of an interactive dashboard for continuous tracking of personal lighting conditions. The first study examines the performance, accuracy, and fabrication challenges of developing a low-cost, wearable and wireless spectrometer

to measure Spectral Power Distributions (SPD) of light sources using ANNs. Neural network was identified as an effective method for improving the accuracy of the developed spectrometer. Additionally, the developed spectrometer offers real-time communication that enables it to be integrated into IoT-based intelligent lighting systems for tailoring indoor lighting systems according to individual circadian needs. The second study examines the practical applicability of developed spectrometer to continuously record personal lighting conditions of office workers in real-world environment. The study provides insights for enhancing occupants health and well-being within the built environment. The third study examines the potential of a web-based app to enable healthier living with light. By engaging the end-user directly throughout the entire process of design and development of the interactive dashboard, the study identified the interactive dashboard as a useful and usable tool for end-users.

This dissertation is one of the first attempts to develop a low-cost and wearable spectrometer together with an interactive application to provide vital information regarding the non-visual effects of light on health by real-time tracking of personal lighting conditions. The findings of this dissertation demonstrates the importance of an affordable and accessible human-centric lighting assist tool as a powerful driver of promoting healthy behavior change in buildings, outlining new directions in the design of buildings that are not only comfortable and energy efficient, but also healthier for their occupants.

Keywords: Non-visual effects of light, Personal circadian monitoring, user-centered design, usability testing, Low-cost spectrometer; Personal lighting condition.

DEDICATION

I dedicate this dissertation to my late father, Mahmoud, without whom I could not have come this far.

ACKNOWLEDGEMENTS

Looking back, it is gratifying to observe how I got to where I am today, especially when I think about the people who supported me, motivated me, challenged me, and not the least distracted me during this journey. BIG thanks to all of you!

First, I would like to thank my advisor Dr. Mona Azarbayjani for providing me with the opportunity to join her team in 2016 at UNCC. Her contagious enthusiasm and passion in the subject of human-building interactions has inspired me to dive deeper and explore unconventional ways to improve the health and well-being of human beings. It has been a valuable experience, as well as a chance to develop new skills and relationships that will undoubtedly continue to grow in the future. Thank you for the constructive criticism and advice. Thank you for encouraging my research and for supporting me throughout my PhD.

I would like to thank my dissertation committee: Dr. Mariana Figueiro, Dr. Dimitris Papanikolaou, and Dr. Isaac Cho for serving as my committee members; and Dr. Jay Wu for serving as the graduate faculty representative. I would also like to thank Dr. Nicholas Davis for serving on my proposal committee. This dissertation would not have been possible without their continuous guidance and support throughout this process. Thank you all for challenging my ideas whenever you thought I needed it and thereby pushing the interdisciplinary boundaries of the project.

Many thanks to Alex Cabral and Robby Sachs for taking the time to answer my questions and for sharing their knowledge about prototyping and fabricating of the developed tool in my dissertation. I would also like to thank Dr. Jianxin Hu for lending me the WaveGo, and also Dr. Faramarz Farahi, Dr. Glenn D. Boreman, and Dr. Michael G. Walter for sharing their expertise and valuable advice.

I wish to express my sincere thanks to Dr. Maziyar Molavi who was always helpful in numerous ways during the past five years. Also for proving helpful feedback on the manuscript and for interesting questions which helped me to improve it.

Most important, none of this would have been possible without the love and patience of my family. My mother, Forough, has been a constant source of love, support, and strength all these years. I am extremely grateful to my sister, Elham, my brother, Arash, my sister-in-law, Hengameh, and my niece, Elina, for always being by my side, in moments of joy and sadness. Thanks should also go to my in-laws, Nosrat Khajeh, Narges Pourebrahim and Nasim Pourebrahim, for their support.

Lastly but most importantly, I would like to thank my wife, Nastaran who is always there for me in the moments of joy and sadness, encouraging me to keep dreaming, and being a true friend when I struggled. No words can describe my love and thanks to her.

TABLE OF CONTENTS

LIST OF TABLES

LIST OF FIGURES

LIST OF ABBREVIATIONS

ANNs Artificial Neural Networks

BP Back-Propagation

CCT Correlated Color Temperature

CMOS Complementary Metal-Oxide-Semiconductor

CRI Color Rendering Index

FWHM Full Width at Half Maximum

ipRGCs Intrinsically Photoreceptive Retinal Ganglion Cells

LEDs Light Emitting Diodes

MLP Multi-Layer Perceptron

MSE Mean-Square Error

NIST National Institute of Standards and Technology

NRMSE Normalized Root-Mean-Square Error

PLA Polylactic Acid

RMSE Root-Mean-Square Error

SPD Spectral Power Distribution

SSE Sum of Squared Errors

CHAPTER 1: INTRODUCTION

Light is essential not only to see things effectively and efficiently, but also synchronizes the timing of our biological clock that consequently affects our health and sense of well-being. The building is a medium for promoting health, comfort, and productivity concerning light. The renewed interest in the concept of human-centric lighting and the discovery of the non-visual effects of light in the past two decades have dramatically changed the way people live and work. Human-centric lighting is defined as "lighting devoted to enhancing human performance, comfort, health, and well-being, separately or in some combination" [1].

Since most people spend more than 87% of their time indoors in modern societies, personal exposure to lighting is more related to indoor lighting conditions [2]. Buildings are lit by daylight or electric light (or both) as the only light sources. Over the last few decades, the invention of electric lighting has radically altered the pattern of light exposure, as we are currently exposed to less natural light during the daytime. Still, we are overexposed to electric light during nighttime. Standard human rhythm in behavior and physiology, such as wake/sleep patterns, has evolved under natural light-dark cycles over millions of years. Thus, inappropriate and insufficient personal light exposure during the day and night can negatively affect this standard rhythm and is associated with a range of psychological, physical, and mental health issues.

For decades, the primary focus in lighting design has generally been on visual aspects of light. The discovery of the third class of ocular photoreceptors in the human eye, called Intrinsically Photoreceptive Retinal Ganglion Cells (ipRGCs) [3, 4], increased attention on the effects of light beyond vision that influence our health and sense of well-being. Illustrating the central role of light in building, human health

can be affected through visual system, and non-visual system (circadian system) [5]. Deviation from the natural light-dark exposure patterns may result in adverse consequences on our sleep [6], alertness [7], mood [8], performance [9], and is associated with a range of health issues such as depression [10], diabetes [11], seasonal affective disorder [12], and even cancer [13]. This breakthrough stresses the importance of creating indoor spaces that mitigate user discomfort and energy consumption and bring health and well-being to their occupants.

One of the main challenges at the early stages of design, or during the post-design evaluation, is to assess how well a proposed plan meets the needs of its intended users in terms of lighting. It has never been so important to capture evidence from human interactions within existing buildings and investigate the impacts of indoor lighting on their health, comfort, and well-being. Although indoor light conditions may satisfy the visual needs, they may be insufficient in spectrum and intensity for biological needs such as alertness and circadian entrainment. To this end, using vision-related quantities such as illuminance (lux) or luminance (cd/m^2) is inappropriate to measure circadian lighting due to the difference between the spectral response of visual and non-visual systems [14, 15].

In addition, since the health effects of light vary from individual to individual, and the movement and activity of humans introduce uncertainty in the prediction of non-visual responses to light, the light conditions around each individual should be investigated separately. Recently, a few devices [16, 17] and techniques [18–20] have been developed to measure the light that stimulates the non-visual system, subsequently influencing the occupant's health and sense of well-being. However, not only these devices are not equipped to measure Spectral Power Distribution (SPD) as the complete form to measure light exposures [21], but also, they are not commercially available, or they are expensive [22, 23]. Moreover, although these devices can continuously record individuals'light exposure and activity level over hours and days, they

do not allow for real-time visualization of the recorded data, which can be a great source of information for post-design evaluation of buildings.

The present dissertation aims to bridge this gap by expanding our knowledge of how light exposure and its interplay with occupant's movements and activities can affect occupant's health and well-being. This dissertation seeks to facilitate the post-design evaluation of architectural space by developing a new human-centric lighting assist tool for more efficient circadian lighting assessment based on the needs and requirements of end-users.

1.1 Context and Background

1.1.1 The Effects of Light on Non-Visual System

With the discovery of a new form of photoreceptors in the human retina (ipRGCs), more attention has been paid to a dual role of the human eyes when exposed to light: enabling humans to perform visual tasks and maintaining health and well-being via the non-visual responses [4]. The non-visual system appears to require high irradiance. It also differs in its time domain from the visual system, with a more sluggish response, resistance to bleaching by light, and adaptation to prior light history.

There are five types of photoreceptors within the human retina: Rods, three types of cones, and ipRGCs [24]. Light as electromagnetic radiation is detected by photoreceptors in the eye in the visible wavelength range between 380 nm and 780 nm. As the photoreceptors absorb a photon, chemical responses in the eye transform light information into neural signals. Each type of photoreceptor contains different light-sensitive pigments that absorb photons in different wavelength ranges, thereby initiating electrical and chemical signals transmitted through neurons to other areas of the brain. The third class of photoreceptors, ipRGCs, does not collect visual information from light and has a different characteristic than rods and cones. While ipRGCs are more sensitive to short-wavelength light (blue light), rods and cones are more suscep-

tible to green-blue and green light, respectively. Although the exact contribution of rods and cones into the non-visual system is still unknown, it is evident that besides ipRGCs as the principal photoreceptor, rods and cones also influence the circadian system [25–27]. Light received at the eye is detected by ipRGCs and transmitted to different brain parts in the non-visual system. Most studies have focused on the path leading to suprachiasmatic nuclei (SCN), which synchronizes the body's circadian rhythm. The circadian rhythm regulates the secretion of a hormone called melatonin, responsible for synchronizing various behavioral and physiological functions such as alertness level, mood, core body temperature, and hormone secretion/suppression. The secretion of melatonin is increased during the night and decreases during the daytime. In the absence of melatonin, cortisol is secreted, which elevates the energy level and helps the transition from sleep-state to wake-state.

The human circadian system is responsible for entraining the circadian rhythms to sync to a roughly 24-hours diurnal cycle. Exposure to light after sunset may shift the circadian rhythm a process called phase shifting. Phase-shifting has been reported mostly among people who work at night, such as nurses and shift-workers or those who traveled across different time zones. Therefore, it is evident that irregular light-dark exposure patterns may disrupt the circadian system and affect human health and well-being. According to the current state of research, the five qualities of light that affect circadian entrainment are intensity, spectrum, timing, duration, and history of light exposure [28]. Thus, as explained above, these five light characteristics, plus spatial distribution and age, need to be considered to effectively investigate the non-visual effects of light in the indoor environment.

A recent study on human subjects suggests that cone photoreceptors contribute identically to non-visual responses at the beginning of light exposure and at low irradiance. In contrast, melanopsin appeared to be the primary non-visual photopigment in response to long-duration light exposure and at high irradiance [29]. The recent

findings indicated that to evaluate the non-visual efficiency of a light exposure, not only the spectral sensitivity of the relevant photoreceptor is required but also the SPD of the illuminant.

1.1.2 Metrics and Devices for Measuring Circadian Light in the Built Environment

There is a lack of consensus on circadian lighting metrics and the exact threshold to support the circadian effectiveness of lighting in working environments. Some standards in the field of light and lighting, such as WELL Building Standard v2 [20], have recently begun to include metrics that address the proper light exposure for supporting physical health and adjusting the circadian rhythm with a natural day-night cycle. The WELL standard recommends using the two most popular circadian lighting metrics for measuring light exposure: Equivalent Melanopic Lux (EML) and Circadian Stimulus (CS). The EML is based on Enezi et al. [30] and Lucas et al. [21] and recommended exposure above specific EML threshold levels that vary in terms of space type. For example, exposure to at least 240 EML between 9:00 AM and 1:00 PM for every day of the year is suggested for work areas. Circadian Stimulus (CS) is proposed by the Lighting Research Center (LRC) [31] to evaluate the circadian-effectiveness of light sources, which range from 0 (no stimulus) to 0.7 (full saturation). The WELL standard suggests exposure to a CS of 0.3 or higher at the eye for at least the hours between 9:00 AM and 1:00 PM.

The effect of light exposure on the circadian system should be calculated by considering the output of all three types of retinal photoreceptors, rods, cones, and ipRGCs in the human eye [14, 32]. CS considers both spectrum and intensity of the light source and ties to all three types of retinal photoreceptors necessary for assessing circadian lighting. However, EML ties to a single photoreceptor and ignores any impacts of the rods and cones. The recent survey conducted by Edward Clark and Natalia Lesniak [33], having more than 100 respondents across the architectural design com-

munity, showed that nearly two-thirds of participants (62%) used CS. In contrast, only 38% of them used EML in practice. This study used CS to measure light's circadian effectiveness using the data collected from the wearable device.

Additionally, there is a lack of low-cost, accurate, and wearable devices to record the characteristics of light exposure as a stimulus that affects the human circadian system. The most common wearable devices have been used to measure the photopic illuminance [34, 35], the irradiance from red, green, and blue of the visible light region [16, 17, 36, 37], or both photopic illuminance and RGB [38]. Due to the difference between the spectral response of visual and non-visual systems, photopic illuminance is improper to quantify circadian-effective light, leading to measurement error up to 98% for measuring circadian lighting [39]. Spectral Power Distribution (SPD) is recommended to measure light exposure. It measures the light in the most comprehensive form that can be used by any metrics currently available or even will be developed in the future [21]. Although only a few portable and wearable devices are designed to measure the SPD of light [15, 23, 40], they are not accessible to researchers and practitioners as they are not commercially available or cost-prohibitive [22]. A recent survey reported that only a few lighting practitioners (28%) always or frequently used photospectrometers or similar devices to verify that the installed lighting meets the design goals [33]. Thus, an affordable, accurate, and wearable device for measuring light spectrum would benefit researchers and lighting practitioners. This study used a wearable device to measure full spectral data of an individual's light exposure in real-time.

1.1.3 Factors Need to be Considered when Investigating the Non-Visual Effect of Light at the Individual Level

Even though there is currently no consensus on the optimal light dosage required to support healthy circadian entrainment, at least six factors that induce non-visual response was determined and categorized into two groups [28, 41]:

- Luminous factors: intensity, spectrum, and directionality of light exposure and;
- Temporal characteristics: timing, duration, and history of light exposure.

Research studies measuring the lighting conditions at the individual level have mainly focused on health effects of light, such as sleep, mood, and circadian rhythm. Little attention has been given to investigating the actual lighting conditions at the individual level, particularly considering inter-individual differences in response to light exposure. Since the biological effects of light vary from individual to individual, and some of these light factors affect the circadian system over an extended period, it is recommended to continuously measure the light conditions around each individual [42]. In addition to luminous and temporal factors, individual differences in response to light exposure need to be considered to investigate the non-visual effects of light in the indoor environment. Previous studies [22,43,44] showed several factors that need to be considered for measuring lighting conditions at the individual level, particularly when considering the effect of light beyond vision, which are listed as below:

- Individual trait. The link between individual traits and light exposure on human circadian rhythm and sleep is evident. Recent evidence strongly suggested considering the individual differences when designing a well-lit environment to satisfy the circadian lighting needs of building occupants [44]. The biological effects of light may differ between individuals based on some Individual factors such as physiological differences (e.g. age [45,46], health-related issues [47–49]), genetic differences [50–52], cultural/behavioral differences (e.g. clothing [53,54], differences in indoor/outdoor-related behavior [53, 55]), and mixed physiological/behavioral differences (e.g. gender [56, 57], chronotype [58, 59], different wake/sleep patterns [60, 61], and different work/social schedules [62–64]). Regarding inter-individual physiological differences, for instance, as the age increased, the light transmission in the eye decreased, and people require higher

light quantity with different spectrums compared to younger populations due to yellowing of the lens and reducing the pupil size [45,46]. Individual differences in response to light exposure may vary due to cultural/behavioral variance. For example, outdoor clothing varies depending on geographical location, climate, and different ethnicities and societies. Different Sleep/wake patterns, work/social schedules, gender, and chronotype, such as morning/evening types, may change the magnitude of the impact of light exposure on the human circadian system.

- Weather conditions. Light intensity and spectrum of daylight constantly change each hour of the day throughout the year. Many studies have investigated the effects of seasonal [7, 65–67] and daily [12, 68] variation of light exposure on humans.

- Workspace characteristics (e.g., office layouts, distance to window [39, 69], the color of surfaces/furniture, building orientation, viewing direction [70], blind condition, amount, and placement of luminaire).

Wearable technologies can investigate individual differences in response to light exposure by continuously measuring personal lighting conditions. Recently, the term "personal lighting conditions" was commonly used by several researchers when referring to lighting conditions at the individual level [42, 71]. The inclusion of this term is recommended, particularly in studies that investigate the non-visual effects of light on humans [72].

1.1.4 Emergence of Human-Centric Lighting

As the modern lifestyle compels us to spend a significant amount of time indoors, we are not exposed to sufficient natural light during the daytime. Still, we are overexposed to electric light during nighttime. In comparison to our ancestors, we experience dimmer days and brighter nights, which can mislead our circadian system's ability to distinguish between "day" and "night", resulting in physiological disruption and

adversely affecting our health and overall well-being. Poor indoor lighting can cause serious health issues and adversely affect the occupants'energy level, mood, and productivity. Therefore, for the lack of access to natural light indoors, human-centric lighting can be a solution to provide the appropriate lighting to address human visual, biological, and behavioral needs. Recently, there has been a renewed interest in HCL for two reasons: 1) the advancement of lighting technology that makes it possible to control the light specifications such as intensity, spectrum, and distribution; and 2) the discovery of the third class of ocular photoreceptor (ipRGCs), which increases our understanding of the non-visual effects of light on human health and well-being [1]. HCL mimics natural light and tailors indoor lighting by modifying the characteristics of light such as intensity, spectrum, CCT, etc., for different times of the day according to special human needs. For example, unlike the early part of a day when exposed to higher intensity and blue-enriched light, which can elicit alertness and promote circadian entrainment, towards the evening, on the other hand, the intensity should be decreased and the spectral composition of the light is shifted to a longer wavelength (red), which avoids circadian disruption as people prepare to sleep.

Temporal patterns of light (timing, duration, and history of light exposure) should be intimated as the most critical variable when designing HCL that explicitly induces the non-visual response [73]. The application of human-centric lighting that mainly stimulates the non-visual system varies depending on building types. Buildings where people typically present during their working hours, such as offices and schools, require only one light setting with a strong biological response. In contrast, buildings where people sleep, such as residential, hospitals, and hotels, require more than one light setting, with strong, weak, or even no biological response during different times of the day. Implementing the HCL becomes even more complex when considering the individual differences such as age and sleep/wake patterns, particularly for buildings that demand more than one light setting. Good outcomes are most likely generated

when a 'personalized smart lighting system' is used by continuously monitoring individual lighting conditions in real-time and controlling these lighting conditions by utilizing an IoT-based intelligent lighting system [74]. For this reason, a low-cost and accurate wearable device that wirelessly, continuously, and in real-time measures personal light exposure in its most complete forms (SPD) is essential for the lighting community.

1.2 Research Scope

This section will outline the present dissertation through an overview of the research problem, objectives, and approach in this work.

1.2.1 Problem Statement

Developing a new connected support technology is necessary for enhancing human health and well-being in the built environment through real-time monitoring of varying internal and external environmental influences from the sun and users. Recently, a growing number of researchers from different research fields have attempted to develop new tools and methods for investigating the non-visual effects of light and their applications in lighting design.

While most lighting design recommendations and standards have been limited to addressing the visual aspects of light, this trend has been criticized, and current standards acknowledge the link between light and human health. Studies have been mostly devoted to investigations in energy or visual aspects of light in architecture and lighting design. However, less attention has been paid to the non-visual effects of light and how to effectively measure the variation in people's daily and seasonal light exposure patterns in buildings. There is a lack of consensus on circadian lighting metrics and the optimal light dosage required to support healthy circadian entrainment. In parallel, the emergence of the new circadian lighting metrics caused new challenges to measuring light exposure and increased the need for specialized lighting

measurement devices.

Although a few devices are available for ambulatory measurement of circadian light exposure, only a few people have access to those devices as they are commercially unavailable, expensive, or inappropriate to measure circadian lighting. The majority of the studies regarding the lighting condition measurements at the individual level have been primarily focused on the health effects of light, such as sleep, mood, and circadian rhythm. Little attention has been given to investigating actual lighting conditions at the individual level, particularly considering inter-individual differences in response to light exposure. Continuous information provided by long-term lighting measurement of the microenvironment around the individual can lead to better design. Accessibility to a low-cost and wearable device that measures the SPD of light exposure, would greatly benefit the research community to better understand the individual variability in response to light exposure. Mainly, continuous measurement of light exposure at the personal level in its most complete form allows an understanding of the effects of various factors that induce the non-visual response, such as intensity, spectrum, timing, duration, and history of light exposure.

In addition, a large proportion of previous studies have been conducted in controlled environments under steady electric light conditions. Therefore, there is not only a lack of understanding of the variability of non-visual effects of light in real-world environments within different geographical locations but also a lack of practical tools to track and measure personal lighting conditions in real-time throughout the 24-hour-day, together with tips on how to improve those individual lighting conditions.

This dissertation aims to fill this gap by developing a new tool to promote healthier living with light by encouraging individuals to engage with their healthcare by managing and keeping track of their health data. I will explore the accuracy and fabrication challenges of developing a low-cost and wearable device in tandem with Artificial Neural Networks (ANNs) to measure light spectrum. Then the practical

applicability of the designed device for continuous measurement of personal lighting conditions will be evaluated in a real-world environment. Finally, the development and usability testing of a novel interactive dashboard to display the data collected by the wearable device by engaging the end-user directly throughout the entire process will be described.

1.2.2 Dissertation Objectives

The present dissertation attempts to address the following research question:

How to equip lighting designers and architects with accessible and affordable tools to evaluate critical parameters related to non-visual aspects of light exposures at the individual level in the building?

Therefore, the primary objective of this dissertation is to employ a human-centric approach for developing a novel tool to promote healthier living with light. To address the research question, three goals are identified as follows, which are addressed in different chapters:

1. Develop a low-cost and wearable device to measure light spectrum using ANNs (Chapter 2)

2. Examine practical applicability of the low-cost and wearable device in monitoring personal lighting conditions in a real-world environment (Chapter 3)

3. Develop and test the usability of an interactive dashboard for continuous tracking and monitoring of personal lighting conditions (Chapter 4)

1.2.3 Dissertation Outline

Chapter 2, 3, and 4 form the core of this dissertation and describe three studies that aimed to provide evidence regarding the objectives of this dissertation. To orient the reader, this section presents an outline of the chapters as follows: Chapter 1 be-

gins with an introduction to the study, followed by reviewing the existing knowledge regarding the non-visual effects of light on human health, as well as the use of methods and factors for investigating the non-visual effect of light at the individual level. Chapter 2 explores the performance, accuracy, and fabrication challenges of developing a low-cost and wearable spectrometer. The ability of Artificial Neural Networks is also analyzed to improve the accuracy of the developed spectrometer. Chapter 3 examines the potential of the developed spectrometer in measuring personal lighting conditions of two-office workers continuously over eight days by utilizing CS to evaluate the circadian effectiveness of various lighting conditions. Next, Chapter 4 describes the process of developing and usability testing of a novel interactive dashboard to provide end-users with easy-to-understand quantities regarding the circadian effectiveness of the light. In addition, Chapter 5 draws the contributions, indicates the limitations, and offers potential future research.

CHAPTER 2: A LOW-COST AND PORTABLE SPECTROMETER FOR MEASURING LIGHT SPECTRUM USING ARTIFICIAL NEURAL NETWORKS

2.1 Introduction

It is widely understood that light has profound effects on our health and sense of well-being. Daylight provides a combination of the suitable types of light with the right spectral content at the correct times, which should be considered a primary light source for human natural lighting needs. The discovery of a new form of photoreceptors in the human retina, called Intrinsically Photoreceptive Retinal Ganglion Cells (ipRGCs) in 2002 [3, 4], ignited increased attention among researchers, in various disciplines, on the unseen effects of light, which influence our mood, alertness, emotion, health, and sense of well-being [75, 76]. This breakthrough stresses the importance of creating indoor spaces, which mitigate user discomfort and energy consumption and bring health and well-being to their occupants.

Advancements in electric lighting have drastically changed the way human beings live by shifting one's light exposure pattern from natural light to artificial light. Currently, people spend more than 87% of their time indoors [2]. Thus, they are not receiving enough light nutrition, which leads to a desynchronization between activity-rest and environmental light-dark cycles, resulting in disrupted circadian rhythms. The human circadian system is responsible for entraining the circadian rhythms to be in sync to a roughly 24-hours diurnal cycle. The emergence of new lighting systems makes it possible to have light everywhere, efficiently, at multiple wavelengths, and in various color tones and temperatures. New types of electric lighting, such as Light Emitting Diodes (LEDs), have considerably been improved in terms of Color Rendering Index (CRI), Correlated Color Temperature (CCT), brightness, life-span,

and power consumption, to overtake traditional light sources such as incandescent and fluorescent [77,78]. Though this breakthrough has been a great benefit for humankind by improving our home, work, and social environments, a growing number of studies have shown that these changes have had negative consequences for human health. Studies have shown that deviation from regular light-dark exposure patterns not only has direct effects on alertness [7], concentration [79], mood [8], sleep [6, 80], and performance [9], but also indirectly, it is associated with a range of health issues such as insomnia [81], depression [10], diabetes [11], seasonal affective disorder [12], cognitive dysfunction [82], and even cancer [13]. To avoid the adverse effects of these changes, electric light sources should be designed per individuals' specific needs by mimicking daylight in the built environment. It has been proven that a good interplay between natural light and light from electric lighting and further adjusting the intensity and spectrum used in varying locations at different times of the day directly affect occupants' health. Hence, there is a need to measure the characteristics of light exposures with reasonable precision and utilize intelligent lighting systems that promote occupants' health, well-being, and comfort in the built environments.

2.1.1 Emergence of New Metrics Lead to New Challenges to Measuring the Light Exposure

The emergence of new metrics to evaluate circadian lighting created new challenges to measuring light exposure and increased the need for specialized lighting techniques and devices. Several researchers attempted to apply short-term or long-term measurement techniques in scene capture [83, 84] or light intensity [17, 34] to assess the circadian lighting values in the built environment. Over the last few years, many studies have been found to employ static measurement devices [39, 83, 85, 86] or personal measurement devices [15–17, 34–37] for measuring circadian lighting in architectural practice. However, most of the individual devices are equipped to gather photopic values. A few were used to measure irradiance from the visible spectrum's red, green,

and blue regions. In addition, many of these devices are not accessible to researchers and practitioners as they are not commercially available, or they are prohibitively expensive [22, 23, 87]. It is proven that the devices and techniques utilized to assess circadian lighting should be reliable and accurate to record the characteristics of light such as intensity, timing, duration, and wavelength that stimulate an individual's non-visual system.

Since 2002, the devices and methods for measuring light have been shifting from vision-related quantities such as illuminance (lux) or luminance (cd/m^2) to those which take into consideration the spectral composition of light radiation by growing knowledge about the link between light and health [21, 30, 31]. Vision-related quantities are weighted by the sum of M and L cones; therefore, they do not consider the effects of light on all three types of retinal photoreceptors in the human eye, which is necessary for assessing circadian rhythm lighting. The recent findings show that the photopic luminous efficiency function alone, $V(\lambda)$, is improper to quantify circadian lighting due to the difference between visual and non-visual systems [14, 15]. A study by Konis [39] confirmed the previous findings and reported that the error, up to 98%, may have occurred by using photopic illuminance for measuring circadian stimulus potential. Therefore, Lucas et al. [31] suggested to record the corneal Spectral Power Distribution (SPD) as the most comprehensive form to measure light exposures due to the complexity of non-visual photosensory systems, since the contribution of each individual photoreceptor is not clear in terms of irradiance response. One of the most notable benefits of recording the SPD of the light sources is that it enables a re-analysis of the collected data by using any unit of measure currently available or developed in the future. However, the metrics related to photopic vision, such as illuminance, are presently used to evaluate circadian lighting due to lack of standard, knowledge, or most importantly, suitable measurement devices.

A range of devices such as spectroradiometers can be used to record the SPD of

the light sources. The calibrated spectroradiometers are precise and accurate as they undergo absolute calibration against National Institute of Standards and Technology (NIST) guidelines. However, there are some limitations associated with the spectroradiometers in the field measurements as they are expensive, bulky, slow, and fragile [88]. It is important to note that only a few laboratories worldwide can measure the spectrum of light sources within 3% uncertainty [89]. To overcome these limitations, the development of array spectrometers such as complementary metal-oxide-semiconductor (CMOS) based sensors is an appealing solution to the problem of spectroradiometers. Compared to spectroradiometers, CMOS sensors are characterized by lower cost, smaller size, faster measurement, energy efficiency, higher signal to noise (S/N) ratio, and higher wavelength precision [90–92]. Yet, they currently do not have the same precision as regulatory reference devices as they deliver higher noise under low illumination, lower sensitivity, and decreased resolution than spectroradiometers [92]. While low-cost sensors have emerged as an alternative to reference devices, these sensors usually provide data with uncertain precision.

One possible solution to improve the precision of the low-cost sensors is to apply different computational techniques to increase their accuracy. Over the past few years, many scholars have used other computational methods such as Artificial Neural Networks (ANNs) to improve the performance of low-cost sensors for light measurement [40], air-quality monitoring [93,94], soil moisture measurement [95], solar irradiance measurement [[96,97], food storage time prediction [98], and occupancy detection [99]. ANNs are computational models that try to simulate the structure and functions of the network of neurons in the brain so that the computer will learn from recognized patterns in data. Ultimately, the decision can be made in a humanlike manner [100].

Recent advancements in various fields such as computer science, architectural engineering, and healthcare have led to increased interest in measurement devices that

are accurate, low-cost, portable, with wireless communication capabilities, and real-time data monitoring and visualization [101–104]. These types of devices will play a significant role in the future of the built environment. It is possible to imagine an IoT-based intelligent lighting system that continuously measures personal lighting conditions and controls these conditions by adjusting the SPD of the electric lighting towards users' preferences and desires in real-time. Essentially, these systems reduce energy consumption and make buildings more comfortable and healthier for the people in them. Portable and wearable devices are an emerging technology that offers continuous tracking and monitoring of an individual's vital data during daily life. They provide a critical opportunity to evaluate the non-visual effects of light on circadian regulation and long-term health, thus allowing individuals to have healthier living about light. These devices employed in the field should consistently and accurately collect characteristics of light exposures such as intensity, spectrum, timing, and duration as a stimulus that may affect the human circadian system. Portable and low-cost spectrometers could also be used as a "dosimeter" to continuously monitor spectral irradiance for assessing the circadian effectiveness of lighting conditions in living and working spaces or light therapy in long-term care facilities for people with dementia or Alzheimer's. Additionally, portable spectrometers can be embedded in smartphones to be helpful in various applications, including food quality inspection, agriculture, and even water quality monitoring. Due to the current lack of availability of an affordable, accurate, and portable device, a personal device to measure occupants' light exposure wirelessly and in a real-time manner would be advantageous for researchers and practitioners.

2.1.2 Objective of the Research

The main objective of the present study was to develop a low-cost, portable, and wireless spectrometer for measuring Spectral Power Distribution by exploring its performance, accuracy, and fabrication challenges. We used ANNs as a method to recon-

struct SPD for improving the accuracy of the developed spectrometer. This study is the first step of a larger project to develop a system and method for real-time monitoring and visualizing personal circadian lighting on a mobile application through an automated process. The device developed in this study will be used in our future studies to measure personal light exposures by employing the metrics recommended by CIE S 026/E:2018 [19] and Well Building Standard v2 [20]. This study had two primary goals:

- Compare various ANNs architectures, activation functions, and learning algorithms to find the best fit with promising performance and the lowest training error.
- Evaluate the performance of ANNs to improve the accuracy of the developed spectrometer for measuring SPD independent of light sources and environmental conditions.

2.2 Materials and Methods

This section presents the hardware used to develop a low-cost and portable spectrometer incorporating a spectral sensor to record the SPD of light sources and the hardware employed in calibration and validation of the performance of the developed spectrometer. To answer the goals of the present study, four experiments were designed: pre-experimental calibration, experiment 1, experiment 2, and experiment 3.

2.2.1 Design Methodology of the Proposed System

The process of developing the proposed system is summarized into the following steps:

- The enclosure of the developed spectrometer was designed in Fusion 360 and built using a 3D printer.

- Different pieces, including a spectral sensor and microcontroller, etc., were assembled together and fixed to the enclosure. The scripting for data acquisition was generated.

- Pre-experimental calibration was performed to evaluate the monochromatic and spectral response of the developed spectrometer across the visible spectrum.

- Experiments 1 and 2 were conducted under different conditions to measure the light source's SPDs. The recorded SPDs were stored in the cloud database for building the initial datasets with 30 and 106 samples for experiments 1 and 2, respectively.

- The initial dataset for each experiment was pre-processed separately by down-sampling and normalizing the SPD of every single one of the light sources.

- In the primary processing, the SPD of each sample of light sources was combined with other samples in predefined percentages to build the final dataset with 5280 and 55,650 samples for experiments 1 and 2, respectively.

- The two final datasets were used to train MLP models and test different algorithms' performance for reconstructing the SPD.

- Three different activation functions and eight different learning algorithms were compared using the two final datasets separately for each experiment to find the most accurate neural network with the best performance.

- Forty measurements under real-world environments were conducted in experiment 3 to assess the ability of the most accurate MLP model obtained from the previous experiment when exposed to unique and complex SPD.

2.2.2 Hardware

In the following sections, the hardware used to develop the low-cost and portable spectrometer, to calibrate the developed spectrometer in pre-experimental calibration, to measure light sourceâs SPDs in the experiments 1 and 2 for building the final dataset to be used in training and testing of MLP models, and to evaluate the developed spectrometer under real-world conditions for measuring SPD using the most accurate MLP model in experiment 3 are described in detail.

2.2.2.1 Low-Cost and Portable Spectrometer

In this study, the development of a portable spectrometer includes a spectral sensor, a microcontroller, a power supply, a battery, a real-time clock, and a micro-SD card adapter that costs only $125 to build. Portable spectrometers have become popular in recent years mainly due to their lower price and smaller size than bulky and expensive spectroradiometers. Currently, the market price of portable spectrometers ranges between $750 and $3000 [[105, 106]. In some cases, there are software options, which would considerably increase the price of the portable spectrometer. Fig. 2.1 shows the exterior view and inner parts of the developed spectrometer. The developed spectrometer size is 77 mm long, 46 mm wide, with a height of 28 mm. Its total weight, including the inner parts and enclosure, is about 50g, and if the device samples every 30s, its battery lasts up to 23h. Table 2.1 shows some important characteristics of the spectral sensor, such as its resolution and peak sensitivities of 18 channels. The developed spectrometer consists of the following parts:

- AS7265X spectral sensor is a CMOS-based sensor consisting of three sensors that detect wavelengths in a range from visible to NIR region, specifically for 18 channels with peak sensitivities at 410 nm, 435 nm, 460 nm, 485 nm, 510 nm, 535 nm, 560 nm, 585 nm, 610 nm, 645 nm, 680 nm, 705 nm, 730 nm, 760 nm, 810 nm, 860 nm, 900 nm, 940 nm, each with 20 full widths at half maximum

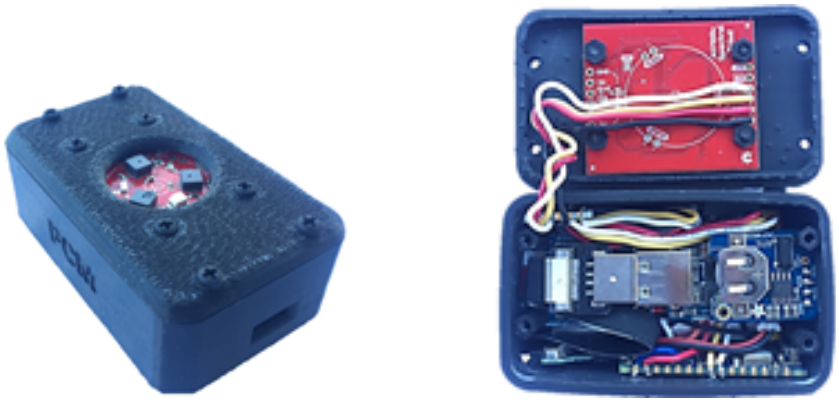

(a) (b)

Figure 2.1: a) The developed spectrometer is 77 mm in length, 46 mm in width, 28 mm in height, weighs about 50g, b) Inner parts include spectral sensor, microcontroller, power supply, battery, real-time clock, and micro-SD card adaptor.

(see Table 2.1).

- It also includes a low-power microcontroller, a power supply, a battery, a real-time clock, and a micro-SD card adaptor to store the collected data internally.

- The enclosure was designed in Fusion 360, a cloud-based CAD/CAM tool, fabricated using a 3D printer with polylactic acid (PLA).

Table 2.1: Characteristics of the AS7265X spectral sensor.

Characteristics	AS7265X	Unit
Sensor	Photodiode	[NA]
A/D Resolution	16	[bits]
Communication	I2C or UART	[NA]
Operating voltage	2.7 - 3.6	[V]
Temperature	-40 to $+85$	[°C]
FWHM	20	[nm]
Wavelength accuracy	± 10	[nm]
Angle of incidence	± 20.5	[°]
Integration time	$2.78-711$	[ms]
Channels	410, 435, 460, 485, 510, 535, 560, 585, 610, 645, 680, 705, 730, 760, 810, 860, 900, 940	[nm]

The different pieces, including microcontroller, spectral sensor, etc., were assembled, and the scripting for data acquisition was generated. These parts were fixed to the enclosure with nylon screws. In addition, this device has internal storage wherever no other types of connection are available. It also offers real-time communication using Bluetooth, Wi-Fi, or SIM card connections. The collected data was stored on a cloud database using a Wi-Fi connection in a real-time manner. As shown in Fig. 2.2, the developed spectrometer will be used in our future studies for real-time tracking and monitoring of personal circadian lighting. For this reason, spectral sensitivities of all five types of photoreceptors: s-cones, m-cones, l-cones, rods, and ipRGCs need to be measured [32, 107]. Therefore, only wavelengths for 14 channels (out of 18) within the visible spectrum (from 410 nm to 760 nm) were considered in this study for calibration and training.

Figure 2.2: Application of the developed spectrometer presented in this study for measuring personal light exposures.

2.2.2.2 Calibration Instrument

The following instrument was used in the pre-experimental calibration to validate the wavelength accuracy of the spectral sensor by measuring the spectral response of all 14 channels.

2.2.2.2.1 Spectrofluorophotometer

For calibration, a spectrofluorophotometer with an operating range between 200 nm to 850 nm and wavelength accuracy of ± 0.2 nm was used to adjust the wavelength manually to acquire the central wavelengths for all 14 channels of the developed spectrometer. The Spectrofluorophotometer consists of a light source, an excitation monochromator, a sample cell, an emission monochromator, and a detector. It should be noted that the Spectrofluorophotometer was only used during pre-experimental calibration.

2.2.2.3 Reference Instruments

In the following sections, the instruments utilized as a reference in different experiments are described in detail. WaveGo and Integrated sphere were employed in experiments 1 and 2 to measure the light source's SPDs. The AvaSpec-Mini2048CL spectrometer was used in experiment 3 to record SPD under real-world conditions.

2.2.2.3.1 WaveGo

The Ocean Insight WaveGo light spectrum meter uses a high-performance spectrometer that is calibrated against NIST standards to analyze light spectrum ranging between 350 nm and 800 nm with 3 nm FWHM optical resolution. The main advantage of WaveGo is the ease of data storage on the cloud account that provides access and analysis of the results anywhere, from an app or desktop. In addition to measuring light spectrum and intensity, it can be used to measure the color and quality of the light source, such as CCT and CRI. We employed the WaveGo to measure the light source's SPDs in experiment 1 (Fig. 2.4) and experiment 2 (Fig. 2.5).

2.2.2.3.2 Integrated Sphere

Integrating spheres are commonly employed in conducting photometric and radiometric measurements. An integrated sphere was used to measure the total light radiated in all directions from a light source uniformly over all the positions within its circular aperture. From one side, getting the light source into the sphere and after numerous reflections, the radiation is dispersed highly uniformly at the sphere walls. The integrated radiation level is easily measured with a detector from another side. The main advantage of using the integrated sphere is to measure all the light scattered from all directions from a light source by averaging the illumination radiated over all angles. The integrated sphere was used as the reference instrument to measure the light source's SPDs in experiment 1 (Fig. 2.4) and experiment 2 (Fig. 2.5).

2.2.2.3.3 AvaSpec-Mini2048CL Spectrometer

AvaSpec-Mini2048CL is a handheld spectrometer that is calibrated against a NIST-traceable irradiance calibration standard. It detects wavelengths in a range between 200 nm and 1100 nm with 0.09 nm FWHM optical resolution. The AvaSpec-Mini2048CL was only used in experiment 3.

2.2.3 Experimental Setup

In the following sections, the process of calibrating the developed spectrometer, developing the ANN models using recorded light source's SPDs from experiments 1 and 2 to reconstruct SPD, and evaluating the developed spectrometer under a real-world environment utilizing the most accurate MLP model, is explained in detail.

2.2.3.1 Pre-experimental Calibration

We conducted the calibration process to test the accuracy of spectral measurements of the developed spectrometer compared to a laboratory-grade spectrofluorophotometer. Fig. 2.3 shows the experimental setup and working mechanism of the Spectrofluorophotometer used to calibrate the developed spectrometer. The calibration process starts by manually adjusting the wavelength for all 14 channels, ranging in wavelengths between 410 nm and 760 nm, using a PC connected to the Spectrofluorophotometer. The excitation wavelength was sent out from the light source, and it passes through the excitation monochromator, which transmits a wavelength specific to the excitation spectrum while blocking other wavelengths. The output of the Spectrofluorophotometer was measured, first by an embedded detector, as a reference value. Then it led to the spectral sensor to be assessed by a microcontroller and stored values on a cloud database to be analyzed by a PC. The collected values were used to quantify the gain of each channel of the spectral sensor, and then by scanning each channel, the spectral response curve of the spectral sensor was reconstructed. The wavelength was recorded by both the developed spectrometer and the Spectrofluorophotometer in nanometers by a four-digit counter. The Spectrofluorophotometer was only used during the calibration process.

2.2.3.2 Artificial Neural Network (ANN) Model Development

In the following sections, described in detail, are the process of collecting data from experiments 1 and 2 for building initial datasets, processing the collected data

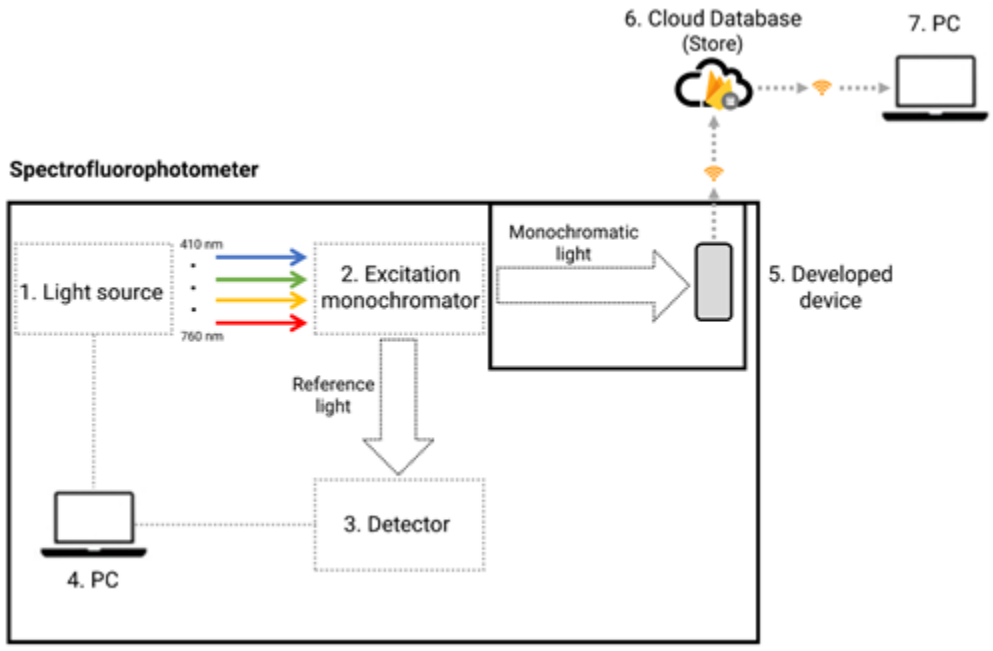

Figure 2.3: Schematic illustration of the calibration process. Light source (1), excitation monochromator (2), detector (3), PC (4), developed spectrometer (5), cloud database (6), and PC (7).

to build final datasets, and using the final datasets to train MLP models and to test the performance of different algorithms for reconstructing the SPD.

2.2.3.2.1 Experiment 1: Control Lab Measurement

To minimize measurement errors, we conducted the first experiment at a controlled laboratory that was completely in darkness with the exception of the light to be assessed for validating the accuracy of the developed spectrometer and the MLP model. Fig. 2.4 shows the experimental setup and the instruments that were used to measure the SPD of 30 LEDs in a controlled laboratory. The WaveGo, the developed spectrometer, and the integrated sphere were employed to measure the SPD of 30 LEDs to build the initial dataset. To avoid entering any light other than the measured light sources into the integrated sphere, a lightbox was designed and 3D printed to fit into the integrated sphere. The lightbox sized $100 \times 100 \times 30mm$, has an opening toward the integrated sphere, and the LED was connected to a mini breadboard at the

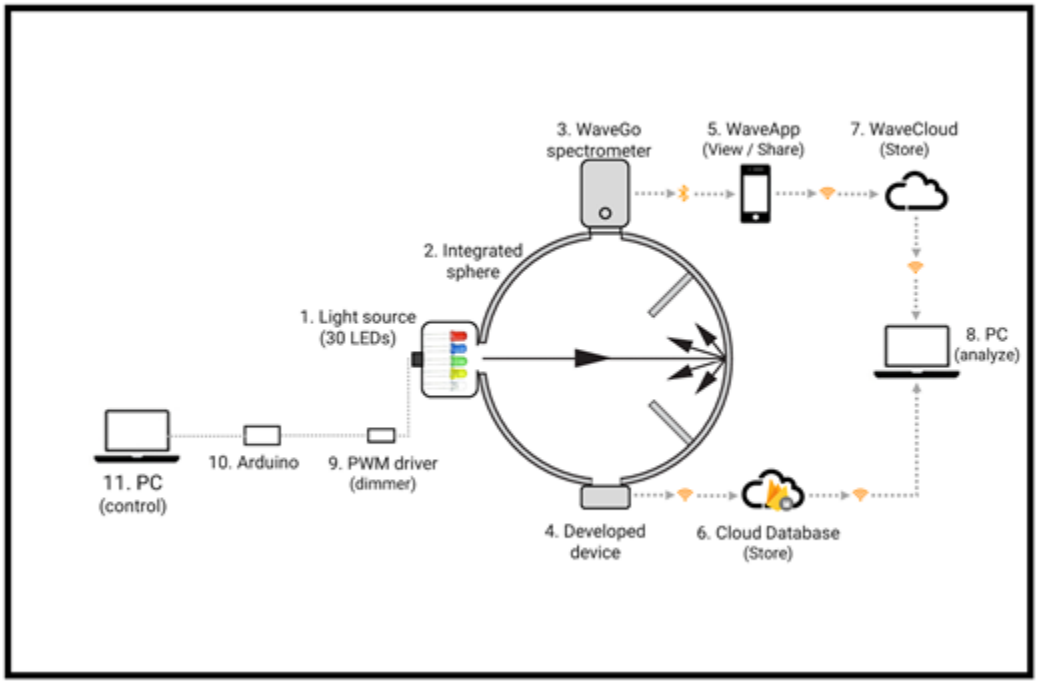

Figure 2.4: Experimental setup used to measure SPDs of 30 LEDs and validate the accuracy of both the developed spectrometer and ANNs in experiment 1.

back. Each of the 30 LEDs was placed individually into the lightbox, and their SPDs were measured several times with the WaveGo and the developed spectrometer. The SPD of each LED was recorded 20 times at 15 seconds intervals over 5 minutes using both the developed spectrometer and the WaveGo. The initial dataset, including the measured SPDs of 30 LEDs by the WaveGo and the developed spectrometer, was stored on the cloud database to be used in the pre-processing and the main-processing phase for developing ANN models.

2.2.3.2.2 Experiment 2: Semi-Real-World Environment Measurement

For the second experiment, we validated the accuracy of the developed spectrometer once without the help of ANNs and then the ability of ANNs to increase the accuracy of the developed spectrometer. Hence, we added various light sources and measured outside the controlled lab to represent a condition close to the real-world environment. Since the designed device will be used in practice with spatially and

spectrally changing light conditions, for the second test, we used a larger number with a greater diversity of light sources, including both electric light and daylight. Fig. 2.5 shows the experimental setup and the instruments used to measure the SPD of 106 different light sources in a semi-real-world environment. The performance of the developed spectrometer without the help of ANNs was investigated in a semi-real-world setting. We hypothesize that the various sources of error, such as stray light, could negatively affect the accuracy of the developed spectrometer. Thus, we tested the MLP model's ability to improve the accuracy of the developed spectrometer when considerable stray light was presented.

We used 106 different types of light sources as an input to the integrated sphere. A variety of commercial electric light sources, including 54 LEDs, 5 Fluorescent, 11 Incandescent, and 3 Halogen, were chosen from different manufacturers. In addition, 33 samples of daylight were measured during sunny days, partly cloudy days, and rainy days to be as close as possible to all conditions that would occur in a real-world environment. As shown in Fig. 5, the integrated sphere was placed at 60 cm from electric light sources and 200 cm from the window. Because both electric light and daylight sources were placed within a distance from the integrated sphere, the measurement was subjected to a significant error from stray light. It is important to note that we turned on the electric light for at least 15 minutes before starting the measurement to reach a steady state. Electric light such as fluorescent and incandescent lamps requires time to warm up, and it varies from lamp to lamp. The SPD of different light sources was measured 15-20 times over five minutes, and the collected data was stored on the cloud to be used in data processing phases. Similar to experiment 1, we used the WaveGo and the developed spectrometer to measure light sources' SPD to build an initial dataset with 106 samples. We used the collected data to train and test MLP models. We used the initial dataset from experiment 2 in the pre-processing phase and the main-processing step for the training and testing of ANN models.

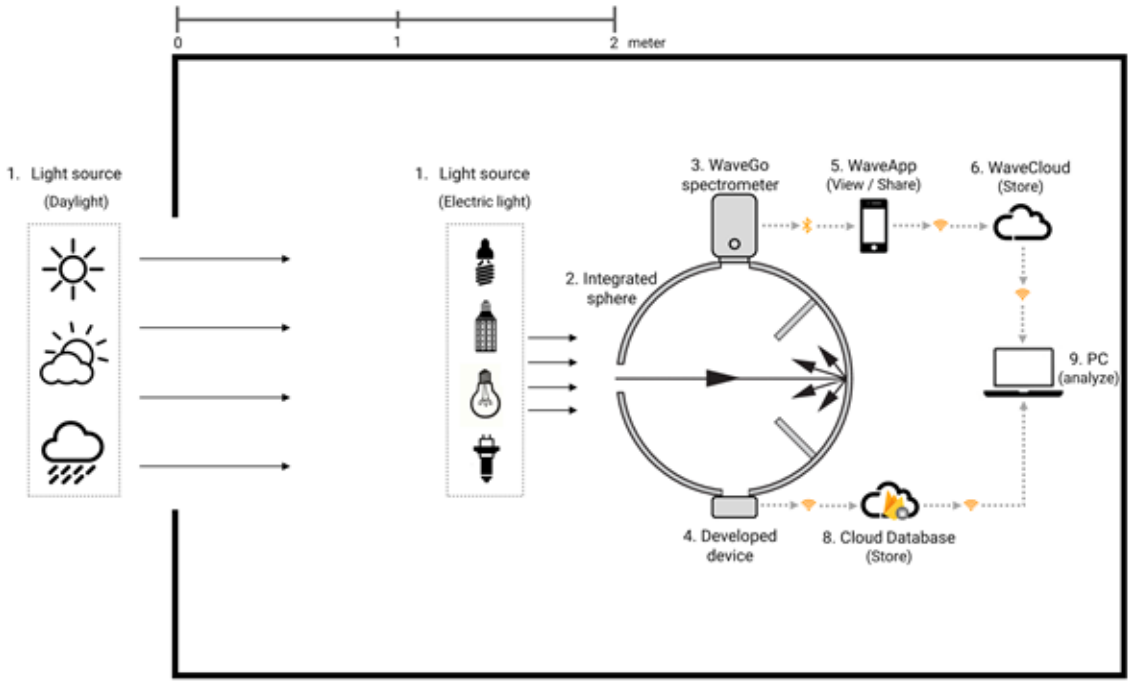

Figure 2.5: Experimental setup used to measure SPDs of 106 different types of light sources and to validate the performance of the developed spectrometer and ANNs in experiment 2.

2.2.3.2.3 Train and Test ANN Models

We designed a two-step procedure; first, the measured SPD from experiments 1 and 2 were processed by downsampling and normalizing in the pre-processing phase. Second, the output of the pre-processing phase was used in the main-processing phase to test and train ANN models for reconstructing SPD.

In the pre-processing phase, the initial datasets collected from experiment 1 and experiment 2 were processed separately by downsampling and normalizing the SPD of every single one of the light sources. For every single one of the light sources, we acquired 14 samples at a wavelength range between 410 nm and 760 nm from the developed spectrometer and 779 samples at a wavelength range between 390 nm and 778.5 nm from the reference instrument (WaveGo). To reconstruct the SPD of the developed spectrometer based on the reference instrument, 111 centers were defined by a resolution of 3.5 nm from 779 samples obtained by the reference instrument. We

downsampled the 779 samples of the reference instrument (WaveGo) to 111 samples as the output of the ANN model by using a window averaging method to fit with the resolution of 3.5 nm. Finally, we normalized 14 samples at a wavelength range between 410 nm and 760 nm from the developed spectrometer and 111 samples resulting from downsampling of the data obtained by the reference instrument to be used as an input and output of the ANN model, respectively. Because the downsampling and normalizing of the SPD reduced the output size of the ANN model and decreased the effect of noises, the speed and accuracy of the ANN model were significantly increased.

We used pre-processing data collected from experiments 1 and 2 to build two final datasets to develop ANN models in the main-processing phase. We employed the two final datasets to train and test different ANNs architectures, activation functions, and learning algorithms for reconstructing SPD. Fig. 2.6 shows the instrument and method used in experiments 1 and 2 to measure SPDs of different light sources, build datasets (initial dataset and final dataset), and use processed data for training and testing the ANN model. We performed the main-processing stage as follows.

First, the SPD of each sample of light sources was combined with other samples to build two final datasets for experiments 1 and 2, separately. The combination percentage for two individual light source samples varied between 10% and 50% for the developed spectrometer and the reference instrument (WaveGo). We built two final datasets with 5280 and 55,650 samples by combining 30 samples in experiment 1 and 106 samples in experiment 2. It is important to note that the different light sources were combined to recreate conditions as close as possible to real-world environments where there is usually more than one type of light source found in indoor environments.

Second, we used the final datasets to train and test different algorithms for reconstructing SPD. In this study, we utilized MLP as the most commonly used type of

ANNs [108], which has been applied in about 70% of ANNs studies [109], as a method to reconstruct SPDs. Fig. 2.6(7) shows the architecture of the MLP, including input, hidden, and output layers. Each layer consists of neurons that transmit data in one direction from one layer to the adjacent layer. The neural network has an input layer with 14 neurons corresponding to the channels of the spectral sensor within the visible spectrum between 410 nm and 760 nm.

Moreover, the number of neurons for the output layer was set to 111, defined according to data collected by the reference spectrometer (Wavego). The number of hidden layers and the number of neurons per layer varied depending on the complexity of the link between the input and output layers. It is a common practice to select the number of hidden layers and their neurons by trial and error [110]. MLP was trained by Back-propagation (BP) learning method, as the most widely used algorithm to train MLP networks [111], and its performance was validated to reconstruct the SPD. We used a 5-fold cross-validation procedure by splitting the dataset into 80% for training and 20% for testing to avoid over-fitting. For this purpose, we employed the neural network toolbox provided by MATLAB in cloud environments that enable us to run multiple jobs simultaneously and increase the training speed considerably. We tested several MLP models with different numbers of hidden layers ranging between 1 and 3, and different numbers of neurons per layer varied between 5 and 35, in increments of 5.

Finally, we tested different parameters that could improve the performance of the MLP model and enhance the data processing performance. We compared three activation functions and eight different learning algorithms to find the neural network with the best performance in terms of training error and training time. We used the linear activation function (purelin) [112], and two non-linear activation functions, Log-Sigmoid (Logsig) [113] and Hyperbolic Tangent Sigmoid (Tansig) [114]. Dorofki, M., et al. [115] compared these three ANNs activation functions to find the most appro-

priate one. In addition, we used eight different learning algorithms: Traingdx [116], Trainlm LevenbergâMarquardt [117], Traincgf Fletcherâreeves [118], Traincgp PolakâRibiere [119], Traincgb PowellâBeale [120], Trainoss [121], Trainbfg BFGS [122], and Traingd [123]. Zhao, Z, et al. [124] compared weaknesses and strengths of different types of learning algorithms employed in this study.

2.2.3.3 Experiment 3: Evaluate the Developed Spectrometer under a Real-World Environment

We compared the performance of the ANN model between experiment 1 and experiment 2 to find the most accurate ANN model to be used in experiment 3. In experiment 3, we utilized the most accurate MLP model directly from the previous experiment without any modification and alteration to challenge its performance for reconstructing the measured SPD in a real-world environment. The ability of the MLP model was evaluated under real-world conditions when it was exposed to SPD from transmitted and reflected light through surfaces with different colors and textures. The AvaSpec-Mini2048CL and the developed spectrometer were positioned side-by-side on a vertical plane at 170 cm above the floor to represent the view at eye level when standing, taking random measurements from different perspectives. It should be noted that the AvaSpec-Mini2048CL and the developed spectrometer were positioned so that they were not exposed to direct irradiance from the light sources. Additionally, we eliminated the integrated sphere, so ambient light enters detectors based on their field of view.

A total of 40 real-world measurements, including 30 indoors and ten outdoors, were taken under different lighting conditions to build the initial dataset. We conducted measurements within two residential buildings for the indoor environment by taking ten measures under electric light (warm and cool LEDs) as the only light source, ten under daylight as the only light source, and five under mixed electric light and daylight. In addition, ten measurements were performed in the outdoor environment.

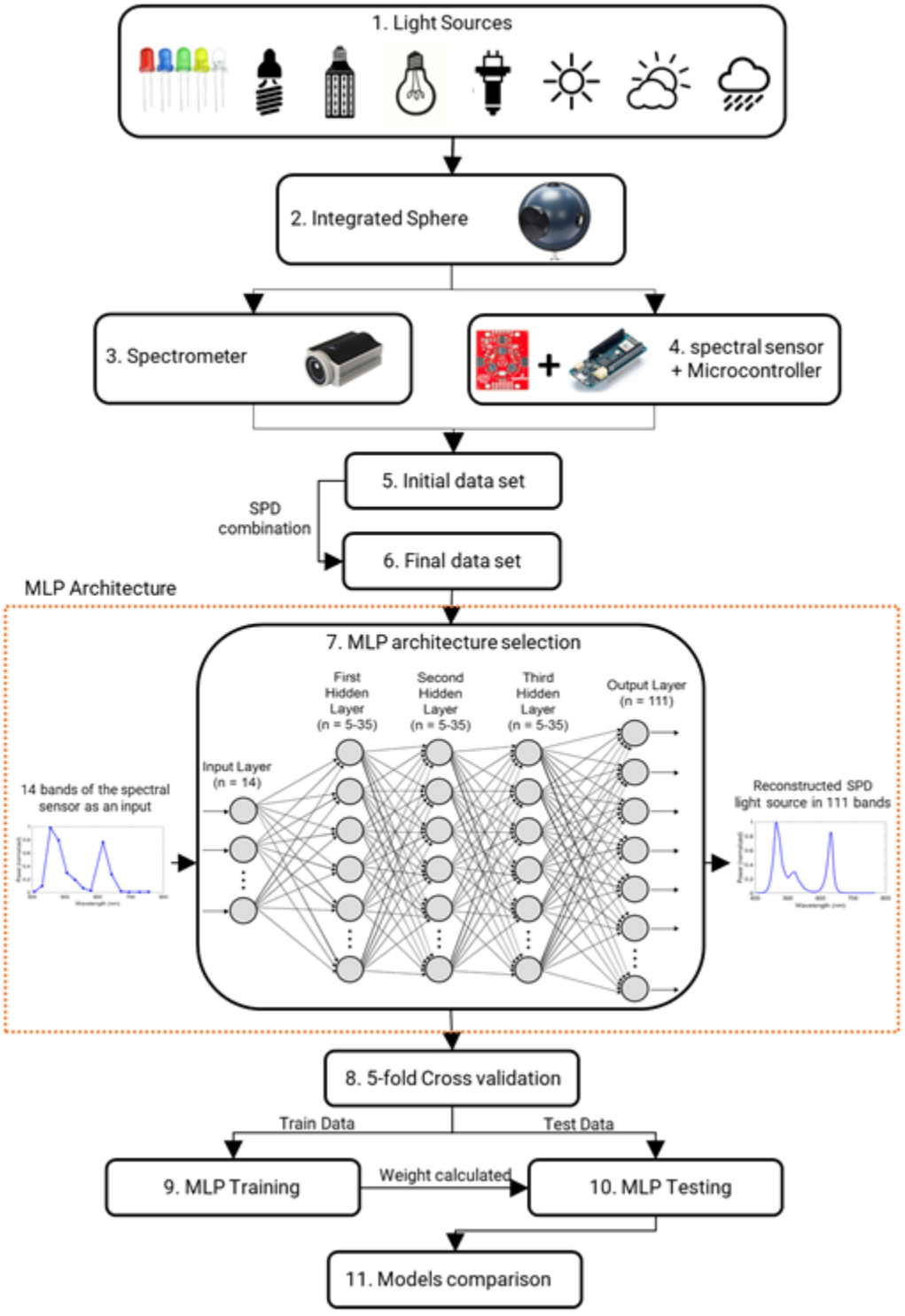

Figure 2.6: Process of collecting data from experiments 1 and 2 using the collected data for training and testing of the MLP model. (1) light sources, (2) integrated sphere, (3) WaveGo, (4) spectral sensor microcontroller, (5) Initial dataset, (6) Final dataset, (7) MLP architecture selection, (8) 5-fold cross-validation, (9) MLP training, (10) MLP testing, and (11) Model Comparison.

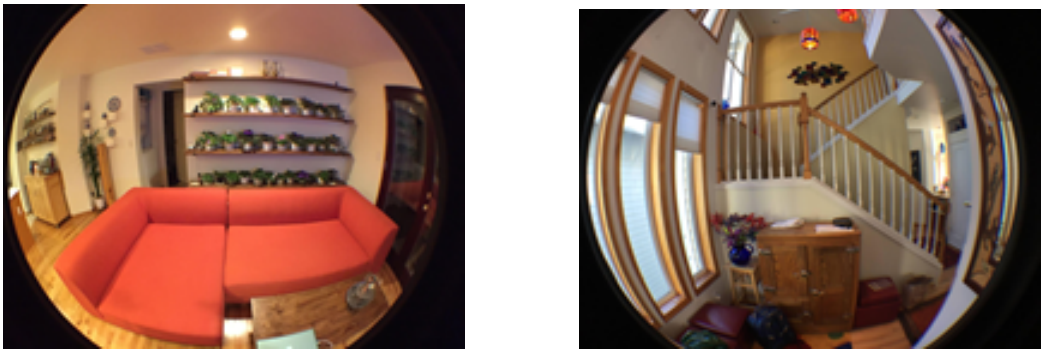

(a) Indoor-warm LED light

(b) Indoor-electric light and daylight

(c) Indoor-daylight

(d) Outdoor

Figure 2.7: Fish-eye view photographs show the full view of the sensors in experiment 3. a) indoor measurement under warm LED light, b) indoor measurement under mixed electric light and daylight, c) indoor measurement under daylight, and d) outdoor measurement.

The measurements were performed between 10 AM and 4 PM from May 15th to May 21st during sunny and partly cloudy days. It is important to note that we used four large background colored surfaces (red, blue, green, and yellow), sized $152.5 \times 214cm$, to cover a significant part of the sensors' view in more than half of the indoor measurements under different light sources (see Fig. 2.7(c)). Fig. 2.7 shows four examples of fish-eye view photographs for real-world measurements, including indoor and outdoor environments. The initial dataset from experiment 3 was pre-processed by downsampling and normalizing the SPD in the most accurate MLP model obtained from the previous experiment.

2.3 Results

This section presents the results of pre-experimental calibration of the developed spectrometer, the development of an ANN model to reconstruct SPD using data collected from experiments 1 and 2, and measurement of SPD in experiment 3 using the most accurate MLP model obtained from the previous experiment.

2.3.1 Pre-Experimental Calibration of the Developed Spectrometer

Fig. 2.8 and Fig. 2.9 show the pre-experimental calibration results that were carried out to check the monochromatic and spectral response of the spectral sensor across the visible spectrum for 14 channels with peak sensitivities between 410 nm and 760 nm. As explained in section 2.2.2, the Spectrofluorophotometer was used to characterize the spectral sensor by adjusting the wavelength manually to obtain the central wavelengths for all 14 channels. The Spectrofluorophotometer was adjusted manually to the central wavelengths of each of the 14 channels of the spectral sensor. At each wavelength, 120 readings were done by one-second intervals over two minutes. Although the Spectrofluorophotometer precisely transmitted a wavelength specific to the excitation spectrum while blocking other wavelengths, in some cases, the adjacent channels of the spectral sensor were also activated. In other words, there was channel interference for all 14 channels; for some, it is negligible, and for some, it is noticeable. As shown in Fig. 2.8, the channel interference for the wavelength 410 nm, 435 nm, 460 nm, 485 nm, 510 nm, 535 nm, 585 nm, 610 nm, 645 nm, 705 nm, 730 nm, and 760 nm was insignificant. However, the channel interference was considerably high for the wavelengths 560 nm and 680 nm as the adjacent channels were highly activated.

Fig. 2.9 presents the spectral response of 14 channels of the spectral sensor measured with the Spectrofluorophotometer to assess the wavelength accuracy of the developed spectrometer. To verify the characteristics of the developed spectrometer, it is crucial to carry out the monochromatic response. The results can be compared

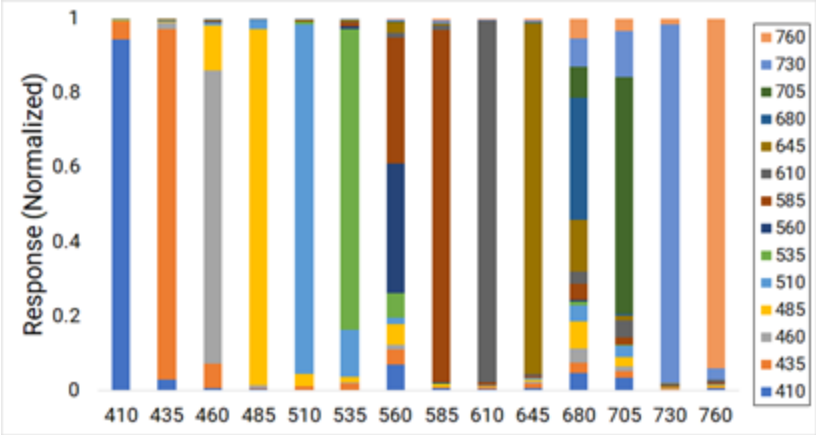

Figure 2.8: Monochromatic response of the spectral sensor measured with the Spectrofluorophotometer for all 14 channels.

with the reported central wavelengths from the manufacturer. The horizontal axis of Fig. 2.9 shows the deviation between the wavelength value acquired in the calibration process from the reported one from the manufacturer (see Table 2.1). The wavelength value differs by 3-5 nm for almost all channels except for two wavelengths (680 nm and 705 nm), where the wavelength value differs by approximately 10 nm. The results show that the AS7265X spectral sensor is a powerful optical inspection sensor with a wavelength accuracy of lower than ±5 nm for 12 channels (out of 14) except for two channels with a wavelength accuracy of ±10 nm. We performed this process once before starting the experiments and under laboratory conditions to evaluate the accuracy of spectral measurement of the developed spectrometer against the manufacturer's reported wavelengths.

2.3.2 Experiment 1

To answer the first goal of this study, we experimented with training the MLP and validating its performance by comparing different architectures, activation functions, and learning algorithms. Additionally, to answer the second goal of this study, we reconstructed the SPD of 30 LEDs measured in the controlled laboratory to evaluate the performance of MLP for improving the accuracy of the developed spectrometer.

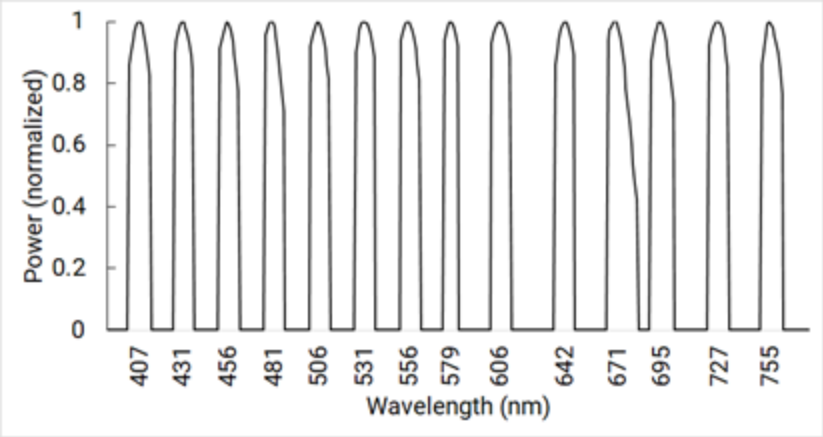

Figure 2.9: Spectral response of the developed spectrometer measured with the Spectrofluorophotometer for assessing the accuracy of all 14 channels.

2.3.2.1 ANNs Architecture Selection

The performance of the neural network can be affected by learning algorithms. The structure of the MLP model is another important factor that could influence the neural network's performance. Table 2.2 shows the effect of different training algorithms and activation functions on the performance of the MLP model in experiment 1. The activation function as a mathematical component in each layer could change the MLP structure. The neural network's performance in terms of the training error and training time when it was trained with different activation functions and learning algorithms is shown in Table 2.2. Three types of activation functions and eight types of learning algorithms were used to find the neural network with the best performance. The non-linear activation function (Tansig) combined with the Trainlm LevenbergâMarquardt algorithm had the lowest training error, while it had the highest training time. Trainlm LevenbergâMarquardt algorithm has the lowest training error between all three activation functions (linear and non-linear activation functions) compared to other learning algorithms.

Table 2.2: The training error and training time for the ANNs trained with three different activation functions and eight different learning algorithms for experiment 1.

Learning Algorithms	Activation Functions					
	Purlin		Tansig		Logsig	
	Training error (MSE)	Training time (sec)	Training error (MSE)	Training time (sec)	Training error (MSE)	Training time (sec)
Traingdx	1.30E+00	28	2.49E-01	42	1.18E-03	50
Trainlm Levenberg-Marquardt	5.35E-07	12,838	6.87E-08	348,265	1.35E-06	35,263
Traincgf Fletcher-reeves	2.26E-05	373	9.47E-01	188	1.63E-03	49
Traincgp Polak-Ribiere	4.13E-04	129	9.47E-01	26	1.59E-03	48
Traincgb Powell-beale	2.85E-05	151	9.47E-01	26	1.59E-03	43
Trainoss	1.49E-04	172	8.54E-01	59	1.76E-03	24
Trainbfg BFGS	5.57E-06	4,096	8.32E-01	595	1.76E-03	36
Traingd	1.91E-02	38	3.49E-02	64	1.19E-03	50

The size of the hidden layers and the number of neurons in each layer were other parameters that had a significant effect on the structure of the MLP model. To find the neural network with the lowest training error, the number of hidden layers and numbers of neurons per layer was selected by trial and error, as mentioned in section 3.2. Fig. 2.10 shows the learning performance of the neural network when

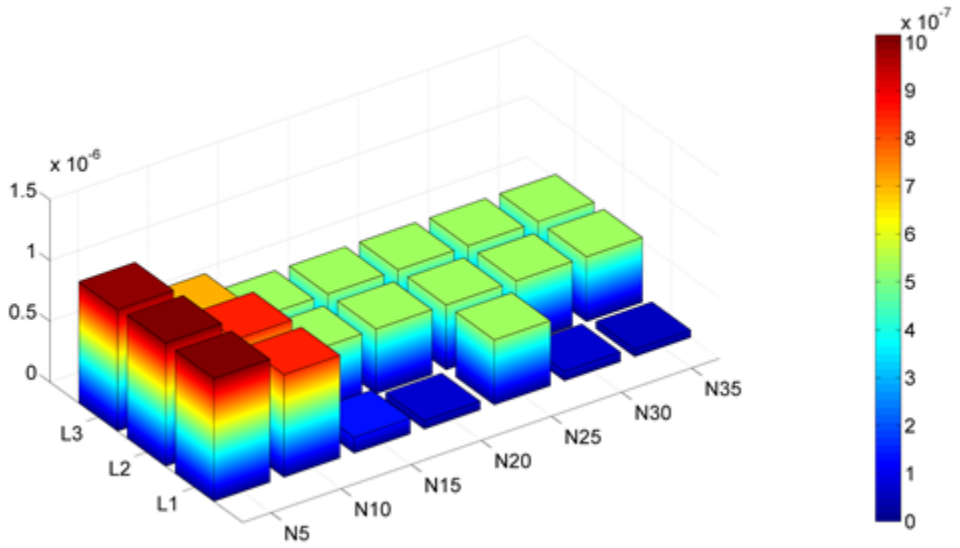

Figure 2.10: Comparing the Mean Square Error (MSE) for different numbers of hidden layers (L) and different numbers of neurons per layer (N), when MLP trained with non-linear activation function Tansig combined with Trainlm LevenbergâMarquardt algorithm in experiment 1.

trained with different numbers of hidden layers (L) versus other numbers of neurons per layer (N) using the non-linear activation function Tansig, combined with Trainlm LevenbergâMarquardt algorithm L1, L2, and L3 represent the neural network with one, two, and three hidden layers, respectively. As shown in the X-axis of Fig. 2.10, the number of neurons per layer varies between 5 (N5) and 35 (N35), in increments of 5. This graph shows that the network with one hidden layer and 20 neurons per layer has the lowest training error. To find the neural network with the lowest training error, the number of hidden layers and numbers of neurons per layer were selected by trial and error, as mentioned in section 2.2.3.2.3.

2.3.2.2 Reconstruction of SPD

Fig. 2.11 shows five examples of reconstruction of the SPD of the LEDs with different colors using the proposed model. The blue line shows the SPD of the light source measured by the WaveGo. In contrast, the direct response from the developed spectrometer is demonstrated by the black line. The SPD estimates by the MLP model

with linear function are shown with a green line, while non-linear Tansig and Logsig functions are shown with a red line and a yellow line, respectively. It is observed that the estimated SPD using MLP with linear and non-linear activation functions is much closer to the SPD measured by WaveGo compared to the direct response from the developed spectrometer. The results clearly show that implementing the neural network affects saving SPD information. Additionally, the non-linear activation function Tansig (red line) is the most accurate MLP model to reconstruct the SPD of light sources.

Closer inspection of Fig. 2.11 shows that the developed spectrometer accurately measured SPDs of light sources as the direct response from the developed spectrometer without the interference of neural networks was significantly close to the source measured by the WaveGo in the experiment with minimum measurement errors. Even though the developed spectrometer had acceptable accuracy for measuring SPDs of light sources, SPDs estimated with neural networks were closer to the source measured by WaveGo. The results indicated that neural networks have a remarkable ability to improve the accuracy of the developed spectrometer.

We evaluated the ability of the neural network to reconstruct the SPD of each light source individually for testing the MLP model. Different error and similarity factors such as correlation coefficient were used to compare the SPD measured by WaveGo and the reconstructed SPD by the MLP model (see Fig. 2.12). Fig. 2.12 shows the value of different types of errors for all 30 LEDs for the most accurate neural network in experiment 1 (Tansig function combined with Trainlm LevenbergâMarquardt algorithm). It shows the Correlation Coefficient (R-value), Sum of Squared Errors (SSE), Mean-Square Error (MSE), Root-Mean-Square Error (RMSE), and Normalized Root-Mean-Square Error (NRMSE). As shown in Fig. 2.12 (e), the maximum NRMSE is 0.6%, and the minimum NRMSE is 0.02%.

Moreover, most of the samples have a correlation coefficient (R-value) near 1.0

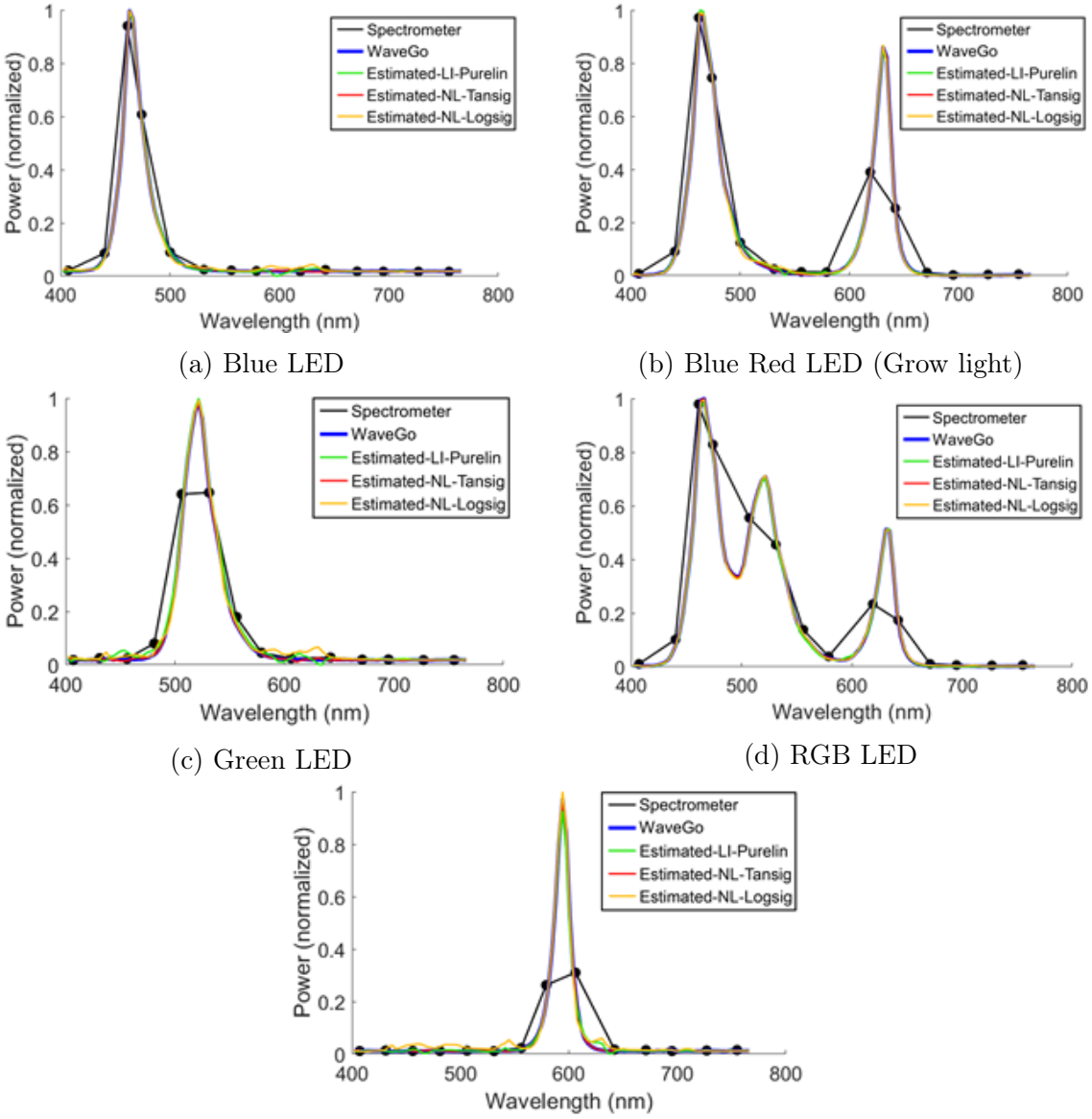

(a) Blue LED

(b) Blue Red LED (Grow light)

(c) Green LED

(d) RGB LED

(e) Red LED

Figure 2.11: Estimated SPD with the two non-linear functions (red and yellow lines) and the linear function (green line), the source measured by WaveGo (blue line), and direct response from the developed spectrometer (black line) for the test in experiment 1.

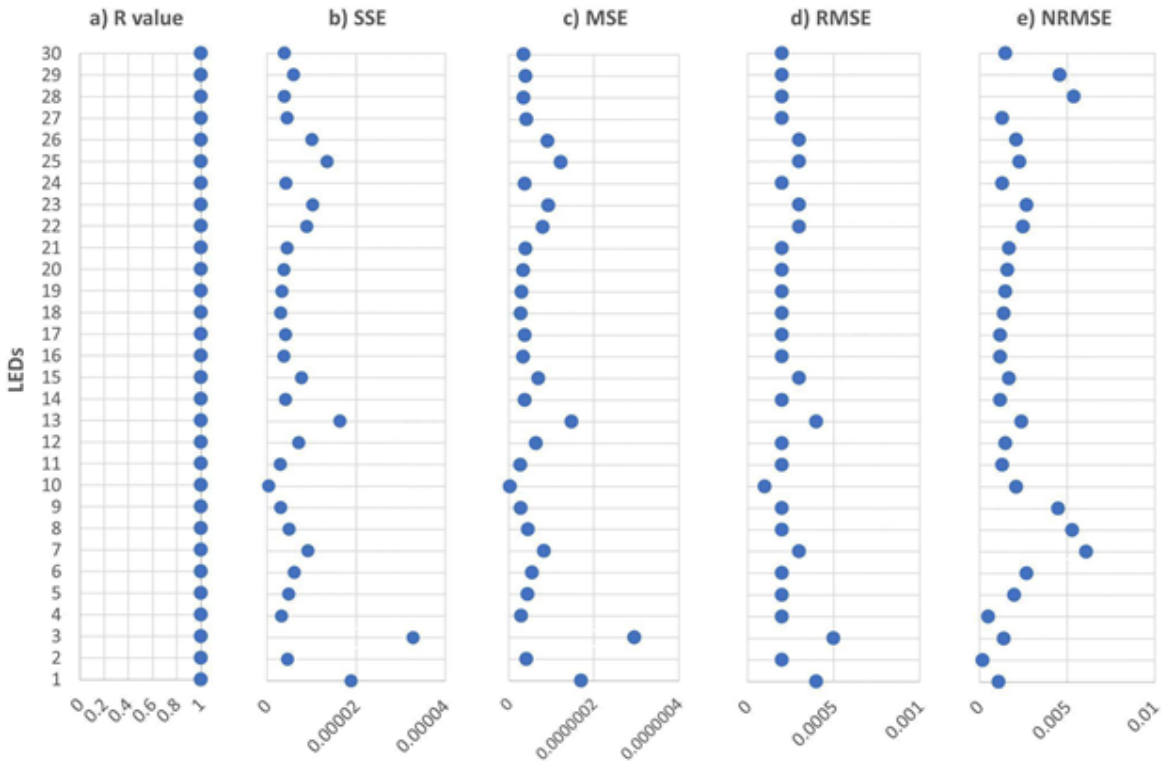

Figure 2.12: Estimated errors for 30 LEDs for the most accurate neural network (Tansig function combined with Trainlm LevenbergâMarquardt algorithm) in experiment 1. a) Correlation Coefficient (R-value), b) Sum of Squared Errors (SSE), c) Mean-Square Error (MSE), d) Root-Mean-Square Error (RMSE), and e) Normalized Root-Mean-Square Error (NRMSE).

that indicates a perfect positive correlation (Fig. 2.12 (a)). These results suggest that the proposed model is very accurate and reliable, with an error lower than 1% to reconstruct the SPD of the light source. The results presented in Fig. 2.12 indicate that using the developed spectrometer in tandem with the neural network can measure SPD with high accuracy.

2.3.3 Experiment 2

To answer the first goal of this study, experiment 2 was performed to train the MLP and validate its performance by comparing different architectures, activation functions, and learning algorithms. To answer the second goal of this study, the SPD of 106 different types of light sources was reconstructed that was measured in the

semi-real-world environment to evaluate the performance of MLP for improving the accuracy of the developed spectrometer.

2.3.3.1 ANNs Architecture Selection

We performed the same procedure to train the MLP network for the second experiment in a semi-real-world environment following the first experiment. Similarly, the effects of learning algorithms and different structures of the MLP model were investigated on the neural network's performance. Table 2.3 compares some of the main characteristics of the neural network with the best performance implemented in experiment 1 and experiment 2. Each experiment shows the best activation functions and learning algorithms in terms of training error and training time. For experiment 2, the neural network with one hidden layer and 25 neurons per layer with Logsig activation function and Trainlm LevenbergâMarquardt algorithm has the lowest training error. Non-linear activation functions perform better than the linear activation function (purelin) for experiments 1 and 2 (see Table 2.3).

The training error (MSE) is 7×10^{-6} for experiment 2, higher than experiment 1. In experiment 2, 85% of samples (all light sources) have NRMSE under 20%, and the Mean NRMSE is below 10%. While experiment 1 has Mean Normalized Root-Mean-Square Error (NRMSE) below 1% and 100% of its samples have the NRMSE under 20%. Although experiment 2 has a higher training error and training time than experiment 1, it still shows an acceptable performance while subjected to a significant amount of measurement errors.

Table 2.3: Specifications of neural network with the best performance in experiment 1 vs. experiment 2.

Experiment	Activation Function	Mean square error (MSE)	Mean NRMSE	Under 20% NRMSE	Mean R-value	Training time (hours)
1	Tansig	0.000000069	0.0046	100	0.999	97
2	Logsig	0.000007154	0.0989	85	0.922	213

2.3.3.2 Reconstruction of SPD

Fig. 2.13 shows reconstructed SPD for five different light sources, Fluorescent, Halogen, LED, and Incandescent, and Daylight, using the proposed model. Because the measurement was subjected to stray light from the surrounding surfaces, there is a discrepancy between the SPD measured by WaveGo (blue line) and the direct response from the developed spectrometer (black line). Despite this test being conducted under a significant source of error, similar to the first test, the reconstructed SPD estimated by the neural network is still very close to the SPD measured by the WaveGo. The SPD estimated with a non-linear activation function called Logsig (yellow line) has the best performance and is closer to the SPD measured by WaveGo than the other two activation functions. The results of non-linear activation functions are more accurate compared to the linear ones.

As shown in Fig. 2.13 (d), the error is higher for daylight than other light sources, which could be due to the complexity of the SPD. Although there is a deviation between the direct response from the developed spectrometer without the help of the neural network (black line) and the source measured by WaveGo (blue line), the accuracy of SPD estimated with the neural network is significantly improved, as it is close to the source measured by WaveGo. The results indicate that the neural network can significantly save the information from the SPD measured by WaveGo

even if considerable stray light is present.

Fig. 2.14 shows the average value of different error types for all samples of light sources to demonstrate the performance and accuracy of the implemented neural network. Additionally, the correlation coefficient (R-value) can be used as a factor to evaluate the similarity between the output of the MLP model and data measured by WaveGo as the reference. The average NRMSE for all five light sources is under 20%. While the average NRMSE of Daylight's samples is around 18%, for Fluorescents' samples the average NRMSE is as low as 0.6% (Fig. 2.14 (e)). As shown in Fig. 2.14(a), all light sources have a high correlation coefficient above 0.9, except Halogen, which is around 0.8.

2.3.4 Experiment 3: Evaluate the Developed Spectrometer under a Real-World Environment

To reconstruct the SPD of 40 real-world measurements in experiment 3, we employed the most accurate MLP model from experiment 2 (one hidden layer and 25 neurons per layer with the Logsig activation function and the Trainlm Levenbergâ-Marquardt algorithm). It should be noted that the most accurate MLP model from experiment 2 without any modification, training, and alteration was directly used to reconstruct the 40 samples (30 indoors and 10 outdoors) of measured SPD in experiment 3. Fig. 2.15 shows the reconstructed SPD of four examples of real-world measurements in experiment 3 using the most accurate MLP model. To help in better understanding of the conditions of the measurements, four examples of fish-eye view colored photographs illustrated in Fig. 2.7 were taken side by side with the developed spectrometer and AvaSpec-Mini2048CL; thus, they represent the position and field of view of the sensors that are shown in Fig. 2.15. The SPD of the light source measured by the AvaSpec-Mini2048CL as a reference is shown by the blue line, while the direct response from the developed spectrometer is demonstrated by the black line, and the SPD estimates by the most accurate neural network are shown with a red line. Even

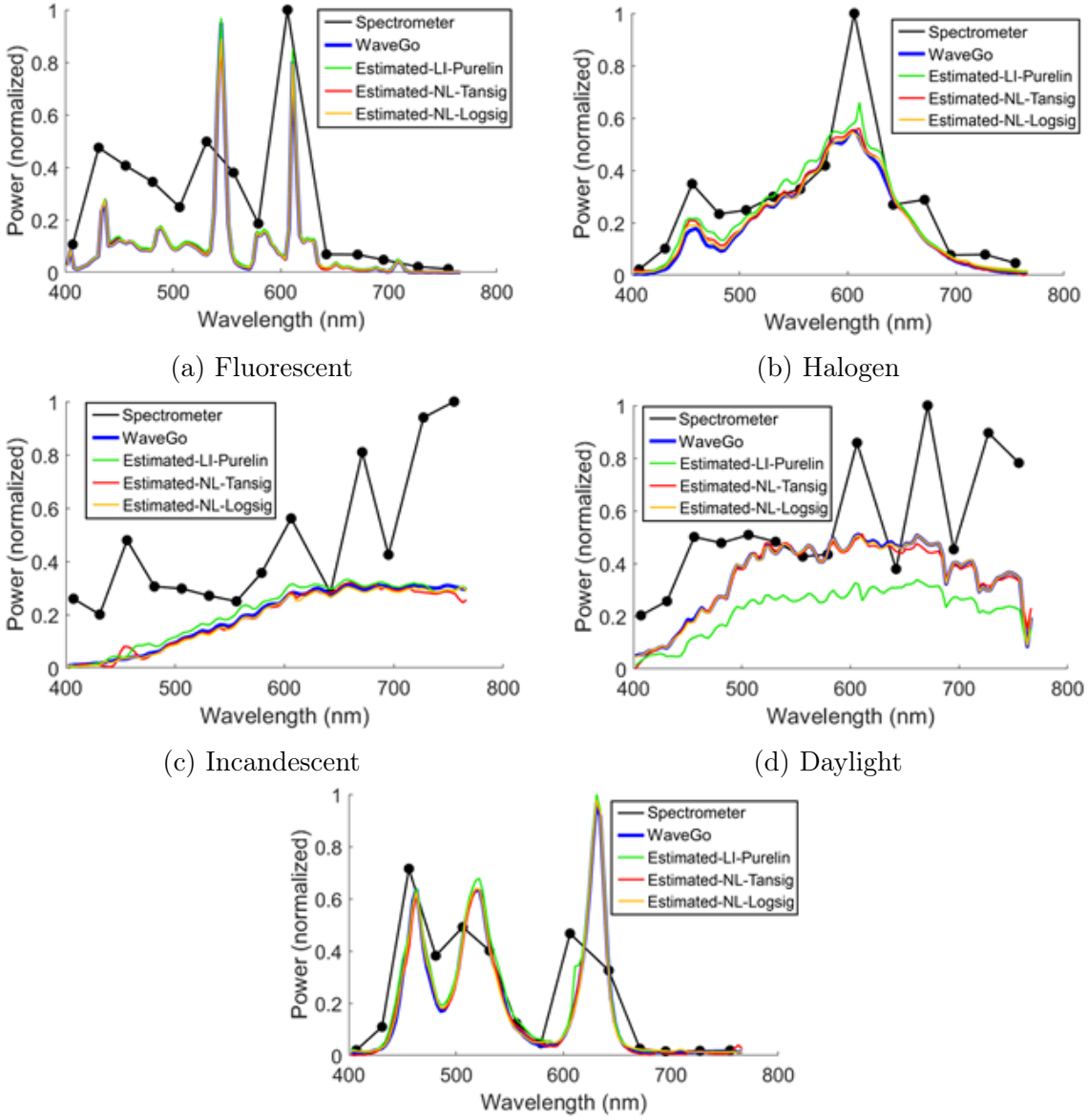

(a) Fluorescent

(b) Halogen

(c) Incandescent

(d) Daylight

(e) RGB LED

Figure 2.13: Estimated SPD with two non-linear functions (red and yellow lines), a linear function (green line), the source measured by WaveGo (blue line), and direct response from the developed spectrometer (black line) for the test in the experiment 2.

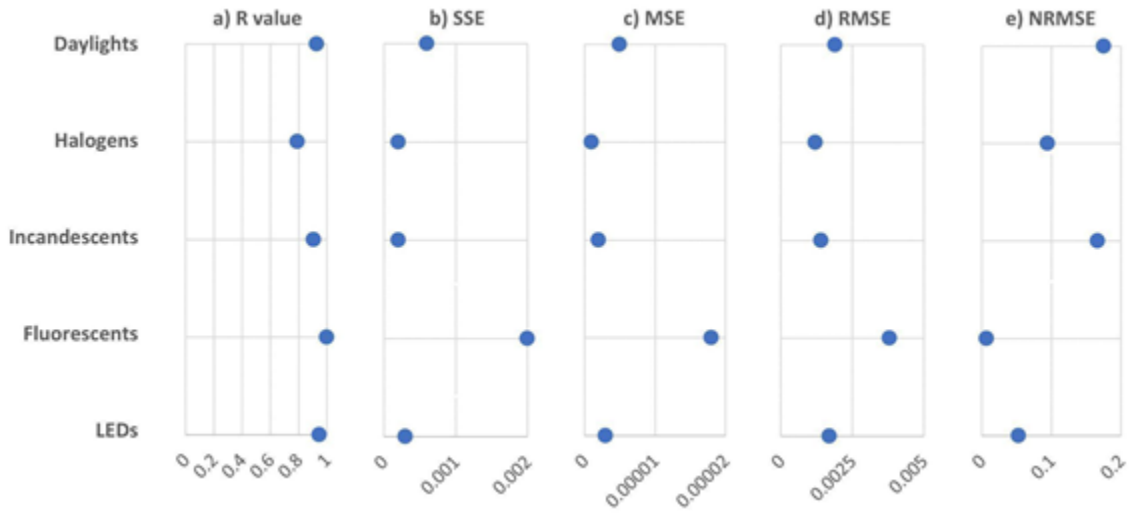

Figure 2.14: Average estimated errors for five different types of light sources for the most accurate neural network (Logsig activation function combined with Trainlm LevenbergâMarquardt algorithm) for experiment 2. a) Correlation Coefficient (R-value), b) Sum of Squared Errors (SSE), c) Mean-Square Error (MSE), d) Root-Mean-Square Error (RMSE), and e) Normalized Root-Mean-Square Error (NRMSE).

though it is observed that the estimated SPD by the most accurate MLP model is much closer to the SPD measured by AvaSpec-Mini2048CL compared to the direct response from the developed spectrometer, there is still a discrepancy between the estimated SPD by the MLP model and the AvaSpec-Mini2048CL as a reference. The results show that the MLP model reconstructed the electric lighting's SPDs in the indoor environment with higher accuracy and lower error than the daylight's SPDs in the outdoor environment.

Fig. 2.16 shows the Correlation Coefficient (R-value) and the value of four different types of errors (SSE, MSE, RMSE, and NRMSE) along with Maximum Error for 40 real-world measurements utilizing the most accurate MLP model that was obtained from experiment 2. Fig. 2.16 (e) shows that the lowest NRMSE was approximately 11% by measuring SPD in the indoor environment under electric light. In comparison, the highest NRMSE was 40% in the outdoor environment under daylight. All of the measurements under electric light have an R-value above 0.85 that indicates a perfect positive correlation between the output of the MLP model and data measured by

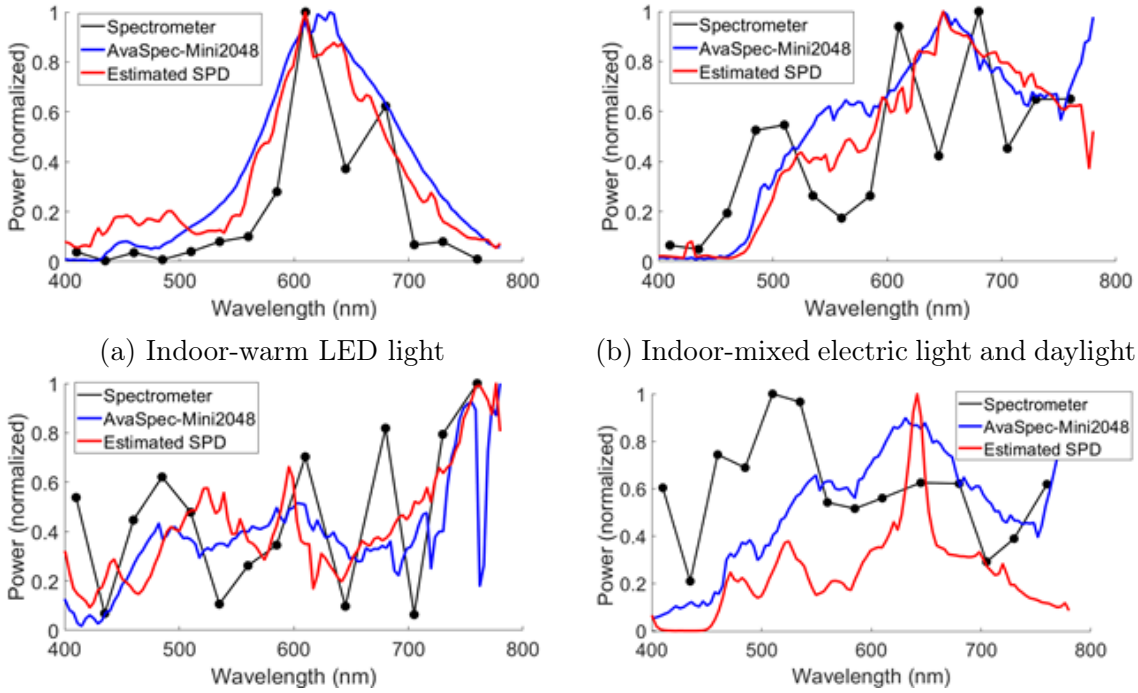

(a) Indoor-warm LED light

(b) Indoor-mixed electric light and daylight

(c) Indoor-daylight

(d) Outdoor

Figure 2.15: Estimated SPD with the most accurate MLP model using 106 samples in four different experiment scenarios: a) indoor space under warm LED as the only light source, b) indoor space under mixed warm LED and daylight, c) indoor space under daylight as the only light source, and d) outdoor space under daylight as the only light source. The SPD of light exposure was measured by AvaSpec-Mini2048 (blue line), the direct response from the developed spectrometer (black line), and the estimated SPD by the most accurate neural network (red line).

AvaSpec-Mini2048CL as the reference. Moreover, all of the real-world measurements under electric light have an error lower than 17%. The measured SPD in the outdoor environment under daylight has higher NRMSE, between 29% and 40%, and a lower R-value, between 0.64 and 0.81, compared with that SPD measured in the indoor environment under electric light. In addition, Fig. 2.16 (f) shows the maximum difference between the estimated SPD by the MLP model and the measured SPD by AvaSpec-Mini2048CL as the reference for all 40 real-world measurements. The mean Maximum Error was 192.6% ± 138.8% for all 40 measurements. Although the indoor measurements under electric light had a mean Maximum Error of 109.3% ± 23.7%, the outdoor measurements had a higher mean Maximum Error of 338.9% ± 207.1%.

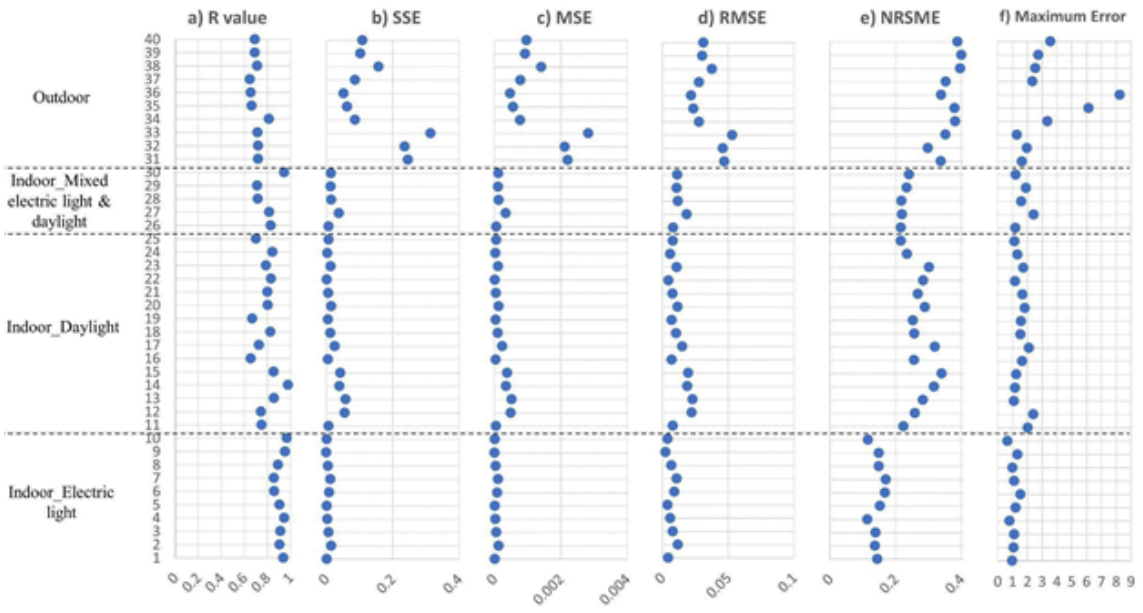

Figure 2.16: Estimated errors for 40 measurements under real-world conditions using the MLP with the best performance (Logsig activation function combined with Trainlm LevenbergâMarquardt algorithm) for experiment 3. a) Correlation Coefficient (R-value), b) Sum of Squared Errors (SSE), c) Mean-Square Error (MSE), d) Root-Mean-Square Error (RMSE), e) Normalized Root-Mean-Square Error (NRMSE), and f) Maximum Error.

2.4 Discussion

This study performed a pre-experimental calibration to assess the developed spectrometer's wavelength accuracy and spectral response across the visible spectrum. We also conducted two experiments to develop ANN models to reconstruct the light source's SPD to improve the developed spectrometer's accuracy. The accuracy and performance of the MLP models were demonstrated at a controlled laboratory that was entirely in darkness in experiment 1 and when a significant source of error from stray light was present in experiment 2. It should be noted that experiment 2 differed from experiment 1 in terms of position and distance of light sources from the integrated sphere and the number and the type of light sources used in each experiment. Finally, in the third experiment (experiment 3), we utilized the most accurate MLP model obtained from the previous experiment (experiment 2) to challenge its

performance by exposing it to complex and unique SPD measured under real-world environments.

Findings from this study suggest that selecting an appropriate ANNs architecture has a significant impact on the accuracy of reconstructed SPD. For example, the results of experiment 1 indicated that the optimum size of the neural network with the best performance was a network with a single layer and around 20 neurons per layer (Fig. 2.10). We found that deviation from the optimum size of the network by increasing or decreasing the number of layers of neurons per layer hurt the accuracy of reconstructed SPD. A possible explanation for this might be that the MLP model in this study was under-fitted when the number of neurons was less than 10. The network could not estimate the SPD accurately compared with a larger-sized network. On the other hand, the model shows a lower performance when the size of the network grew, and the number of neurons surpassed 20, specifically for the multi-hidden layer networks. In this case, the network could be over-fitted, not learning anymore, and memorized the data instead [125].

Reconstructed SPD by the non-linear function combined with Trainlm Levenbergâ-Marquardt algorithm had the lowest training error for experiments 1 and 2. While the Trainlm LevenbergâMarquardt algorithm had the best performance with the lowest training error, training time dramatically increased compared to other learning algorithms (Table 2.2). These results agree with previous studies [126,127], which showed that the Trainlm LevenbergâMarquardt algorithm was the most efficient method with non-linear characteristics to learn the features based on related datasets.

The findings show the significant benefits of using ANNs to improve the precision of the developed spectrometer (Fig. 2.11, Fig. 2.13, and Fig. 2.15). The estimated error for reconstructing the SPD ranged from 0.02% to 0.6% for experiment 1 using 30 samples of the light source (Fig. 2.12). Even in experiment 2 with 106 different light sources, when the test was subjected to the significant source of error from stray light,

the highest reported error was lower than 18% (Fig. 2.14). The error was increased under daylight in real-world measurements due to the complexity and uniqueness of the SPD. Moreover, in experiment 3, we challenged the most accurate MLP model obtained from the previous experiment by exposing the developed spectrometer to unique SPDs from reflected light off surfaces with different colors within indoor and outdoor environments under other lighting conditions. We found that the neural network was very effective in reconstructing SPD with the known patterns in data, while it had a higher error rate (up to 40%, Fig. 2.16) when exposed to SPDs with unrecognizable patterns. We also found that the MLP model could learn from recognized patterns in data under electric lighting in real-world measurements and ultimately reconstructed SPD with reasonable accuracy (below 17%, Fig. 2.16).

The MLP model was trained by measuring the SPD of 106 different types of light sources, including LEDs, fluorescents, incandescent, halogens, and daylight in experiment 2. Moreover, to build the final dataset, we combined the different light sources to recreate conditions as close as possible to real-world environments. Although we measured 33 SPDs of daylight during sunny, partly cloudy, and rainy days for experiment 2, the spectral characteristics of natural daylight in real-world environments can change dramatically during a single day, and from season to season, day to day, and at different geographical locations. There were also significant differences between the initial conditions used to measure SPD in experiments 2 and 3 in terms of the experimental setup, position and direction of light sources, and the time and season of the measurements. Additionally, excluding the integrated sphere considerably increased the instrument-related source of error from stray light and interference in experiment 3 due to a change in the collecting optics. The higher error for the real-world condition (experiment 3) can be attributed to the considerable differences between the measured SPD used to train the MLP model in experiment 2 and the SPD that the developed spectrometers and the reference instruments were exposed

to in experiment 3.

Although the idea of improving the accuracy of the low-cost sensors using ANNs is not new and has been used by many researchers over the past few years [93–99], only one study [40] attempted to develop a spectrometer using ANNs for measuring light source's SPDs. However, this study did not consider errors introduced by stray lights and interferences within the real-world measurements. In addition, the size and diversity of samples that we used to train the MLP model in experiment 2 were much larger (106 samples) compared with only 81 samples used in the previous study. In the current study, the inclusion of a significant source of error from stray light increased the NRMSE from under 1% in experiment 1 (control laboratory) to 18% in experiment 2 (semi-real-world environment). In experiment 3, the developed spectrometer was exposed to transmitted and reflected light from surfaces with different colors and textures in the paths from the light sources to the developed spectrometer. Therefore, it created a unique SPD that was not exactly similar to previous samples, even if it comes from the known pattern of light sources. Previous studies showed that deep learning methods such as Convolutional Neural Network (CNN) have much better learning efficiency and outperform the older types of networks such as multilayer perceptron (MLP) [128–130]. Providing more samples from different light sources and using deep learning techniques to improve the device's accuracy under real-world conditions remains for future study.

The accurate measure of accuracy for low-cost personal devices is unknown. Except daylight, the accuracy of the developed device when exposed to both known and unknown SPD of electric light sources matches the reported accuracy (7-20 %) of personal devices measuring circadian lighting [131] and also the accuracy of (5-20 %) low-cost devices that measure luminance distribution of light in the building realm [132–134]. It should be noted that these devices only measured light exposures of irradiance from red, green, and blue in the visible light spectrum and did not measure

SPD within the entire visible spectrum. While the accuracy within these ranges would not qualify as laboratory-grade devices, a range based on previous studies seems appropriate for a practical personal measurement device.

The work we presented in this paper is novel in at least four aspects. First, the developed spectrometer used the most advanced low-cost spectral sensor (AS7265X) in the market regarding accuracy and resolution that measures spectral irradiance in a range between 410 nm and 760 nm. This sensor can be used to assess circadian lighting as it considers the spectral sensitivities of all five types of photoreceptors. Second, the most popular portable devices measure irradiance from red, green, and blue regions of the visible spectrum or record photopic value (lux) and store the collected data in internal memory. However, the developed spectrometer can measure SPD as the complete form to measure light exposures with wireless communication. It enables it to connect with a cloud-based web service to store collected data in real-time. Measuring SPD allows us to re-analyze the collected data using any unit of measure currently available or that may be developed in the future. The device can be integrated into intelligent lighting systems for turning indoor lighting sources into proper human-centric lighting. It can also be used as a connected technology using an App to monitor how light affects individuals' health and get tips to control their living conditions. Third, utilizing the neural network for reconstructing the SPD of light sources considerably increased the resolution and accuracy of the spectral sensor with 14 channels from over 20 nm to 111 points around 3.5 nm, which is close to the resolution of the expensive commercial devices. Finally, we used various light sources, including electric light and daylight (106 samples). We employed an integrated sphere to design a reliable measurement process to compare the performance of a non-calibrated spectrometer developed in this study with the calibrated one (WaveGo).

This study is part of the larger project, for which spectral irradiance measured

by the developed device is converted to W/m^2 to measure personal light exposures by employing the metrics recommended by different standards such as Well Building Standard and CIE. The developed device will be used in our future studies for real-time monitoring of personal circadian lighting and to visualize collected data in a real-time manner on an application. Thus, as previously mentioned, we only use 14 bands out of the 18 bands of the spectral sensor in the wavelength between 410 nm and 760 nm to address the peak sensitivity for all five human photoreceptors.

Providing continuous information by long-term measurement of the micro environment around the individuals can mitigate user discomfort and energy consumption and bring health and well-being to occupants in existing buildings. Capitalizing on the potential of monitoring personal lighting exposures, our developed device incorporates a spectral sensor that records varying internal and external environmental influences from the sun and users. The proposed device holds promise for a healthier built environment by offering real-time tracking and monitoring of an individual's lighting conditions and control these conditions (e.g., via a connected lighting system) towards the individual's needs and desires. Outcomes of the study contribute to a body of evidence that can inform significant design decisions related to the current use and future design of office, educational, and healthcare facilities.

2.4.1 Limitations of the Study

We measured a limited number of light sources, 30 samples in experiment 1 and 106 samples in experiment 2, to build the final datasets, and utilized a limited number of ANNs architecture, activation functions, and learning algorithms for training the MLP model for reconstructing the SPD. Therefore, the most accurate MLP model is most effective when reconstructing the SPD of light sources, similar to the SPD utilized to build the final dataset. Its accuracy decreases when it is generalized to all types of light sources. Additional research is needed to improve the performance of neural networks when it is subjected to significant error and unique SPD of day-

light under real-world conditions (experiment 3) by providing more samples of light sources as an input and/or applying more advanced techniques such as deep learning. In contrast, the present study focused specifically on evaluating the performance of one type of low-cost spectrometer, which is commercially available. Future studies can integrate different types of spectral sensors or mini spectrometers with various computational techniques to increase the accuracy of measurement devices.

2.5 Conclusions

There is a lack of an accurate, affordable, and portable spectrometer to measure light source's SPDs, which affects the human circadian system. The current study demonstrated the development of a low-cost, portable and wireless spectrometer in tandem with Artificial Neural Networks to improve the accuracy of the measured light source spectrum. We used an MLP model to reconstruct the light source's SPDs measured in 14 bands in the wavelength between 410 nm and 760 nm to an SPD of 111 points. We found that the MLP with a single layer and neurons ranged between 20 and 25 per hidden layer with non-linear activation functions in combination with Trainlm LevenbergâMarquardt learning algorithm can estimate the SPD with an error lower than 1% in experiment 1 and lower than 18% in experiment 2 affected by the existence of considerable stray light. Although the neural network learned the pattern of SPD of the electric lighting effectively by an error lower than 17% in real-world conditions, it had a higher error rate when exposed to daylight with unrecognizable patterns due to the complexity and uniqueness of the SPD. Findings from this study suggest that the more samples used to train neural networks, the more accurately neural networks can reconstruct SPD.

This study has been one of the first attempts to integrate a low-cost spectrometer with artificial intelligence to provide valuable insights to lighting designers, researchers, and architects. The spectrometer prototype developed in this study can be integrated into an IoT-based intelligent lighting system to measure personal light-

ing conditions continuously. The intelligent lighting system can further tailor indoor lighting conditions according to individual needs and desires. Additionally, the developed device offers several applications by monitoring individuals' vital information, such as real-time tracking of personal light exposures and visualizing the collected data on a mobile device. The recorded data can help individuals or their health coaches control their living conditions, health, and lifestyles.

CHAPTER 3: EVALUATING THE CIRCADIAN-EFFECTIVENESS OF LIGHT THROUGH PERSONAL LIGHT EXPOSURE MEASUREMENT: RESULTS OF A FIELD STUDY USING A LOW-COST AND WEARABLE SPECTROMETER IN HOME-OFFICE

3.1 Introduction

Natural light is an essential element of building design that influences human health, comfort, performance, and well-being. Natural light provides a combination of suitable types of light with the right spectral content at the correct times. Humans' daily rhythms in behavior and physiology, such as wake/sleep patterns, have evolved under natural light-dark cycles over millions of years. However, the invention of electric lighting has dramatically changed human home, social, and work environments by shifting the light exposure pattern from natural light to electric light over the past decades. Currently, exposure to natural light is significantly reduced in the US as people spend more than 87% of their working hours indoors compared to the 1800s where they spent about 90% of their time working outside [2]. Despite the advantages of this invention for humankind, lack of natural light exposure during the day and increased exposure to electric light during the night are associated with psychological, physical, and mental health issues that can disrupt circadian rhythms and sleep.

Circadian rhythm is a natural process that regulates the sleep-wake cycle by synching the internal clock to roughly a 24-hours diurnal cycle in an outdoor environment. Disruption of circadian rhythm may result in mood disorders, displacement of wake/sleep cycle, melatonin suppression, and phase-shifting of the circadian system. Ocular light exposure provides measurable benefits for both visual and non-visual systems. Even though we interact with our environment through a visual system, the

discovery of the third class of photoreceptors within the eye [3], named Intrinsically Photoreceptive Retinal Ganglion Cells (ipRGCs), placed increased attention on unseen effects of light that influence our mood, alertness, emotion, health, and sense of well-being. Deviation from regular light-dark exposure patterns negatively affects sleep [6], mood [8], performance [135] and is associated with a range of health issues such as seasonal affective disorder [12] and even cancer [13].

Nowadays, as we spend a large proportion of our time in the built environment, we are exposed to less light during daytime hours and more light during nighttime hours than what we would have naturally received across day and night [136]. For the past seven decades, the exposure to electric light has increased between 3% and 6% annually as people are mostly indoors, which may increase the likelihood of disrupting the circadian rhythms [137]. In recent years, the work landscape has changed dramatically, as companies have started to cut costs by downsizing their office spaces and allowing their employees to work-from-home (WFH). The number of people remotely WFH surged by 173% from 2005 to 2018 [138]. The pace of this change is increasing as a direct result of the COVID-19 pandemic, as currently, an ever-increasing number of people are WFH. Studies show strong links between an irregular natural day-night cycle and disruption of circadian rhythms, poorer sleep quality, impairment of cognitive function, and the onset of depression in office workers without or with less access to natural light [[139]. Therefore, it has never been more important to capture evidence from human interactions within existing buildings and investigate the impacts of indoor lighting conditions on human health, comfort, and wellbeing.

Currently, there is a lack of consensus on circadian lighting metrics and/or the exact threshold to support circadian effectiveness of lighting in working environments. Some standards in the field of light and lighting such as, WELL Building Standard v2 [20], have recently begun to include metrics that address the proper light exposure for supporting physical health and adjusting the circadian rhythm with a natural day-

night cycle. The WELL standard recommends using the two most popular circadian lighting metrics for measuring light exposure: Equivalent Melanopic Lux (EML) and Circadian Stimulus (CS). The effect of light exposure on the circadian system should be calculated by considering the output of all three types of retinal photoreceptors, rods, cones, and ipRGCs, in the human eye [32]. CS considers both spectrum and intensity of light source and ties to all three types of retinal photoreceptors, which are necessary for assessing circadian lighting [14]. However, EML ties to a single photoreceptor and ignores any impacts of the rods and cones. This study used CS to measure the circadian effectiveness of light using the collected data from the wearable device.

Tailoring indoor lighting conditions per individuals'specific needs and desires can promote health and wellbeing in the built environments. Previous studies suggested we consider at least six factors (timing, duration, history, intensity, spectrum, and directionality of light exposure) when assessing the effects of light beyond vision [42]. The spectrum and intensity of the light exposure need to be aligned with the human circadian system throughout the day to avoid circadian disruption and enhance human health and productivity. For example, exposure to light in the early morning advances the timing of the circadian clock; however, receiving bright light during the evening delays the timing of the biological clock and may cause circadian disruption, which consequently reduces sleepiness [140]. Thus, people who spend a large proportion of the day under electric light expose themselves to steady light intensities and spectrum, specifically during the evening/night hours, which may shift the human biological clock [141]. In the field of architecture and lighting design, different metrics, techniques, and devices need to be utilized other than what traditionally have been used by lighting designers to address human biological needs for light. In this way, wearable technologies can be used to measure personal light conditions continuously in their most complete forms (Spectral Power Distribution of light), which is essential

for the lighting community. Recently, the term âpersonal lighting conditionsâ was commonly used when measuring lighting conditions continuously at the individual level [42]. The inclusion of this term is recommended, particularly in studies that investigate the non-visual effects of light on humans [72].

The objective of the present study was to measure the personal lighting conditions of two-office workers continuously over eight days in a home office using a recently developed wearable spectrometer. We used CS to evaluate the circadian effectiveness of various lighting conditions during the study period. We further explore the effect of work schedules in response to light exposure between two office workers.

3.2 Method

We conducted a field study using a novel wearable spectrometer to measure participants'light exposures continuously in a home office over eight days in Seattle, WA. Fig. 3.1 shows the processes used in this study for data processing and analysis. The following sections describe the process of collecting and analyzing the data and the instrument used for data collection in detail.

3.2.1 Test Space Selection Criteria and Participants

During the COVID pandemic, an ever-increasing number of people have been WFH. Therefore, data collection was performed at a home office on the third floor of a residential building located in Seattle, WA. Fig. 3.2 shows the schematic plan of the home office and its surrounding urban context. The home office has five separate spaces, including a working area, a kitchen, a bathroom, a living room furnished with a TV for resting time, and a bedroom for sleep at night. The working space had one West-side window that was covered with a Venetian blind. Except for the distance to the window, we attempted to minimize the variation between the features in participants working spaces. Features are similar for both participants included: room size; wall and furnishing color; siting orientation; amount and placement of

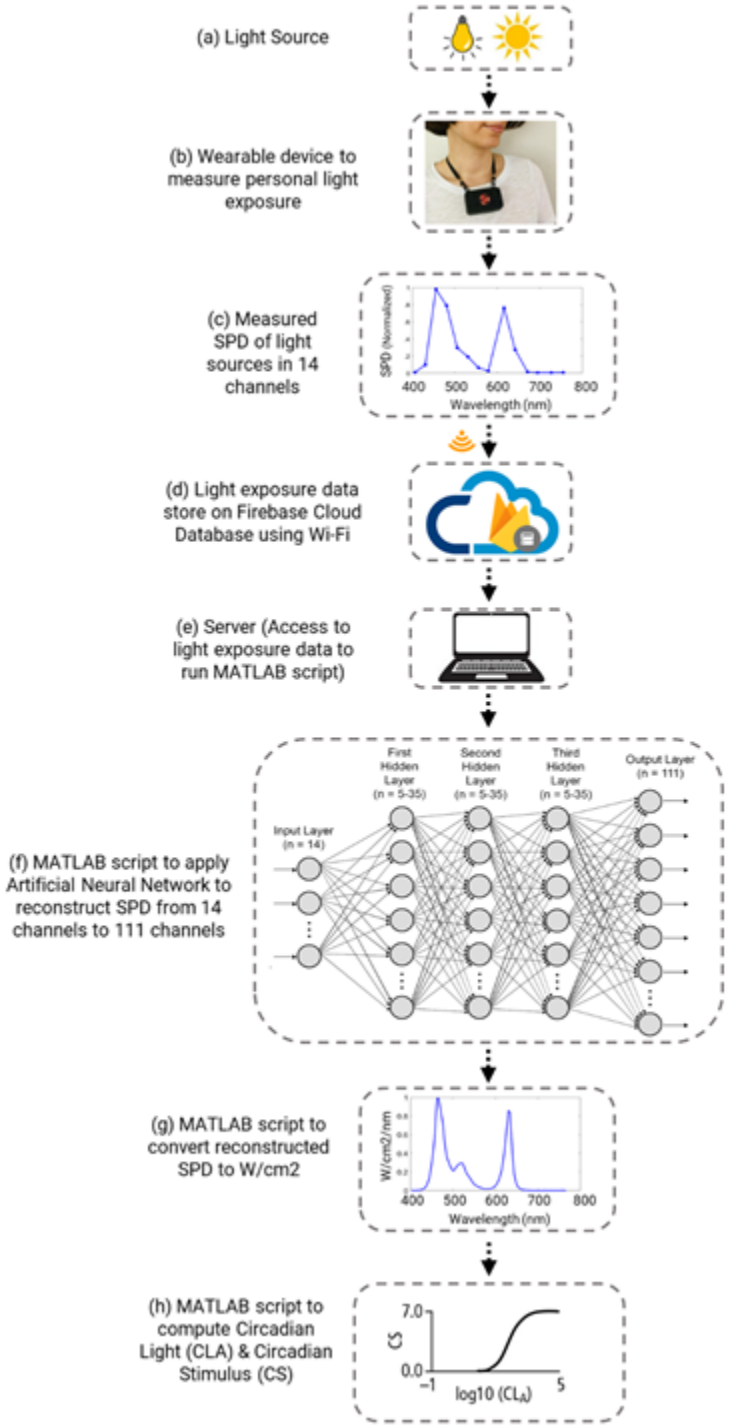

Figure 3.1: Procedure used for collection, processing, and analysis of data. (a) only daylight/electric light and mixed daylight/electric light used as light source, (b) wearable light measurement device used to measure complete spectral data at the individual level, (c) SPDs measured by a low-resolution spectral sensor in 14 channels, (d) SPDs stored on cloud database using Wi-Fi, (e) processed and analyzed collected SPDs on the server, (f) Using ANNs to reconstruct SPD, (g) reconstructed SPDs calculated in terms of W/cm2, and (h) CLA and CS calculated for two participants across the three-day study period.

(a) (b)

Figure 3.2: Example of home-office layout. a) plan shows where the subjects were seated, positions of computer monitors, LED smart bulb, locations, and view orientations of HDRI sensors, b) surrounding urban context.

furniture and luminaire; size, building orientation, blind condition of the window (as well as size, number, and the height of the monitors). The living room had a west-facing window with a fully closed blind during this study, and there was a small source of lighting coming from a TV that could be ignored. The bedroom had an east-facing window covered by a fully closed blind during the nighttime because this space was only used for sleep.

We chose Seattle as the cloudiest major US city in the lower 48 states [142]. On average, Seattle has 226 days (62% of days) with clouds covering more than three-quarters of the sky and 308 days (84% of days) with clouds covering over one-quarter of the sky in a year. Thus, with fewer sunny days, there is limited access to daylight as an ideal light source for the human circadian system. The length of the day varied significantly in Seattle for the year. Fig. 3.3 shows how the length of the day changes throughout the year in Seattle, WA. The present study was conducted between September 27 and August 4, when sunrise was about 07:00 and sunset was around 19:00, with total daylight of fewer than 12 hours. Two office workers (one

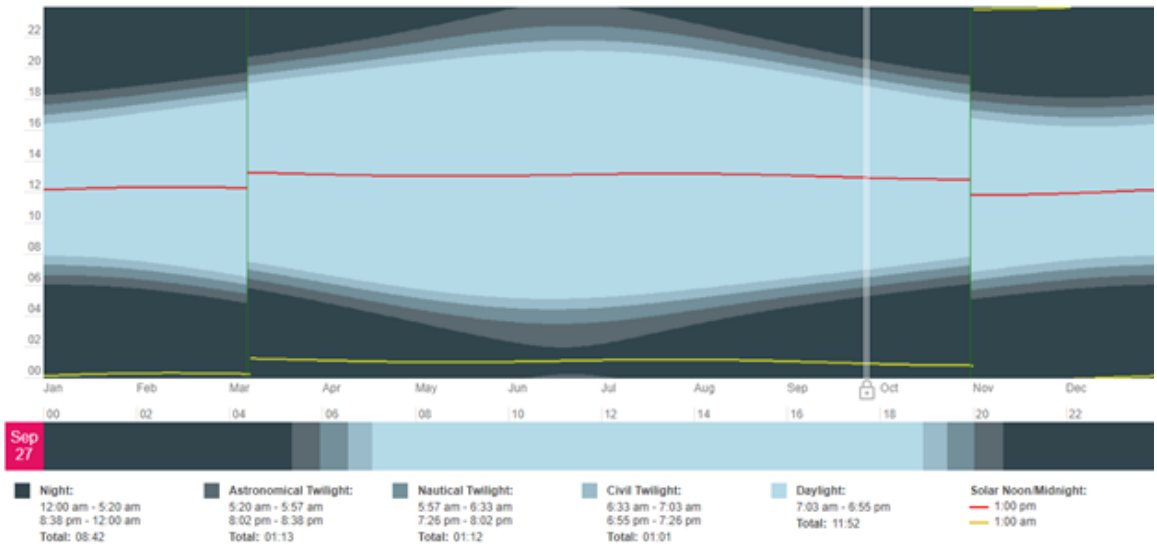

Figure 3.3: Sun graph shows the sunrise and sunset for September 27th, 2020, in Seattle, WA.

male: age 36 years and one female: age 36 years) volunteered for the study.

3.2.2 Wearable Lighting Measurement Device

We used a low-cost and wearable device with 14 channels that detect wavelengths within the visible spectrum with 20 FWHM to continuously measure Spectral Power Distributions (SPD) of light sources every 30 seconds. The device incorporates a CMOS-based sensor (AS7265x Smart Spectral Sensor, AMS AG, Austria) consisting of three sensors that detect wavelengths ranging from 410 to 760 nm. To validate the spectral sensitivity, accuracy, and linearity of the device, we calculated the calibration equations for fourteen channels according to simultaneous measurements with a calibrated spectrometer (Ocean Insight WaveGo light spectrum meter, UNC Charlotte, North Carolina, USA) using 106 different types of light sources including both daylight and artificial lighting to represent all possible lighting conditions. Utilizing Artificial Neural Networks enabled us to increase the resolution of the spectral sensor from over 20 nm to around 3.5 nm, which is close to the resolution of expensive commercial devices such as calibrated spectroradiometers.

3.2.3 Outdoor Context

We monitored the outdoor lighting conditions during the study period from 08:00 to 19:00 between September 27 and August 4. For this purpose, we employed two low-cost and programmable High Dynamic Range Image (HDRI) sensors consisting of Raspberry Pi microcomputers with fisheye cameras modules to provide the visual record of interior and exterior scenes at the working space. The HDR images collected from two sensors were used in the present study to compare any variations of outdoor lighting conditions during the entire period that the analysis was performed. As shown in Fig. 3.2, the two HDRI sensors were positioned on a vertical plane at 1.2 m above the floor to represent the view from seated eye height. The first HDRI sensor was placed at 1 m from the window with a window-facing view. The second one was attached to the window from outside to capture the exterior scene. A Python script was embedded in the Raspberry Pi to schedule the camera to capture a series of low dynamic range (LDR) images with different exposures value (EV), ranging from very dark (-3 EV) to very bright (+3 EV) for all three days from 08:00 to 19:00 at 15-minute intervals from window-facing view and exterior scene. It took about 50 s to capture a full set of LDR images at a given time interval. An open-source command-line software HDRgen was used to combine LDR images into an HDR image.

3.2.4 Lighting Interventions

We built a custom luminary for the study using one ilumi BR30 Bluetooth LED Smart bulb [143] inserted into a luminaire head on the ceiling of the working space to be only used during Day 7 and Day 8 of the study. A warm LED (2700 K) was used between Day 1 and Day 6 that was replaced with a new ilumi BR30 Bluetooth LED Smart bulb. The color temperature of this multicolor light source is adjustable from 2700 K to 6500 K, at nearly any brightness level. The Ilumi app automatically turned the light source on at 7 AM and turned it off at 11 PM between Day 7 and Day

8. An additional layer of control called “Circadian Experience” was used to improve the daily routine to schedule lighting brightness and color setting depending on the time per human circadian rhythm. The lighting automatically transitioned from a cool, energetic white (6500 K) morning to a relaxing, warm (2700 K) evening. The Circadian Experience was utilized to replicate the natural light cycle. The luminaire was placed in the middle of the working space to affect both participants equally.

3.2.5 Data Collection and Protocol

We provided the required materials and instructions to participants before the commencement of the study. We asked participants to wear the wearable spectrometer as a pendant (at chest height) for eight consecutive days during data collection periods. The device was attached to the participants'clothes at the left-hand side of the chest and measured light exposure at a similar view direction of the eye in the vertical plane (see Fig. 3.1(b)). We asked participants to keep the wearable device always uncovered. Each participant wore a device during waking hours and placed it next to their bed at the charging station during sleep. Participants had different working schedules as one started working at 7 AM (± 30 minutes) and the other one from 11 AM (± 30 minutes), but they went to bed at the same time (11 pm). To compare light-dark patterns between the two participants, we asked them to log their bedtimes, waketimes (waking hours), and working times (when they are behind the desk) during the data collection period. To evaluate the circadian efficacy of different indoor lighting conditions, we designed other lighting conditions for each day of the data collection period (see Fig. 3.4).

Fig. 3.4 shows the protocol designed for the present study. The study was performed over eight days. From Day 1 to Day 5, the participants had the freedom to close the blind if they experienced excessive direct sunlight entering from the window or open the blind if there was a need for more daylight in the working area. Additionally, the participants had the freedom to turn on/off a warm LED (2700 K) placed

Figure 3.4: The eight-day protocol for the study. Participants wore the wearable devices for all eight study days during waking hours and placed the device next to their bed during sleep. The blind was fully retracted during Day 6 and 8 but fully closed during Day 7. The lighting interventions were operational on Day 7 and Day 8.

in the middle of the room. During day 6, the blind was fully retracted, and electric light was kept off to record the lighting conditions in the working space entering from the West-facing window. During day 7, we turned on the ilumi BR30 Bluetooth LED Smart bulb in the working area and closed the blind to investigate the effects of lighting intervention. Finally, during day 8, the blind was fully retracted, and the ilumi BR30 Bluetooth LED Smart bulb was turned on to allow for both natural light and electric light in the working space.

3.2.6 Analysis of Measured SPD Data

We employed a mathematical model of human circadian phototransduction proposed by Rea et al. to calculate Circadian Light (CLA) and Circadian Stimulus (CS) for any spectral irradiance distribution [31, 144]. The CLA metric is the weighted irradiance of light incident at the cornea to reflect the spectral sensitivity of the human circadian system. Additionally, the CS metric is determined by how much melatonin is suppressed by nocturnal lighting after one-hour light exposure from threshold (CS = 0.1) to saturation (CS = 0.7) to reflect the absolute sensitivity of the circadian system [18]. We used MATLAB to analyze each SPD collected from the wearable device to calculate circadian light (CL) and circadian stimulus (CS). First, we converted the corneal SPD into CLA, and then, second, CLA is transformed into CS. CS metric was employed to quantify the effectiveness of corneal spectral power distribution to stimulate the human circadian system.

It should be noted that a new light measurement strategy is currently recommended to report corneal spectral irradiance in five illuminance quantities by calculating the effective irradiance for rhodopic, melanopic, cyanopic, chloropic, and erythropic independently [19]. However, currently, there is a lack of biological lighting metrics that utilize these five illuminance quantities to assess the lighting conditions in indoor environments. Therefore, we reported the results in units of CS, as the WELL Building Standard recently recommended this unit of analysis [20].

We analyzed the data collected from the wearable device to compare the total light exposure among all eight days for both participants. As we only altered the lighting conditions in the working space, we analyzed the collected data based on the time participants spent in this space (working hours) to better understand the circadian effectiveness of different lighting conditions. Moreover, we analyzed the data from the wearable device to assess the total light exposure during both working hours and the total light exposure during waking hours for each participant. We calculated the total light exposure during both working hours and waking hours based on the times participants reported being at the working space and being awake, respectively. Additionally, we went one step further to analyze the light exposure on an hourly basis during both working hours and waking hours and for different parts of a day, which included Morning (0600-1200), Afternoon (1200 - 1700), Evening (1700 - 2000), and Night (2000 - 0600). This helped us to better understand the circadian stimulus potential of light for each participant during their waking and working hours within different hours and different parts of the day. It is important to note that each participant has a different schedule, so each participant's working hours and waking hours differ from that of the other.

3.2.7 Statistical Analysis

Statistical analysis was performed with SPSS Version 27. statistical software package (IBM, Armonk, NY, USA). A one-way ANOVA was conducted on light exposure

data with the factors "days" (eight days: day 1, day 2, day 3, day 4, day 5, day 6, day 7, and day 8) to determine the effects of the light intervention across the eight-days study period. Tukey′s post hoc analysis was further applied to compare the significant main effects and interactions of attributes where significant differences were found in ANOVA. A two-way ANOVA was conducted to explore how the participants schedule (3 states: sleep, waking, and working) and daytime periods (4 parts: 6 a.m−12 p.m. = morning, 12 p.m−5 p.m. = afternoon, 5 p.m−8 p.m. = evening, and 8 p.m−6 a.m. = night) affect light exposure (CS) throughout the study. Results were considered to be statistically significant when $p < 0.05$.

3.3 Results

3.3.1 Monitoring the Variations of Outdoor Lighting Conditions

As shown in Fig. 3.5, we monitored the outdoor lighting conditions by utilizing two low-cost and programmable High Dynamic Range Image (HDRI) sensors consisting of Raspberry Pi microcomputers with a 5-megapixel fisheye lens with a 180-degree field of view (FOV) to provide the visual record of interior and exterior scenes at the working space. We applied a false-color luminance mapping on each HDR to visualize the luminance distribution of the window-facing view and external setting and monitor any variations of outdoor lighting conditions during the study period from 08:00 to 19:00 between September 27 and August 4. A comparison between Day 1 and Day 8 of exterior scenes (Fig. 3.5(b)) shows that outdoor lighting conditions were almost the same among all eight days with a clear sky and no cloud cover.

For the window-facing view of the interior scenes, Fig. 3.5(a) shows a significant decrease in window light exposures during Day 7 compared to Days 6 and 8, as the blind was fully closed for the entire day. Closer inspection of Fig. 3.5(a) shows that the participants closed the blind mainly during the afternoon between Day 1 and Day 5 to reduce the excessive sunlight entering the window. During Day 6 and Day 8, the blind was fully retracted for the entire day.

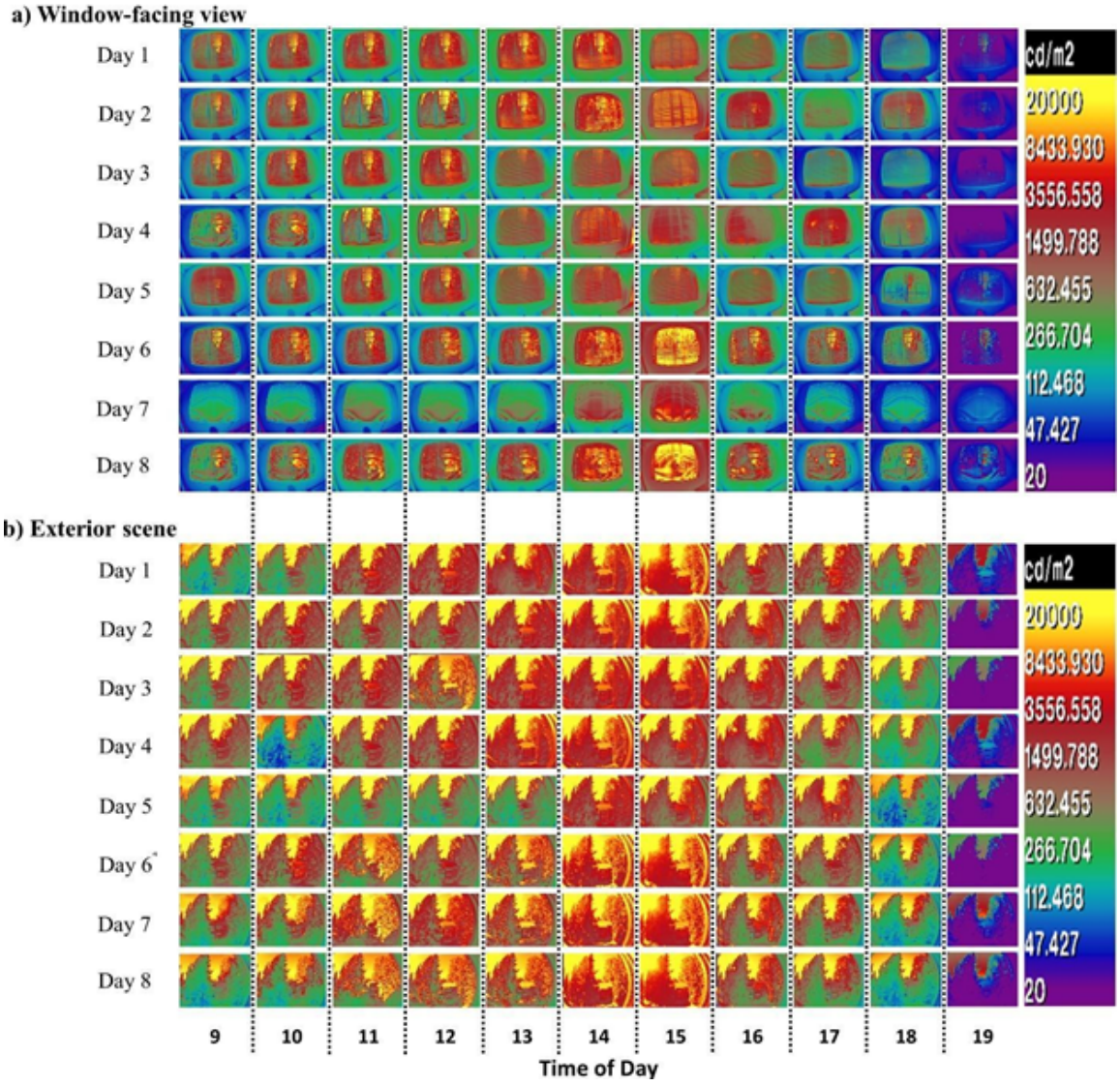

Figure 3.5: False Color luminance mapping of a) window-facing views and b) exterior scenes from 09:00 to 19:00 between Day 1 and Day 8.

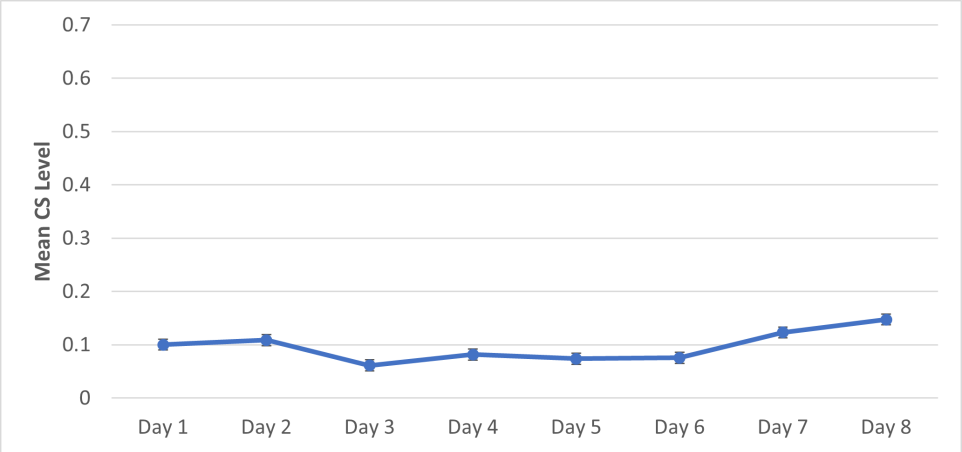

Figure 3.6: Mean CS values measured for an entire day for each study day. The error bars represent the standard error of the mean.

3.3.2 Exploring the Circadian Effectiveness of Various Lighting Conditions

Circadian stimulus (CS) was estimated by analyzing SPD collected from the wearable device worn by the participants. Fig. 3.6, Fig. 3.7, and Fig. 3.8 summarize the outcomes in terms of the mean CS level over the eight-day study period grouped into the entire day, working and waking hours, and daytime periods. As expected, the one-way ANOVA revealed significant differences in CS values for the study days, $F(7, 43261)=163.665$, $p<0.001$. Post-hoc analysis using the Tukey HSD model show significant ($p<0.001$) difference in mean CS levels between two intervention days (Day 7 ($M = 0.12$, $SD = 0.19$), and Day 8 ($M = 0.14$, $SD = 0.21$)) and the first six days.

Fig. 3.6 shows two intervention days (Day 7 and Day 8) had the highest CS value compared with other study days. As shown in Fig. 3.7, the mean CS level dramatically increased from Day 6 to Day 8 during waking and working hours. For different daytime periods, there is a surge in mean CS level from Day 6 to Day 8 during morning and evening, except for afternoon as there was a slight decrease from $CS = 0.31$ to $CS = 0.3$ between Day 7 and Day 8, respectively (Fig. 3.8).

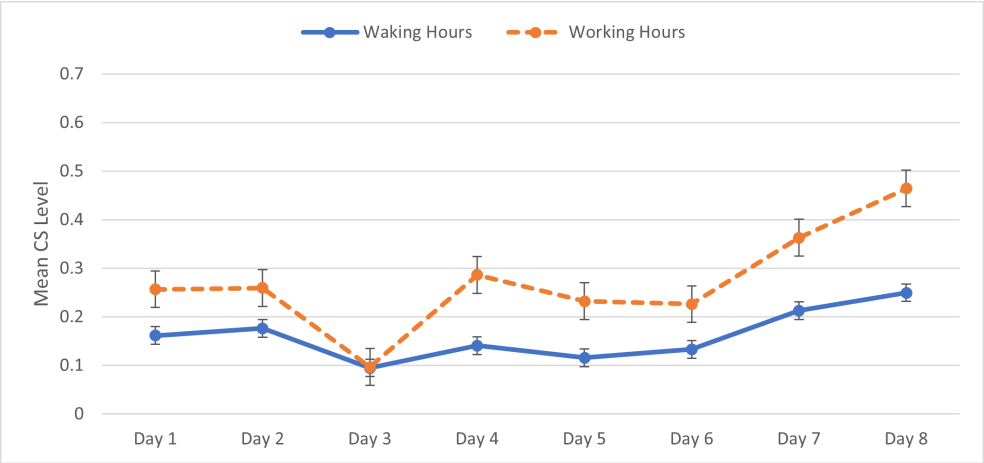

Figure 3.7: Mean CS values measured during working hours and waking hours for each study day. The error bars represent the standard error of the mean.

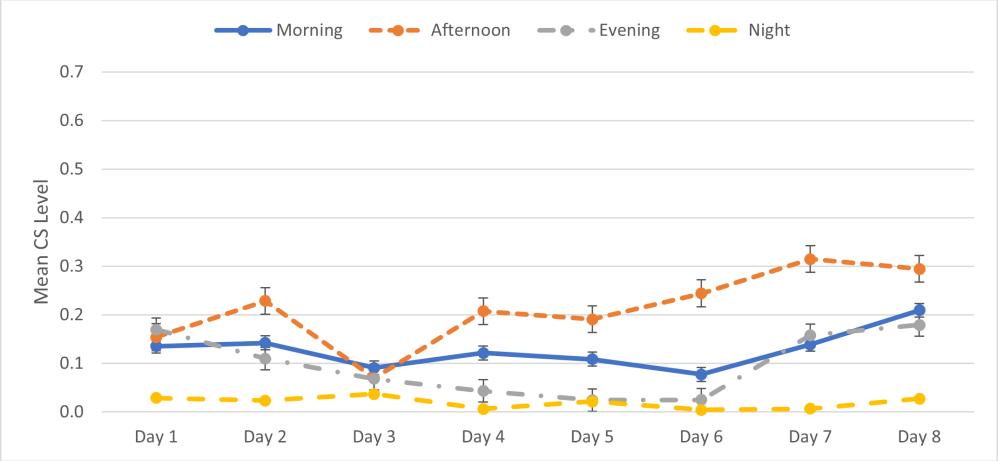

Figure 3.8: Mean CS values measured during different daytime periods for each study day. The error bars represent the standard error of the mean.

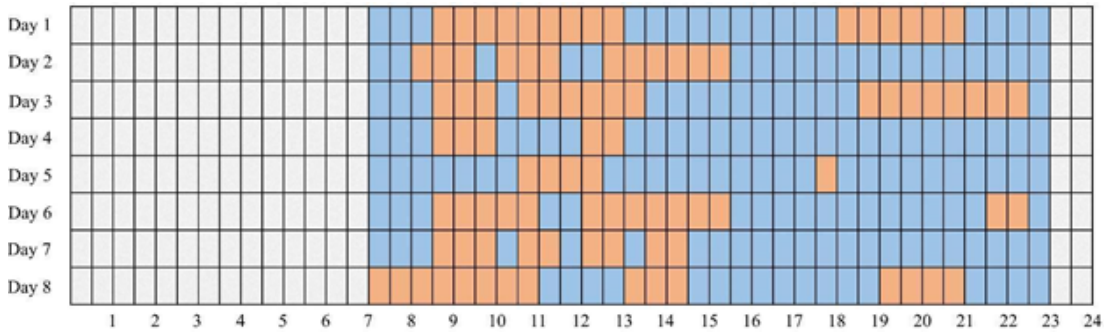

(a) Participant 1

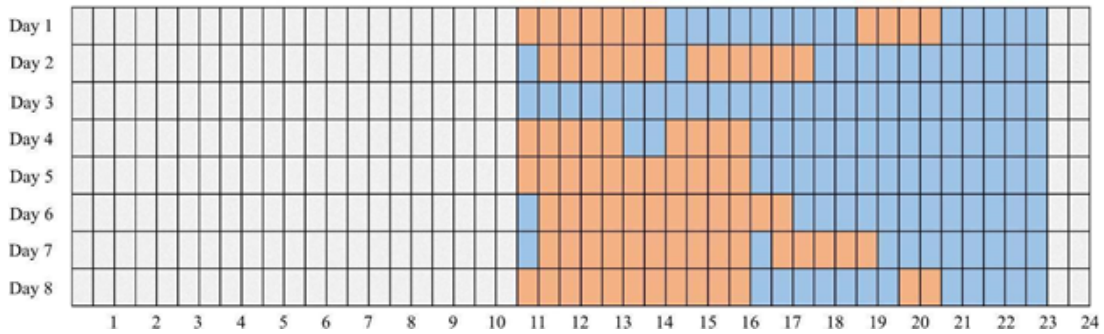

(b) Participant 2

Figure 3.9: Participant profiles and their daily schedule and locations for all eight-day study periods. Orange, blue, and grey cubes indicate each participant's hours working, waking, and sleeping, respectively.

3.3.3 Exploring Personal Lighting Conditions per Individual

Fig. 3.9 presents the daily schedule of both office workers for all eight-day study periods. Each participant self-reported their daily schedules and locations during the entire study period. Participants had different sleep-wake schedules (blue and grey cubes) and working schedules (orange cubes). As shown in Fig. 3.9, the average reported duration of working hours was 345 minutes (SD = 140) and 315 minutes (SD = 138) for participant 1 and participant 2, respectively. The sleep-wake schedule of each participant was different from one another. The average reported duration of waking hours was 960 minutes (SD = 30) and 720 minutes (SD = 50) for participant 1 and participant 2, respectively. In general, participant 2 had a longer sleep duration by approximately 12 hours compared with 8 hours for participant 1. It should be noted that participant 2 was not presented in the working area during Day 3.

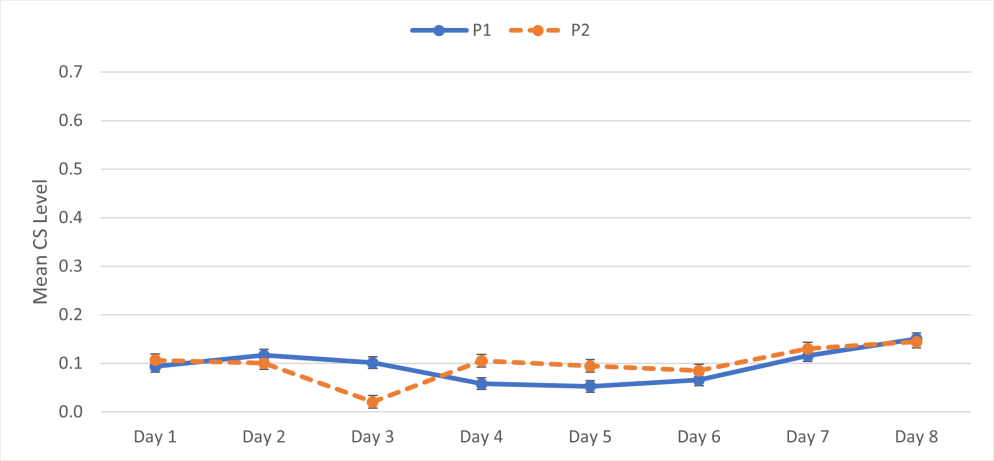

Figure 3.10: Mean CS values measured at the chest of each participant for an entire day. The error bars represent the standard error of the mean.

Fig. 3.9−Fig. 3.12 can be used to understand the significant impact of individual differences between participants on measured light exposure data reported in units of CS. Fig. 3.10, Fig. 3.11, and Fig. 3.12 compared the measured levels of CS between two participants during each study day, waking hours, and only working hours for the study. The two-way ANOVA revealed significant main effects of the participant's schedule, $F(2, 43130)=4697.851$, $p<0.001$. The mean CS level increased from Day 6 to Day 8 for both participants. Fig. 3.12 shows mean CS values during working hours were significantly higher for participant 2 during all study periods ($CS > 0.3$), except Day 3, compared with participant 1.

Fig. 3.13 presents the mean CS level for four different daytime periods acquired by taking light exposure data of each participant throughout the study. There was a significant main effect of daytime periods, $F(3, 43130)=203.431$, $p<0.001$. For participant 1, the mean CS level decreased from morning to night during all three study days. For participant 2, the mean CS level increased between morning and afternoon, followed by a decrease towards the night during all eight-study days, except for an unexpected surge on mean CS level during the evening on Day 7. Except a slight increase between afternoon and evening on Day 1 and Day 8 and an unexpected

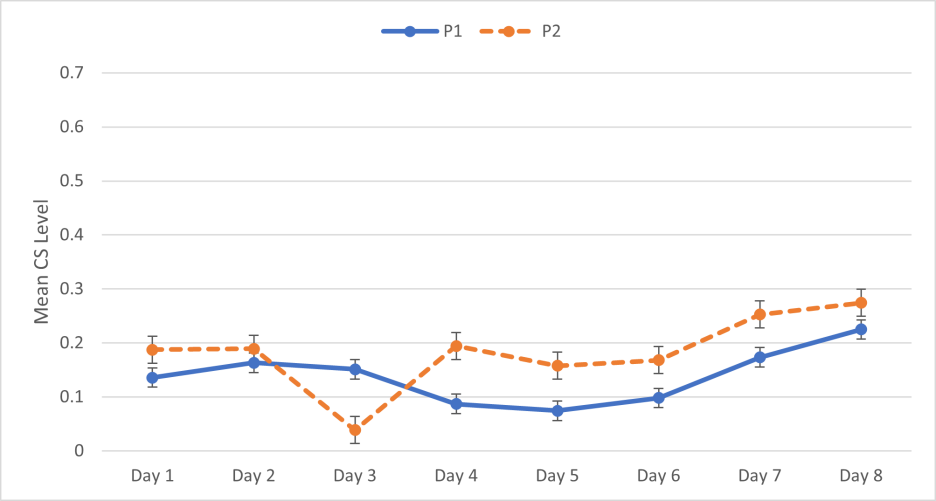

Figure 3.11: Mean CS values measured at the chest of each participant during waking hours. The error bars represent the standard error of the mean.

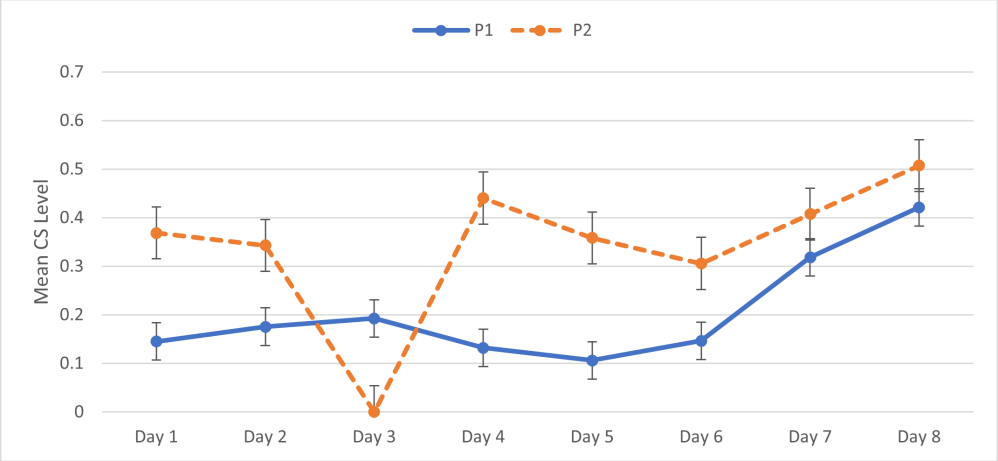

Figure 3.12: Mean CS values measured at the chest of each participant during only working hours. The error bars represent the standard error of the mean.

increase from morning to afternoon on Day 5.

3.4 Discussion and Conclusions

This research assessed the practical applicability of an affordable and wearable spectrometer in the context of aiding individuals to have healthier living with relation to light. In this study, the circadian effectiveness of light was measured in terms of CS across the eight-day study period. Previous studies showed that the office workers who received CS ≤ 0.15 in the morning had difficulty sleeping at night with higher levels of depression compared to those who received CS ≥ 0.3 in the morning [7, 8]. Hence, in the present study, CS ≥ 0.3 is considered a high circadian-effective light level that reduces sleepiness and improves energy and alertness in office workers. It should be noted that each participant used the same wearable device on each day of the study.

We evaluated the circadian effectiveness of lighting during a two-day intervention (Day 7 and Day 8) following the baseline between Day 1 and Day 6 for two office workers. The findings show a significant difference between the first six days and Days 7 and 8 in terms of CS value that indicated the potential of utilizing dynamic electric lighting in combination with daylight to impact the circadian stimulus potential of indoor lighting significantly. As expected, participants were exposed to higher amounts of circadian-effective light during working hours compared to waking hours (Fig. 3.7). CS values during waking hours for the two intervention days were above 0.2 (see Fig. 3.7). We found that the two office workers received high circadian-effective light levels (CS ≥ 0.3) while at work (during working hours) on intervention Day 7 and Day 8 compared to baseline days (Fig. 3.7). The average CS value for both participants was 0.37 on Day 7, followed by a considerable increase to 0.45 on Day 8. Increasing circadian stimulation during Day 8 was because of access to a mixture of daylight and electric light compared to Day 7, where electric light was the only source of lighting. The importance of daylight and its impact on improving the level

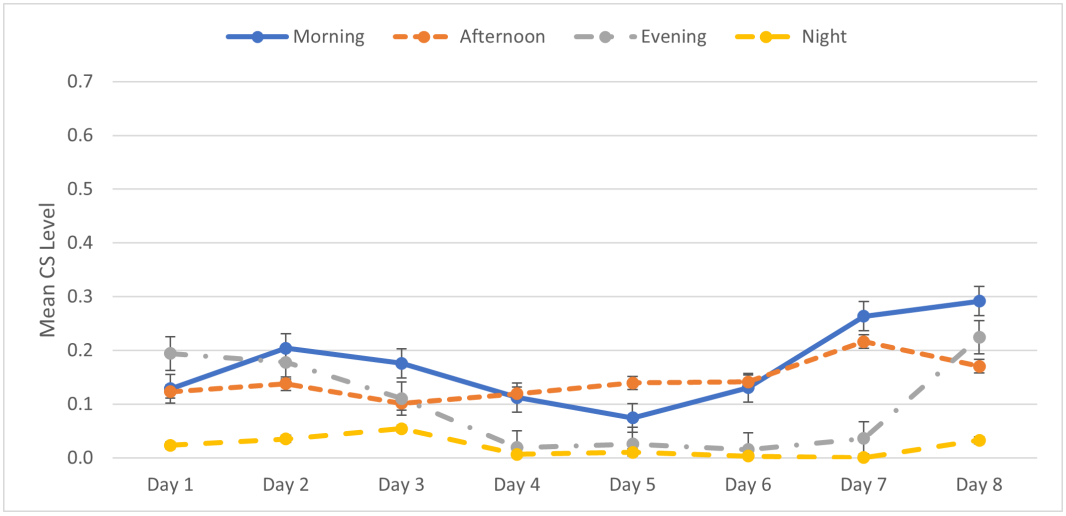

(a) Participant 1

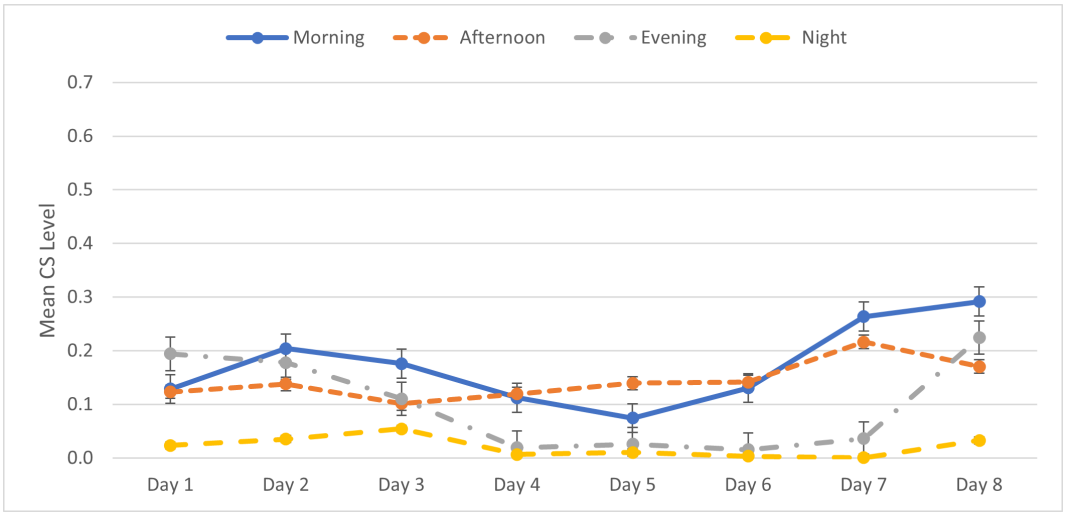

(b) Participant 2

Figure 3.13: Mean CS values measured at the chest during different daytime periods for a) participant 1 and b) participant 2. The error bars represent the standard error of the mean.

of circadian-effective light in indoor spaces is comparable to the studies presented by Konis et al. [39] and Boubekri et al. [145]. They showed the benefits of daylit spaces in comparison with windowless environments regarding increasing circadian stimulation. Participants were exposed to a significantly higher amount of circadian-effective light in the afternoon for most of the study days compared to other daytime periods (Fig. 3.8). The mean CS value increases during the afternoon can be explained by the more significant proportion of time that both participants spent at their working space with higher circadian-effective light levels than other spaces such as the living room and bedroom (see Fig. 3.9).

Even though we performed this study in summer 2020 and we only have two participants doing the same job tasks in the exact location, we still found large individual differences between the two participants in their lighting conditions. These differences between the personal lighting conditions of two participants may be explained by mixed physiological/behavioral differences and workspace characteristics such as different wake/sleep patterns, work schedules, and distance to the window. As mentioned in section 2.1, the variation between workspace characteristics was minimized for both participants. Variations as siting orientation, amount and placement of furniture and luminaire, size of the building, building orientation, blinds and condition of window coverings, and the size, number, and height of the monitors were similar for both participants.

Even though the study was performed on sunny days during the summer season, both office workers were generally exposed to low circadian-effective light levels (CS $\leq$ 0.3) during waking hours (Fig. 3.11). We can speculate on a few reasons why the measured amount of circadian light for both participants for the entire day (Fig. 3.6) and during waking hours (Fig. 3.7) on all eight study days was low. One is due to the building design, a narrow facade, and a small window-to-wall ratio that had been poorly designed to provide enough daylight availability in the space (Fig. 3.3).

Another is due to the building orientation, as the West-facing window had only about two hours of direct sunlight (Fig. 3.5). In contrast, the East-facing window did not provide enough daylight availability for even the bedroom during the daytime period. The third reason would be the lack of enough number, placement, intensity, and spectrum of electric lighting installed in the building where less daylight is available.

As expected, distance from the West-side window at the working space was associated with a difference in participants' lighting conditions. Except for Day 3, the average CS values during working hours for participant 2 were above 0.3 (Fig. 3.12). In contrast, for participant 1, the average CS value during working hours was above 0.3 only on two intervention days (Day 7 and Day 8). As shown in Fig. 3.12, a 2-meter increasing distance to the West-facing window resulted in a significant increase in the mean CS level between Day 6 and Day 8 when daylight was the source of light for the working space. The CS level reduces for an increasing distance can be explained by the limited penetration depths of daylight in a room [146]. These results are consistent with previous studies showing distance-to-window has a significant impact on the personal lighting conditions [43], particularly the amount of circadian-effective light that participants were exposed to during daytime [66]. These findings highlight the importance of considering the impact of distance to the window when measuring the personal lighting conditions within daylit spaces.

The difference in personal lighting conditions between the two participants was also found and can be impacted by changing the office workers'sleep-wake schedules and working schedules. As mentioned in section 2.6, the working hours and waking hours were calculated based on the amount of time each participant spent at the working space and being awake, respectively. Although participant 2 woke up about 4 hours later than participant 1, the percentage of time spent at the working space was much higher compared to participant 1 (Fig. 3.9). Participant 2 received a higher amount of circadian-effective light in the afternoon than other daytime periods during

all eight-day study periods, except Day 3 when participant 2 was not present in the working area for the entire day (Fig. 3.13). However, participant 1 was exposed to the highest level of circadian-effective light in the morning for intervention on Day 7 and Day8.

Additionally, a low CS level on Day 4 and Day 5 compared with other study days for participant 1 can be explained by the lower number of working hours during these days (see Fig. 3.9). Similarly, for participant 2, a considerable decrease in CS level on Day 3 resulted from a significant reduction in the number of working hours. Future research is recommended to include a more substantial number of participants with different age groups, jobs, cultures, and genders to explore a complete set of factors to better understand the actual lighting conditions at the individual level.

The present study is the first to employ a low-cost and wearable spectrometer that allows us to measure light source′s SPDs in real-time and store personal light exposure data on an external Firebase cloud database using wireless communication. The concept of a "personalized smart lighting system" can be deployed by continuously monitoring individual lighting conditions in real-time using the spectrometer prototype developed in this study and controlling these lighting conditions by utilizing an IoT-based intelligent lighting system.

3.4.1 Limitations of the study

Firstly, due to the impact of the COVID pandemic, we had a limited number of participants in this study. The small sample size does not allow us to investigate the inter-individual differences in response to light exposure between larger populations with different ages, genders, and jobs. Physiological, genetic, behavioral, and cultural differences may cause different biological reactions even under the same lighting conditions.

Finally, this study was performed in the summer, and the specific weather conditions with much longer daylight hours per day may vary when compared with win-

tertime. The previous studies demonstrated that the average lighting conditions are lower in winter and autumn compared with summer [65 – 67]. This may have caused the level of circadian-effective light to be considerably higher during the summer compared to other seasons.

3.4.2 Future research directions

Future research needs to consider four aspects. First, it is recommended to include a larger number of participants with different age groups, jobs, cultures, and genders to explore a complete set of factors to better understand the actual lighting conditions at the individual level. Secondly, additional research is needed to evaluate the personal lighting conditions in other space types with different light settings, such as hospitals and residential spaces. It will help us better understand the circadian effectiveness of indoor lighting within a broad range of building types and populations. Thirdly, as briefly mentioned in section 3.4.1, "limitations of the study", the inclusion of different seasons and even other locations for recording personal lighting conditions may result in more robust recommendations to enhance the level of circadian-effective light in indoor spaces. Therefore, additional research is needed to repeat this study in winter/autumn conditions and the south/near the equator. And fourth, further research is required to explore the personal lighting conditions in buildings using similar IoT-based wearable devices equipped with wireless communication to be integrated with intelligent lighting systems to adjust the spectrum and intensity according to individual needs and desires in real-time.

CHAPTER 4: USER-CENTERED APPROACH TO BUILDING AN INTERACTIVE DASHBOARD FOR ASSESSING THE CIRCADIAN EFFECTIVENESS OF LIGHT: DEVELOPMENT AND USABILITY STUDY

4.1 Introduction

Light affects human health, well-being, and performance through the visual and circadian systems. The suitable types of light with the right spectral content at the correct times can support the 24 hours of human circadian rhythms. In turn, light exposure with the right spectral content at the wrong times can disrupt human circadian rhythms. For example, lack of natural light in winter and long daylight hours in summer in Canada and Northern Europe is associated with a mismatch between sleep/wake schedules that disrupt circadian rhythms [147]. Disruption of circadian rhythm may result in mood disorders, displacement of sleep/wake cycle, melatonin suppression, phase-shifting of the circadian system, and lead to a range of health issues such as depression, diabetes, seasonal affective disorder, and even cancer [10–13, 148].

Since 2002, by growing interest in the link between light and health, tools, and methods for measuring light exposure have been shifted from vision-related quantities (e.g., lux) to those considering the spectral composition of light radiation. To address humans' biological needs for light, the effect of light exposure on the circadian system should be calculated by considering the output of all three types of retinal photoreceptors: rods, cones, and ipRGCs, in the human eye [32, 149]. Recently, a metric called Circadian Stimulus (CS) was proposed by the Lighting Research Center (LRC) [31] to evaluate the circadian-effectiveness of light sources. The WELL standard suggests exposure to a CS of 0.3 or higher at the eye for at least the hours

between 9:00 AM and 1:00 PM [20]. CS considers both spectrum and intensity of light source and ties to all three types of retinal photoreceptors. Despite the significant effect of light exposure on the circadian system, there is still a lack of practical tools to measure and deliver the CS to non-expert end-users as an easy-to-understand outcome. Individuals who are exposed to irregular patterns of light and darkness such as office workers and nurses receive less natural light during daytime hours and more artificial light during nighttime hours, which lead to lower productivity, lower physical and psychological well-being, and a higher risk of accidents and errors [150, 151]. Technologies such as web-based and mobile apps have a great potential to engage individuals in their health care by supporting real-time personalized health monitoring and promoting healthy behavior change [152–154]. Our study developed an interactive dashboard specifically for these groups to manage and track their lighting conditions data.

This study is the second step of a larger project to develop a novel connected support technology, including a low-cost and wearable spectrometer and an interactive dashboard to help people live healthier with light. The main objective of the present study is to develop an interactive dashboard through a user-centric approach by engaging the end-user directly throughout the entire process, from needs finding to usability testing of medium- and high-fidelity prototypes.

4.2 Materials and Methods

4.2.1 System and Details

We developed a novel human-centric lighting assist tool including a low-cost and wearable spectrometer and an interactive dashboard to enable individuals to continuously track and monitor their lighting conditions throughout a 24-hour day (Fig. 4.1). Past studies describe the fabrication challenges, calibration, and validation of the wearable spectrometer. The interactive dashboard aims to provide non-expert users with meaningful and easy-to-understand quantities on how much circadian-

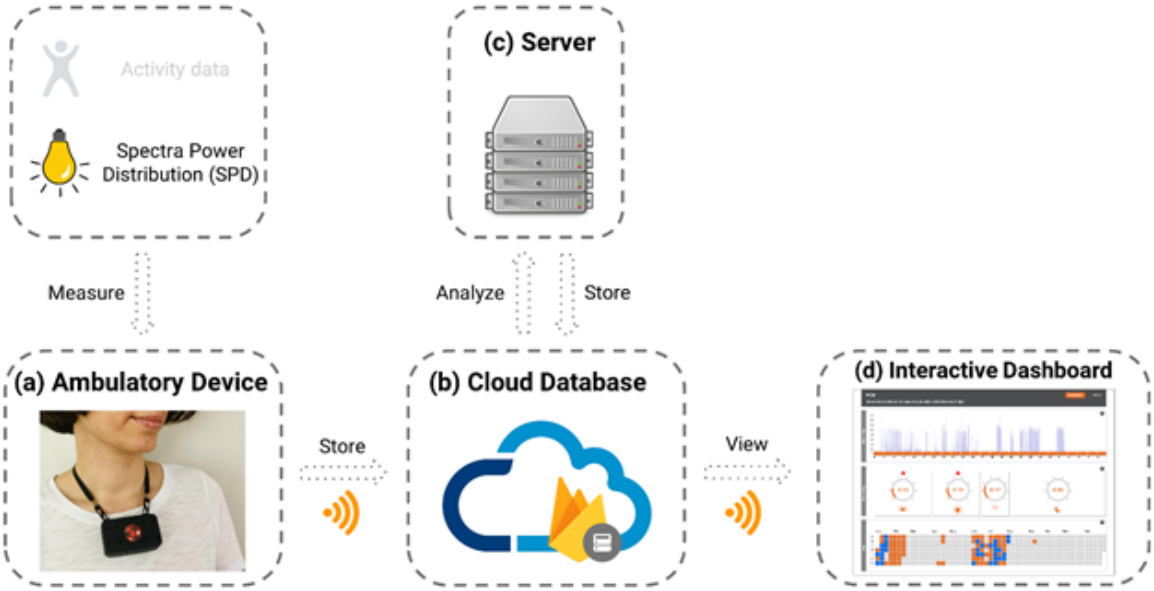

Figure 4.1: The proposed human-centric lighting assist tool includes a) a low-cost and wearable spectrometer to record SPD, b) a cloud database to store collected SPD, c) a server to analyze data, and d) an interactive dashboard to visualize the data in meaningful and easy to understand quantities.

effective lighting they receive, together with improving indoor lighting systems into proper human-centric lighting. The interactive dashboard allows the users to explore the effect of circadian-effective lighting within three different time frames: (1) the yearly and monthly time frame includes the holistic overview of the average CS for each day of the recent or previous years (2) Hourly time frame includes the average CS for every hour of the specific day, and (3) the part-of-day time frame includes the average CS during the morning, evening, afternoon, and night. In addition, if individuals' everyday life is not aligned with their circadian rhythms, the app provides tips and/or live updates as a state of emergency for enhancing an individual's lighting conditions. The high (good) and low (poor) circadian effectiveness of light are shown by different colors. The same color codes are used for different time frames to increase consistency throughout the application. Information such as the definition of CS and the app's purpose can be found on the "About" page.

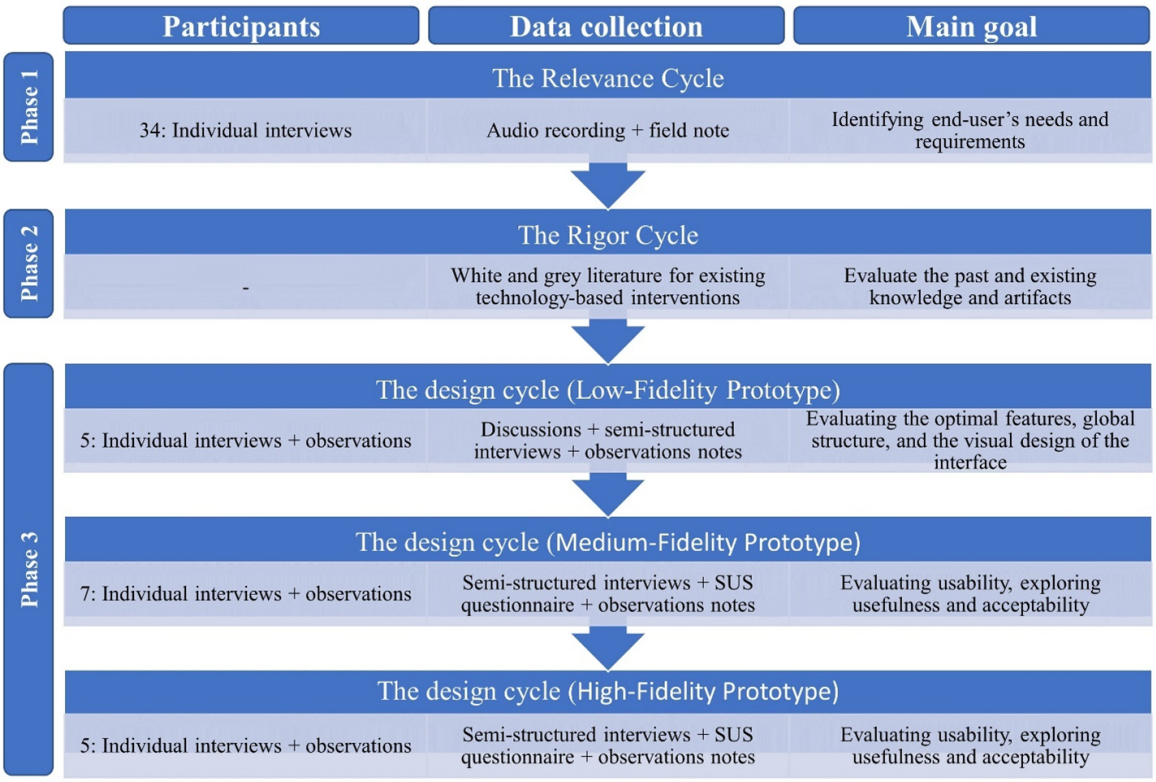

Figure 4.2: Study overview.

4.2.2 Study Design

We implemented a user−centered approach guided by Information System Research (ISR) framework to develop a functional interactive dashboard through a three−phase iterative process (Fig. 4.2) [155, 156]. We engaged the end−user directly throughout the process of design and development of the interactive dashboard to provide the most beneficial outcome [157]. We performed a three−cycle iterative user−centered approach spread over 20 months consisting of relevance, rigor, and design cycles. During the relevance cycle, we identified the end-user's needs and requirements through a series of interviews with various stakeholders. We evaluated the past and existing knowledge and artifacts during the rigor cycle to ensure the interactive dashboard innovation. Finally, during the design cycle, we developed and assessed low−, medium−, and high−fidelity prototypes of the interactive dashboard to enhance the design and increase its acceptance likelihood.

4.2.3 Phase 1: the Relevance Cycle

The goal of phase 1 was to identify the end user's needs and requirements. We conducted a series of in-person interviews with intended end-users. Inclusion criteria included: (1) non-expert users such as office workers who spend most of their time indoors and are exposed to less natural light during daytime hours and more artificial light during nighttime hours; and (2) expert users who improve the indoor lighting conditions such as lighting designers. Exclusion criteria included: those who spend a large proportion of their time working outdoors under natural light.

We conducted 34 semi-structured interviews between June and August 2019 with 15 office workers and 19 lighting designers ages between 31 and 60 years to determine the interactive dashboard's desired functional and design requirements. All interviews were audio-recorded and transcribed. The duration of each interview was between 20 and 60 minutes.

4.2.4 Phase 2: the Rigor Cycle

The goal of phase 2 was to evaluate the past and existing knowledge and artifacts to ensure the interactive dashboard innovation. We reviewed both white and grey literature for existing artifacts, including web-based and mobile apps with the functional specifications and systems qualities drawn from the relevance cycle. We searched for artifacts designed to evaluate the effects of light on human health, specifically on the circadian system.

4.2.5 Phase 3: the Design Cycle

Phase 3 comprises two stages: Develop/Build and Evaluate. For the first stage, we developed a low-fidelity prototype using findings from interviews with intended end-users during phase 1 to evaluate the optimal features, global structure, and visual design of the interface. We performed two usability tests for the second stage using the medium- and high-fidelity prototypes to evaluate the developed prototypes'usability,

usefulness, and acceptability. During the design cycle and through an iterative process, we applied the lesson learned from participants'feedback and literature review from the previous phases to improve the design and increase the likelihood of the proposed app acceptance. We performed three iterative studies with low-, medium-, and high-fidelity prototypes explained in detail in the following sections (Fig. 4.2). For each iteration, we recruited 5 participants, which is typical sample size for usability studies to acquire the majority of usability issues [158, 159]. We collected usability data both qualitatively and quantitatively using questionnaires, observations, and individual interviews. All interviews were conducted remotely. Each session was video-recorded using the Zoom video conferencing platform and lasted less than 45 minutes.

4.2.5.1 Develop/Build: Low-Fidelity Prototype

The goal of the develop/build stage was to identify the global structure, optimal features, and the visual design of the interface and acceptability of the proposed app. We incorporated the output drawn from relevance and rigor cycles, including a list of functional requirements and features based on analyzing interviews, reviewing the literature, and identifying the existing web-based and/or mobile apps. Before designing the low-fidelity prototype, several paper-based prototypes were created based on the need's analysis (interviews with end-users) and literature review to define the potential functions and features included in the proposed app. We designed a low-fidelity prototype of the interactive dashboard in Figma [160]. Five participants were recruited in March 2020 from previous participants in the relevance cycle.

At the beginning of the interview, we provided a brief introduction and the project's goal for each participant. Then, we shared our screen with participants through Zoom to show the low-fidelity prototype. We discussed the functions and features that could be included in the interactive dashboard. The participants shared their ideas on the information, content, and features presented in the low-fidelity app. During

the discussion, we asked probing questions to stimulate discussion, such as "What would improve some of the current features that are presented in the prototype?" and "What information do you need from a web-based app related to quality and quantity of light you receive throughout a 24-hour day?".

At the end of each interview, we reviewed all the transcripts, notes, and observations obtained from the interviews. We used the AI software program named Otter.ai [161] to transcribe the recording of the interview. This software provided accurate speech-to-text along with metadata such as the date and time stamps. Using a low-fidelity prototype immensely helped us explore our end-users needs and desires related to functional content and features of the interactive dashboard. The finding from the develop/build phase provided information for further refinement of the prototype in terms of the interface's visual design and functional requirements.

4.2.5.2 Evaluate: Usability Testing

The goal of the evaluation stage was to evaluate usability and explore the usefulness and acceptability of the proposed app. We conducted two usability testing using medium- and high-fidelity prototypes to assess the usefulness and acceptability of the proposed app. Similar to phase 1, we designed the medium- and high-fidelity prototypes in Figma.

We conducted the usability testing using Zoom and asked participants to share their screens to observe their interaction with the prototype. We prompted participants to "think-aloud" their thoughts during each interview as much as possible while working through the prototype. Each interview was video-recorded and lasted for about 45 minutes. Each participant completed the System Usability Scale (SUS) at the end of the session. SUS was one of the most frequently used, validated, easy to interpret, and reliable with small sample sizes instruments for assessing subjective usability [162–167].

All interviews were transcribed, coded, and analyzed for generalizable themes. We

used Excel for descriptive quantitative analysis of participant characteristics and the SUS scores. We analyzed qualitative data using a content analysis approach to identify usability issues and navigation problems to create themes [[168]. Additionally, we used a rainbow spreadsheet proposed by Tomer Sharon [169, 170] to analyze interview transcripts and observation notes. We coded participants' statements and comments from transcribed recordings. To identify themes, we coded all participant comments under six categories: visibility, navigation, aesthetic, understandability, usefulness, workflow, and content. In the following sections, the process of usability testing using medium- and high-fidelity prototypes is explained in detail.

4.2.5.2.1 Medium-Fidelity Prototype

We conducted usability testing using a medium-fidelity prototype. We performed two types of usability assessments in February 2021: (1) expert review of the prototype using 2 participants who have experience in the field of User Interface (UI) design and human-computer interaction and (2) end-users usability testing with two office workers and three lighting designers. The procedure included a semi-structured interview with each participant as follows: (1) brief introduction of the project and goal of testing; (2) asking five open-ended warm-up questions; (3) describing the full functionality of the medium-fidelity app; (4) providing six tasks and observing participant's interaction using the prototype; (5) asking follow-up questions after completing each task; (6) filling the SUS questionnaire. According to Bangor's adjective rating scale, a product is qualified as a "good product" when a SUS score is above 70 (acceptable) [162, 163].

4.2.5.2.2 High-fidelity prototype

We designed a high-fidelity prototype incorporating the usability issues evaluated from the previous usability test to improve the functionality and user interface of the prototype. To test the usability of the high-fidelity prototype, we performed

the remote usability testing with five intended end-users (2 office workers and three lighting designers) during June 2021 who did not participate in the previous sessions. We used the same six-steps usability testing procedures (section 4.2.5.2.1) to conduct a semi-structured interview with each end-user. Interviews were video-recorded. We took observation notes during each session. The analysis was based on transcriptions, observation notes, and the SUS questionnaire.

4.3 Results

4.3.1 Population Descriptive Statistics

We had 51 participants aged between 31-60. Thirty-four participants in phase 1 (between June and August 2019) identified the end-user's needs and requirements of the proposed app. For phase 3, we recruited 15 eligible participants between March 2020 and June 2021. Of those, 5 participants evaluated the low-fidelity prototype in terms of global structure and the interface's visual design, 5 tested the usability of the medium-fidelity prototype, and 5 assessed the usability and explored the usefulness and acceptability of the high-fidelity prototype. Additionally, two expert reviewers evaluated the medium-fidelity prototype. Table 4.1 shows the participants'characteristics.

Table 4.1: Sociodemographic characteristics of the participants (n=51).

Number and types of participants at each phase	(n)	(%)
Subgroup		
Lighting designer	27	52.9
Office worker	22	43.1
Expert reviewer	2	3.9
Gender		
Female	23	45
Male	28	55
Phase 1		
Lighting designer	19	56
Office worker	15	44
Phase 3		
Low-fidelity prototype		
Lighting designer	3	17.6
Office worker	2	11.7
Medium-fidelity prototype		
Lighting designer	2	11.7
Office worker	3	17.6
Expert reviewer	2	11.7
High-fidelity prototype		
Lighting designer	3	17.6
Office worker	2	11.7

4.3.2 Phase 1

Overall, all participants like the idea of the proposed app as they think it is noble and would greatly help them track their lighting conditions. They were primarily interested in the solution that would greatly help for improving their lighting conditions. The interview transcripts'thematic analysis resulted in identifying four categories of functional requirements: track personal lighting exposures, staying healthy, my information management, and resources (Table 4.2).

Table 4.2: Findings from interviews with intended end-users.

Category	Content
Track personal lighting exposure	Different hours, days, months, and years
Staying healthy	An ideal spectrum of light for individuals, solution for improving lighting conditions
My information management	Log of previous measurements
Resources	Importance of circadian lighting for health

4.3.3 Phase 2

There is a growing interest among researchers within different fields in investigating the non-visual effects of light on human health and well-being. The extensive review of the previous and existing artifacts revealed that there are only a few mobile apps available to evaluate the effects of light on humans by tracking users'sleep, activity levels, and in some cases measuring lighting conditions. We did not find any apps using metrics such as Circadian Stimulus (CS) to monitor the biological effects of light on human health in real-time. Two web-based online tools have recently been developed to explore non-visual spectrum lighting for human health [171] and calculate the relevant physiological quantities for light [172]. We also found one connected technology, including a wearable device and a mobile app to record vertical illuminance

(lux) with a real-time recording of how much light they receive over time [38]. We considered these artifacts in the next phase (design cycle) to increase the acceptance likelihood of the proposed app.

4.3.4 Phase 3: Low-Fidelity Prototype

All participants (n = 5) appreciated the possibility of accessing detailed information about an individualâs lighting conditions. Three participants, two office workers, and one lighting designer commented on the global structure and the visual design of the static interactive dashboard. They thought minimizing the text and the number of clicks to accomplish a task would greatly help improve the app's functionality. They stressed the need to enhance the visual design of the bottom bars by combining them into one graph with less text to minimize the number of clicks for selecting a specific date. Furthermore, they emphasized reducing texts by removing legend at the left side of the dashboard.

All participants (n=5), except one, were confused by the purpose of the app. They indicated that providing instruction on using this app and what the metric implied would greatly help them. Two participants (office workers) preferred attaching the hourly average to the top bar by relocating the hours of a day from the top to the bottom to improve the visual design of the interactive dashboard. The evolution from low- to medium-fidelity prototype is illustrated in Fig. 4.3 (b).

4.3.5 Phase 3: Medium-Fidelity Prototype

Three office workers and two lighting designers participated in usability testing of the medium-fidelity prototype. The median SUS score of 76 (SD = 5.48) indicated that the medium-fidelity prototype was relatively intuitive (Table 4.3). The findings from the qualitative data showed that overall, the participants had positive feelings about the prototype. Table 4.4 shows some examples of the usability issues identified by participants in testing medium-fidelity prototypes. Additionally, two experts re-

viewed the medium-fidelity prototype to check for possible usability issues. We used the recommendations made by two expert reviewers and five end-users to modify the app design. Fig. 4.3(c) shows the evolution from medium- to high-fidelity prototype.

Table 4.3: System usability scale score for medium- and high-fidelity prototypes. (Scores of the ten items were transformed into a summary score ranging from 0 to 100; higher = more user friendly).

System usability scale items (SD) (1 = Strongly disagree; 5 = Strongly agree)	Medium-fidelity (SD)	High-fidelity (SD)	All (SD)
1. I think that I would like to use this app frequently.	3.60 (0.55)	3.80 (0.84)	3.70 (0.69)
2. I found the app unnecessarily complex.	1.60 (0.55)	1.20 (0.45)	1.40 (0.50)
3. I think the app was easy to use.	3.60 (0.89)	4.20 (0.45)	3.90 (0.67)
4. I think that I would need the support of a technical person to be able to use this app.	1.80 (0.45)	1.60 (0.55)	1.70 (0.50)
5. I found the various functions in this app were well integrated.	4.20 (0.84)	4.00 (1.00)	4.10 (0.92)
6. I think there was too much inconsistency in this app.	2.00 (0.00)	1.80 (0.45)	1.90 (0.22)
7. I would imagine that most people would learn to use this app very quickly.	4.80 (0.45)	4.40 (0.55)	4.60 (0.50)
8. I found the app very cumbersome to use.	1.80 (0.45)	2.00 (0.00)	1.90 (0.23)
9. I felt very confident using the app.	3.80 (0.84)	4.00 (0.00)	3.90 (0.42)
10. I needed to learn a lot of things before I could get going with this app.	2.40 (0.55)	2.00 (1.00)	2.20 (0.78)
Total System Usability Scale score	76 (5.48)	79.50 (4.47)	77.75 (4.98)

Table 4.4: Modifiable usability issues identified by participants with related themes after testing the medium- and high-fidelity prototype.

Category	Themes	Examples of participant comment
1. Visibility: Ability to quickly recognize critical messages and instructions provided by the interactive dashboard	• Visibility improved when providing tips on how to enhance CS	• I need to see a list of recommendations on enhancing CS (medium- and high-fidelity prototype).
		• User-definable metrics help set limits for people of different ages like kids and the elderly (high-fidelity prototype).
	• Visibility improved when instructions and information are added	• I do not know what to do with the app? The purpose of the app is unknown to me (medium-fidelity prototype).
		• Put a legend on the dashboard to show the CS metric (medium- and high-fidelity prototype).
		• What PCM stands for? Pl define it (high-fidelity prototype).

Continued on next page

Table 4.4 – continued from previous page

Category	Themes	Examples of participant comment
	• Visibility improved when the help button is located in the dashboard	• Instruction is too longâtoo much text in the last paragraph of the about page. I want to see something graphically (high-fidelity prototype). • Put some legend in the dashboard to describe what different colors are. Not intuitive at this point. Nice to have a legend to show high and low circadian rhythms by hovering over the blue and orange cubes (medium- and high-fidelity prototype). • Change the title from hour/day to Hourly in the dashboard (high-fidelity prototype). • I like the hourly average starts from midnight instead of 6 am (high-fidelity prototype). • Write noon for noon and midnight for 12 am on an hourly average (high-fidelity prototype).
Continued on next page		

Table 4.4 – continued from previous page

Category	Themes	Examples of participant comment
		• I want to understand why between 2-5, the data is high and then drops; what happened between those hours? Somebody was moving to the window or waking from point A to point B? (high-fidelity prototype). • The warning sign is not intuitive; make it better (high-fidelity prototype). • The tips do not mention how much should I deem light (high-fidelity prototype)? • The help button icon was not clear enough (high-fidelity prototype). • Nothing here to indicate the year. Specify the year (high-fidelity prototype). • Shade the upper limit or make a line on 0.3 to show the threshold between acceptable and not acceptable on the upper graph (high-fidelity prototype).

Continued on next page

Table 4.4 – continued from previous page

Category	Themes	Examples of participant comment
		• Like the tips to pup-up automatically when there is any suggestion for improving CS instead of a danger sign, put a piece of information with the blue bar to catch my attention (high-fidelity prototype).
2. Navigation: Ability in recognizing and using buttons and moving easily through the app	• The title should appear on the left location of each of the three sections and add a little horizontal distance between them to facilitate navigation	• I am confused about where each section starts. Add distance between each section. The title for each section would help to find the date or hourly average easily (medium-fidelity prototype).
		• A marker to show where each month starts and ends (high-fidelity prototype).
		• Not easy and intuitive to find out what day you want. Make a black line between different months (high-fidelity prototype).

Continued on next page

Table 4.4 – continued from previous page

Category	Themes	Examples of participant comment
3. Aesthetic: The color and look and feel of the program	• Aesthetic improves when the color changed with blue and orange • Add icons for each part of the day to find morning and night much easier (medium-fidelity).	• White line between each hour to the top (high-fidelity prototype). • Connect each part of the day to the representative hour by copy the moon and sun to the top part (high-fidelity prototype). • Replace current colors or use patterns instead of colors (medium-fidelity). • More visually pleasing when adding icon beside each part of a day. • Make text smaller in the middle of the circle in part of a day (high-fidelity).

Continued on next page

Table 4.4 – continued from previous page

Category	Themes	Examples of participant comment
4. Understandability: Ability to quickly comprehend the meaning of the text, instructions, and the purpose of the interactive dashboard	• Using a complete circle with a CS label from 0 to 0.7 improves understandability	• Use a complete circle for different parts of the day like morning, afternoon, etc. (medium-fidelity).
		• I am confused by a good CS for a different part of the day. Why is there tip and issue for the night and not evening in some days (high-fidelity prototype)?
	• Understandability improves when using common terminology with precise instructions on about page	• Vocabulary such as âCSâ was not understandable by most office workers (high-fidelity prototype).

Continued on next page

Table 4.4 – continued from previous page

Category	Themes	Examples of participant comment
5. Usefulness: Ability of the app to improve speed, decreasing the cognitive burden, and/or enhancing the accuracy of the interactive dashboard	• Implementing supplementary functionalities are essential to improve usefulness and so acceptability	• I like to have a legend on the left side of the dashboard to describe the meaning of different colors (high-fidelity prototype). • Label part of the day by putting 0.3 on each circle (high-fidelity prototype). • Add all days of the week in yearly (medium-fidelity). • The graphic for different parts of the day is not clear. Just keep them and write morning (high-fidelity prototype). • Add some instructions in the dashboard (medium- and high-fidelity).

Continued on next page

Table 4.4 – continued from previous page

Category	Themes	Examples of participant comment
		• Find the way to show results for multiple users (high-fidelity prototype). • Besides, add another value that is user-definable to say too much light or poor light. A scoring system from 0 to 10 shows that CS is good or bad for different hours and parts of the day (high-fidelity prototype). • Track the mood of people. Pop up in the computer every hour to ask your mood (high-fidelity prototype). • As it is a desktop app, I want little access that can bring down and show me what is below 0.3 means (high-fidelity prototype).

Continued on next page

Table 4.4 – continued from previous page

Category	Themes	Examples of participant comment
6. Workflow:	• To prevent workflow disturbance, the PCM app should be accessible on various devices and provide additional functionalities	• The PCM app user interface should be adapted to be usable on smartphones and tablets (high-fidelity prototype).
7. Content: Appropriateness of the interactive dashboard information	• Content improves when having another page to provide instruction on how to use the app and what the metric implies	• Better to have another page for a short demo video and instructions. Have a walkthrough tutorial like other apps we used for the first time (medium- and high-fidelity prototype). • It could be an added value to have access to older data for up to several years. For example, compare the personal lighting conditions for specific times between different years (high-fidelity prototype).

Continued on next page

Table 4.4 – continued from previous page

Category	Themes	Examples of participant comment
		• I might put a hyperlink (publications and standards) to describe circadian rhythm in-depth (high-fidelity prototype).

4.3.6 Phase 3: High-Fidelity Prototype

The results of usability testing of the high-fidelity prototype revealed that the median SUS score was slightly improved from 76 (SD=5.48) to 79.5 (SD=4.47) after modification of the interactive dashboard (Table 4.3). A total of 37 changes were made to the high-fidelity prototype based on the end-users recommendations. Qualitative feedback indicated that participants appreciated the refinement and modifications of the prototype. Testing of the high-fidelity prototype of the interactive dashboard revealed more concerns regarding visibility, usefulness, and navigation. Some usability issues by the participant for further improvement of the prototype are listed in Table 4.4.

4.4 Discussion

In this study, a user-centered approach guided by the ISR framework was performed through a three-phase iterative process to develop a novel interactive dashboard for real-time monitoring of personal lighting conditions. At each phase of the study, significant improvements were made to the interactive dashboard. Throughout the entire process, we focused on the end user's needs, recommendations, and feedback

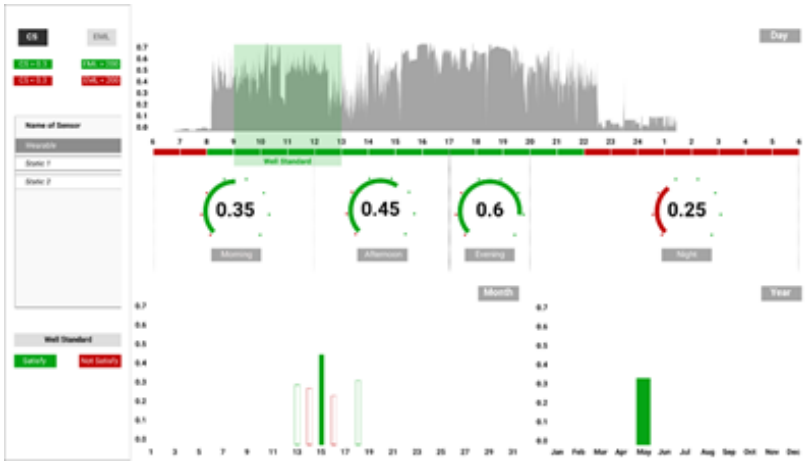

(a) Low-fidelity prototype

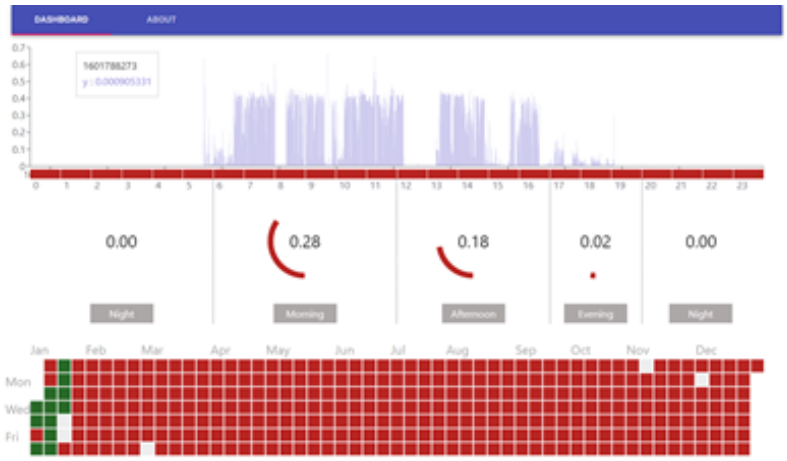

(b) Medium-fidelity prototype

(c) High-fidelity prototype

Figure 4.3: Changes between the low-fidelity (a), medium-fidelity (b) and high-fidelity (c) prototypes.

as a foundation for developing a highly usable and useful interactive dashboard. A critical advantage of the user-centered approach implemented in this study is that it enabled us to evaluate usability issues of an interactive dashboard and modify them before launching the actual app.

We found that the medium- and high-fidelity prototypes were considered acceptable with SUS scores of 76 and 79.5, respectively. No significant changes in SUS score between medium- and high-fidelity prototypes might result from the small sample sizes and a limited number of usability issues identified by participants [173–175]. Although there is no agreement on an acceptable SUS score [176], Bangor et al. [162] recommended considering a product with SUS score above 70 as a "good product".

The results of phase 1 enabled identifying four categories of end-users functional requirements used in designing the low-fidelity prototype. Results of phase 2 revealed the unavailability of an interactive dashboard for real-time tracking and monitoring of biological effects of light on human health. We found two previously developed web-based online tools for exploring the non-visual spectrum lighting for human health [171] and calculating the physiological relevant quantities of light [172]. Our interactive dashboard differed from existing tools because it enables individual non-expert users to continuously monitor how much circadian-effective lighting they receive throughout the 24-hours day, together with how to improve their lighting conditions. Results of phase 3 allowed identification of several usability issues of testing the medium- and high-fidelity prototypes. The usability issues identified during the usability testing of the high-fidelity prototype need to be addressed before being assessed in a fully functional app. Most importantly, because more concerns were expressed regarding the usability issues related to visibility, usefulness, and navigation, they should be prioritized when modifying the high-fidelity prototype.

There are several limitations to this study. First, we conducted usability testing of medium- and high-fidelity prototypes with 5 participants, a typical sample size

used to find the most usability issues of a product [159,175]. However, future studies should be performed on a larger sample size with more diversity to identify a higher number of usability issues along with a significant difference in SUS score. Second, future study is needed to perform usability testing of a fully functional prototype of an interactive dashboard. Our funding was limited due to the evaluation of the medium- and high-fidelity prototypes. Third, future research can utilize the same approach for developing a mobile app for tracking personal lighting conditions.

4.5 Conclusion

Implementation of a user-centered approach with three-phase iterations led to developing a novel interactive dashboard for real-time monitoring of the biological effects of light on human health. First, we started by identifying the end user's needs and requirements; second, we evaluated the past and existing knowledge and artifacts; third, we assessed the global structure and the visual design of the interface; and finally, we evaluated usability, exploring usefulness and acceptability of the proposed app. We found that the interactive dashboard was usable, useful, and satisfying for the participants. Both qualitative and quantitative analyses gave us an in-depth understanding of different usability issues. Even though we addressed the usability issues identified during the testing of the medium-fidelity prototype, some issues still need to be addressed in our future developments.

This study is one of the first attempts to develop an interactive application to provide vital information regarding the non-visual effects of light on health through real-time tracking of personal light exposures. Tracking personal lighting conditions can significantly help individuals or their health coaches to take more control over their living conditions, health, and lifestyles.

CHAPTER 5: CONCLUSION

5.1 Contribution

Light has a profound impact on our health and general well-being. Today more than ever, we depend on electric lighting for a considerable portion of the day, as we spend most of our time indoors. Due to technological advances in lighting and the discovery of the non-visual effects of light, the use of human-centric lighting has become an attractive option as we reconsider our relationship with light. Human-centric lighting can provide a range of evidence-based solutions to promote better health and well-being in the built environment by tailoring indoor lighting conditions according to individual circadian needs in real-time. Using human-centric lighting, however, first requires a consistent and constant recording of lighting characteristics that affect the circadian system over the entire course of the 24-hour day. Developing a tool to track and record circadian light exposure is one of the most promising responses to this problem.

This dissertation proposed a novel user-centric lighting assist tool consisting of a wearable spectrometer and an interactive dashboard. The low-cost and wearable spectrometer records different light characteristics that stimulate the circadian system characteristics such as intensity, spectrum, timing, duration, and history of light exposure. The spectrometer displays vital information regarding the non-visual effects of light on humans through an interactive dashboard to improve personal knowledge of lighting and increase end-user awareness to help them live healthier about light. This research can be referenced as guidance towards a healthier lit environment in the post-design evaluation of existing buildings.

Numerous studies have shown the necessity of developing a portable, low-cost,

and accurate tool with wireless communication capabilities and real-time data monitoring and visualization [40, 101–104]. A few wearable measurement devices have been used for measuring personal light exposure within the field of lighting research [15–17, 35–37, 40, 177, 178]. However, these devices are typically expensive, commercially unavailable, or have questionable accuracy in measuring circadian lighting. Currently, most studies have been utilizing wearable devices that measure vision-related quantities such as photopic illuminance [34, 35], or the irradiance from red, green, and blue of the visible light region [16,17,36,37] or both [38] to assess the non-visual effects of light. This could be problematic as it is recommended to measure SPD of the light exposure due to the complexity of non-visual photosensory systems and limited knowledge regarding the contribution of each individual photoreceptor in terms of irradiance response. The devices that record SPD enable researchers to re-analysis the collected data using any unit of measure currently available and any unit that may be developed in the future. Further, several field studies have been carried out using expensive hand-held and portable spectrometers to measure circadian lighting in the built environment [39, 179]. Other researchers have applied measurement techniques using high dynamic range (HDR) photography [39,83,85] or lighting simulation techniques [180–184] to evaluate the non-visual effects of light in the built environment.

This research has bridged the gap by developing a low-cost, wearable, and accurate device to measure personal light exposure in the most comprehensive form recommended by lighting communities. My study departs from previous investigations in at least three aspects. First, the user-centric lighting assist tool incorporates a low-cost, wearable, and wireless spectrometer to continuously measure SPD of light exposure with a resolution of 3.5 nm in the visible spectrum using Artificial Neural Networks (ANNs). Second, the developed spectrometer offers real-time communication to transmit the collected SPD for storage on a cloud-based database using Blue-

tooth, Wi-Fi, or SIM-card connection. This capability enables it to be integrated into IoT-based intelligent lighting systems for tailoring indoor lighting systems according to individual circadian needs. Third, the user-centric lighting assist tool allows visualizing the circadian-effectiveness of light exposure for end-users on an interactive dashboard to track and monitor their personal lighting conditions easily. It also provides recommendations on how to improve indoor lighting conditions according to individual circadian needs. To this end, through a user-centered approach, the end-users were engaged throughout the entire process, from design to build an interactive dashboard.

This tool can be a great source of information for lighting designers and post-design evaluation of buildings. Moreover, it provides non-expert end-users with meaningful and easy-to-understand information to take more control over their living conditions and health by promoting healthy behavior change in buildings.

5.2 Limitation and Future Research Directions

First, the research has looked at only one type of neural network called multilayer perceptron (MLP) to improve the accuracy of the wearable spectrometer. In addition, a limited number of samples (light sources) and a few neural network architectures, activation functions, and learning algorithms have been used to train and test the MLP model for reconstructing the SPD. Future research can overcome this shortcoming by applying more advanced computational techniques such as deep learning, with higher samples of light sources, to facilitate the performance of the neural network, which consequently could improve the accuracy of the developed spectrometer.

Second, due to the impact of the COVID pandemic, this study had some limitations for conducting the field experiments intended to explore the performance of the wearable spectrometer in real-world environments. Another possible future research direction would be to understand the practical applicability of the wearable spectrometer with a higher number of participants and with greater diversity during different

seasons and in geographical locations. In addition to evaluating the performance of the wearable spectrometer, this would greatly help investigate the inter-individual differences in response to light exposure.

Third, the future study must consider the sensitive group of non-expert end-users as the eventual customer for the interactive dashboard, not just the academic elite. The potential segment for our technology could be those who spend most of their time indoors, who are exposed to less natural light during daytime hours and more artificial light during nighttime hours than what we would have naturally received during day and night people such as nurses with rotating work schedules, and the elderly. Nurses'working hours are often outside the standard working schedule, leading to poorer quality and shorter sleeping hours, extended periods of wakefulness, and circadian disruption. Those nurses commonly have lower productivity, lower physical and psychological well-being, and a higher risk of accidents and errors. Therefore, shift work-related fatigue is a direct consequence of circadian disruption and sleep loss and considerably affects nurse and patient safety. This tool would greatly help end-users like nurses to initiate healthy behavioral change by engaging them with their health data.

Fourth, future research is recommended to integrate the human-centric lighting assist tool into an IoT-based intelligent lighting system for turning indoor lighting sources into accurate human-centric lighting. This goal is achieved by continuously measuring personal lighting conditions and tailoring indoor lighting conditions by adjusting the spectrum and intensity according to individual circadian needs in real-time.

Lastly, in recent years, sensor-enabled mobile health (mHealth) apps such as Fitbit has emerged to enhanced users' consciousness of their health status. Using wearable sensors with mHealth apps empower users to be more involved in their health by tracking and monitoring data related to users' behavior (activity and motion) and

characteristic (lighting exposure and body temperature). It also promotes behavior change by providing a huge amounts of data for individuals or their health coaches. However, there has been surprisingly lack of study in this area due to unavailability of an affordable and accessible tools for real-time tracking and monitoring of biological effects of light on human health. Current tools are either inappropriate to measure circadian lighting, commercially unavailable, or not able to visualize the collected data in meaningful and easy to understand quantities. Future study is recommended to focus on conducting usability testing of the tool that is developed in this study to investigate how users adopt and sustain healthy lifestyle choices through the use of personalized approach for self-monitoring of biological effects of light in real-time. This tool can drive the behavior change process by supporting users in optimizing personal light exposure, activity, and overall health. Use of innovative technologies such as sensor-enabled mHealth apps have been proven as an effective way to re-engineer healthcare system throughout the world by improving healthcare access and affordability, and reducing healthcare costs by engaging users and encouraging meaningful behavior change.

REFERENCES

[1] P. Boyce, "Exploring human-centric lighting," 2016.

[2] N. E. Klepeis, W. C. Nelson, W. R. Ott, J. P. Robinson, A. M. Tsang, P. Switzer, J. V. Behar, S. C. Hern, and W. H. Engelmann, "The national human activity pattern survey (nhaps): a resource for assessing exposure to environmental pollutants," *Journal of Exposure Science & Environmental Epidemiology*, vol. 11, no. 3, pp. 231–252, 2001.

[3] D. M. Berson, F. A. Dunn, and M. Takao, "Phototransduction by retinal ganglion cells that set the circadian clock," *Science*, vol. 295, no. 5557, pp. 1070–1073, 2002.

[4] S. Hattar, H.-W. Liao, M. Takao, D. M. Berson, and K.-W. Yau, "Melanopsin-containing retinal ganglion cells: architecture, projections, and intrinsic photosensitivity," *Science*, vol. 295, no. 5557, pp. 1065–1070, 2002.

[5] P. R. Boyce, "The impact of light in buildings on human health," *Indoor and Built environment*, vol. 19, no. 1, pp. 8–20, 2010.

[6] M. G. Figueiro and M. S. Rea, "Evening daylight may cause adolescents to sleep less in spring than in winter," *Chronobiology International*, vol. 27, no. 6, pp. 1242–1258, 2010.

[7] M. Figueiro, M. Kalsher, B. Steverson, J. Heerwagen, K. Kampschroer, and M. Rea, "Circadian-effective light and its impact on alertness in office workers," *Lighting Research & Technology*, vol. 51, no. 2, pp. 171–183, 2019.

[8] M. G. Figueiro, B. Steverson, J. Heerwagen, K. Kampschroer, C. M. Hunter, K. Gonzales, B. Plitnick, and M. S. Rea, "The impact of daytime light exposures on sleep and mood in office workers," *Sleep Health*, vol. 3, no. 3, pp. 204–215, 2017.

[9] M. M. Mallis and C. DeRoshia, "Circadian rhythms, sleep, and performance in space," *Aviation, space, and environmental medicine*, vol. 76, no. 6, pp. B94–B107, 2005.

[10] M. G. Figueiro, B. A. Plitnick, A. Lok, G. E. Jones, P. Higgins, T. R. Hornick, and M. S. Rea, "Tailored lighting intervention improves measures of sleep, depression, and agitation in persons with alzheimerâs disease and related dementia living in long-term care facilities," *Clinical interventions in aging*, vol. 9, p. 1527, 2014.

[11] Y. Gan, C. Yang, X. Tong, H. Sun, Y. Cong, X. Yin, L. Li, S. Cao, X. Dong, Y. Gong, *et al.*, "Shift work and diabetes mellitus: a meta-analysis of observational studies," *Occupational and environmental medicine*, vol. 72, no. 1, pp. 72–78, 2015.

[12] H. C. Thorne, K. H. Jones, S. P. Peters, S. N. Archer, and D.-J. Dijk, "Daily and seasonal variation in the spectral composition of light exposure in humans," *Chronobiology International*, vol. 26, no. 5, pp. 854–866, 2009.

[13] E. Cordina-Duverger, F. Menegaux, A. Popa, S. Rabstein, V. Harth, B. Pesch, T. Brüning, L. Fritschi, D. C. Glass, J. S. Heyworth, *et al.*, "Night shift work and breast cancer: a pooled analysis of population-based case–control studies with complete work history," 2018.

[14] M. S. Rea and M. Figueiro, "Light as a circadian stimulus for architectural lighting," *Lighting research & technology*, vol. 50, no. 4, pp. 497–510, 2018.

[15] S. Rabstein, K. Burek, M. Lehnert, A. Beine, C. Vetter, V. Harth, S. Putzke, T. Kantermann, J. Walther, R. Wang-Sattler, *et al.*, "Differences in twenty-four-hour profiles of blue-light exposure between day and night shifts in female medical staff," *Science of The Total Environment*, vol. 653, pp. 1025–1033, 2019.

[16] L. Price, M. Khazova, and J. O'Hagan, "Performance assessment of commercial circadian personal exposure devices," *Lighting Research & Technology*, vol. 44, no. 1, pp. 17–26, 2012.

[17] A. Bierman, T. R. Klein, and M. S. Rea, "The daysimeter: a device for measuring optical radiation as a stimulus for the human circadian system," *Measurement Science and Technology*, vol. 16, no. 11, p. 2292, 2005.

[18] M. S. Rea, M. G. Figueiro, A. Bierman, and J. D. Bullough, "Circadian light," *Journal of circadian rhythms*, vol. 8, no. 1, p. 2, 2010.

[19] S. CIE, "026/e: 2018 cie system for metrology of optical radiation for iprgc-influenced responses to light," *CIE Central Bureau: Vienna, Austria*, 2018.

[20] C. SEMINAR, "The well v2 building standard and how floor covering impacts health and well-being,"

[21] R. J. Lucas, S. N. Peirson, D. M. Berson, T. M. Brown, H. M. Cooper, C. A. Czeisler, M. G. Figueiro, P. D. Gamlin, S. W. Lockley, J. B. OâHagan, *et al.*, "Measuring and using light in the melanopsin age," *Trends in neurosciences*, vol. 37, no. 1, pp. 1–9, 2014.

[22] M. Münch, A. Wirz-Justice, S. A. Brown, T. Kantermann, K. Martiny, O. Stefani, C. Vetter, K. P. Wright, K. Wulff, and D. J. Skene, "The role of daylight for humans: gaps in current knowledge," *Clocks & sleep*, vol. 2, no. 1, pp. 61–85, 2020.

[23] M. Adamsson, T. Laike, and T. Morita, "Comparison of static and ambulatory measurements of illuminance and spectral composition that can be used for assessing light exposure in real working environments," *Leukos*, 2018.

[24] M. L. Ámundadóttir, "Light-driven model for identifying indicators of non-visual health potential in the built environment," tech. rep., EPFL, 2016.

[25] D. M. Dacey, H.-W. Liao, B. B. Peterson, F. R. Robinson, V. C. Smith, J. Pokorny, K.-W. Yau, and P. D. Gamlin, "Melanopsin-expressing ganglion cells in primate retina signal colour and irradiance and project to the lgn," *Nature*, vol. 433, no. 7027, pp. 749–754, 2005.

[26] J. A. Perez-Leon, E. J. Warren, C. N. Allen, D. W. Robinson, and R. Lane Brown, "Synaptic inputs to retinal ganglion cells that set the circadian clock," *European Journal of Neuroscience*, vol. 24, no. 4, pp. 1117–1123, 2006.

[27] L. S. Mure, C. Rieux, S. Hattar, and H. M. Cooper, "Melanopsin-dependent nonvisual responses: evidence for photopigment bistability in vivo," *Journal of biological rhythms*, vol. 22, no. 5, pp. 411–424, 2007.

[28] P. Khademagha, M. Aries, A. Rosemann, and E. Van Loenen, "Implementing non-image-forming effects of light in the built environment: A review on what we need," *Building and Environment*, vol. 108, pp. 263–272, 2016.

[29] J. J. Gooley, S. M. Rajaratnam, G. C. Brainard, R. E. Kronauer, C. A. Czeisler, and S. W. Lockley, "Spectral responses of the human circadian system depend on the irradiance and duration of exposure to light," *Science translational medicine*, vol. 2, no. 31, pp. 31ra33–31ra33, 2010.

[30] J. a. Enezi, V. Revell, T. Brown, J. Wynne, L. Schlangen, and R. Lucas, "A âmelanopicâ spectral efficiency function predicts the sensitivity of melanopsin photoreceptors to polychromatic lights," *Journal of biological rhythms*, vol. 26, no. 4, pp. 314–323, 2011.

[31] M. S. Rea, M. G. Figueiro, A. Bierman, and R. Hamner, "Modelling the spectral sensitivity of the human circadian system," *Lighting Research & Technology*, vol. 44, no. 4, pp. 386–396, 2012.

[32] S. Hattar, R. J. Lucas, N. Mrosovsky, S. Thompson, R. Douglas, M. W. Hankins, J. Lem, M. Biel, F. Hofmann, R. G. Foster, *et al.*, "Melanopsin and rod–cone photoreceptive systems account for all major accessory visual functions in mice," *Nature*, vol. 424, no. 6944, pp. 75–81, 2003.

[33] E. Clark and N. Lesniak, "Circadian lighting solutions are real and importantâwhy arenât they being used," *Metropolis, New York*, 2017.

[34] S. Hubalek, D. Zöschg, and C. Schierz, "Ambulant recording of light for vision and non-visual biological effects," *Lighting Research & Technology*, vol. 38, no. 4, pp. 314–321, 2006.

[35] R. Arguelles-Prieto, M.-A. Bonmati-Carrion, M. A. Rol, and J. A. Madrid, "Determining light intensity, timing and type of visible and circadian light from an ambulatory circadian monitoring device," *Frontiers in physiology*, vol. 10, p. 822, 2019.

[36] M. V. Dias, A. Motamed, P. S. Scarazzato, and J.-L. Scartezzini, "Toward proper evaluation of light dose in indoor office environment by frontal lux meter," *Energy Procedia*, vol. 122, pp. 835–840, 2017.

[37] G. Martin, "Lightlog–brighten your day,(2015)."

[38] K. van Creveld, "Measuring real daylight exposure afforded by various architectural environments and the implications for our health and wellbeing," tech. rep., Jean Heap Research Bursary Society of Light and Lighting, 2020.

[39] K. Konis, "Field evaluation of the circadian stimulus potential of daylit and non-daylit spaces in dementia care facilities," *Building and Environment*, vol. 135, pp. 112–123, 2018.

[40] J.-S. Botero-Valencia, J. Valencia-Aguirre, D. Durmus, and W. Davis, "Multi-channel low-cost light spectrum measurement using a multilayer perceptron," *Energy and Buildings*, vol. 199, pp. 579–587, 2019.

[41] M. S. Rea, M. G. Figueiro, and J. D. Bullough, "Circadian photobiology: an emerging framework for lighting practice and research," *Lighting research & technology*, vol. 34, no. 3, pp. 177–187, 2002.

[42] J. van Duijnhoven, M. P. Aarts, and H. Kort, "Personal lighting conditions of office workers: An exploratory field study," *Lighting Research & Technology*, vol. 53, no. 4, pp. 285–310, 2021.

[43] J. van Duijnhoven, M. P. Aarts, E. R. van den Heuvel, and H. S. Kort, "The identification of variables influencing personal lighting conditions of office workers," *Lighting Research & Technology*, p. 1477153520976950, 2020.

[44] S. L. Chellappa, "Individual differences in light sensitivity affect sleep and circadian rhythms," *Sleep*, vol. 44, no. 2, p. zsaa214, 2021.

[45] R. P. Najjar, C. Chiquet, P. Teikari, P.-L. Cornut, B. Claustrat, P. Denis, H. M. Cooper, and C. Gronfier, "Aging of non-visual spectral sensitivity to light in humans: compensatory mechanisms?," *PloS one*, vol. 9, no. 1, p. e85837, 2014.

[46] P. L. Turner and M. A. Mainster, "Circadian photoreception: ageing and the eyeâs important role in systemic health," *British Journal of Ophthalmology*, vol. 92, no. 11, pp. 1439–1444, 2008.

[47] M. Münch, L. Léon, S. Collomb, and A. Kawasaki, "Comparison of acute non-visual bright light responses in patients with optic nerve disease, glaucoma and healthy controls," *Scientific reports*, vol. 5, no. 1, pp. 1–12, 2015.

[48] M. L. Maynard, A. J. Zele, and B. Feigl, "Melanopsin-mediated post-illumination pupil response in early age-related macular degeneration," *Investigative ophthalmology & visual science*, vol. 56, no. 11, pp. 6906–6913, 2015.

[49] M. T. S. Barboni, C. Bueno, B. V. Nagy, P. L. Maia, K. S. M. Vidal, R. C. Alves, R. J. Reiter, F. G. Do Amaral, J. Cipolla-Neto, and D. F. Ventura, "Melanopsin system dysfunction in smith-magenis syndrome patients," *Investigative ophthalmology & visual science*, vol. 59, no. 1, pp. 362–369, 2018.

[50] A. Azzi, R. Dallmann, A. Casserly, H. Rehrauer, A. Patrignani, B. Maier, A. Kramer, and S. A. Brown, "Circadian behavior is light-reprogrammed by plastic dna methylation," *Nature neuroscience*, vol. 17, no. 3, pp. 377–382, 2014.

[51] K. A. Roecklein, K. J. Rohan, W. C. Duncan, M. D. Rollag, N. E. Rosenthal, R. H. Lipsky, and I. Provencio, "A missense variant (p10l) of the melanopsin (opn4) gene in seasonal affective disorder," *Journal of affective disorders*, vol. 114, no. 1-3, pp. 279–285, 2009.

[52] D. S. Pereira, S. Tufik, F. M. Louzada, A. A. Benedito-Silva, A. R. Lopez, N. A. Lemos, A. L. Korczak, V. D´ Almeida, and M. Pedrazzoli, "Association of the length polymorphism in the human per3 gene with the delayed sleep-phase syndrome: does latitude have an influence upon it?," *Sleep*, vol. 28, no. 1, pp. 29–32, 2005.

[53] M. M. Mendes, A. L. Darling, K. H. Hart, S. Morse, R. J. Murphy, and S. A. Lanham-New, "Impact of high latitude, urban living and ethnicity on 25-hydroxyvitamin d status: a need for multidisciplinary action?," *The Journal of steroid biochemistry and molecular biology*, vol. 188, pp. 95–102, 2019.

[54] W. B. Grant, H. P. Bhattoa, and P. Pludowski, "Determinants of vitamin d deficiency from sun exposure: a global perspective," in *Vitamin D*, pp. 79–90, Elsevier, 2018.

[55] A. Darling, K. Hart, S. Arber, J. Berry, P. Morgan, B. Middleton, S. Lanham-New, and D. Skene, "25-hydroxyvitamin d status, light exposure and sleep quality in uk dwelling south asian and caucasian postmenopausal women," *The Journal of steroid biochemistry and molecular biology*, vol. 189, pp. 265–273, 2019.

[56] S. L. Chellappa, R. Steiner, P. Oelhafen, and C. Cajochen, "Sex differences in light sensitivity impact on brightness perception, vigilant attention and sleep in humans," *Scientific reports*, vol. 7, no. 1, pp. 1–9, 2017.

[57] I. Abramov, J. Gordon, O. Feldman, and A. Chavarga, "Sex and vision ii: color appearance of monochromatic lights," *Biology of sex differences*, vol. 3, no. 1, pp. 1–15, 2012.

[58] T. Roenneberg, "Having trouble typing? what on earth is chronotype?," *Journal of biological rhythms*, vol. 30, no. 6, pp. 487–491, 2015.

[59] T. Roenneberg, A. Wirz-Justice, and M. Merrow, "Life between clocks: daily temporal patterns of human chronotypes," *Journal of biological rhythms*, vol. 18, no. 1, pp. 80–90, 2003.

[60] W. P. Van Der Meijden, J. L. Van Someren, B. H. Te Lindert, J. Bruijel, F. Van Oosterhout, J. E. Coppens, A. Kalsbeek, C. Cajochen, P. Bourgin, and E. J. Van Someren, "Individual differences in sleep timing relate to melanopsin-based phototransduction in healthy adolescents and young adults," *Sleep*, vol. 39, no. 6, pp. 1305–1310, 2016.

[61] L. A. Watson, A. J. Phillips, I. T. Hosken, E. M. McGlashan, C. Anderson, L. C. Lack, S. W. Lockley, S. M. Rajaratnam, and S. W. Cain, "Increased sensitivity of the circadian system to light in delayed sleep–wake phase disorder," *The Journal of physiology*, vol. 596, no. 24, pp. 6249–6261, 2018.

[62] A. Kawasaki, S. Wisniewski, B. Healey, N. Pattyn, D. Kunz, M. Basner, and M. Münch, "Impact of long-term daylight deprivation on retinal light sensitivity, circadian rhythms and sleep during the antarctic winter," *Scientific reports*, vol. 8, no. 1, pp. 1–12, 2018.

[63] D. Leger, V. Bayon, M. Elbaz, P. Philip, and D. Choudat, "Underexposure to light at work and its association to insomnia and sleepiness: A cross-sectional study of 13 296 workers of one transportation company," *Journal of psychosomatic research*, vol. 70, no. 1, pp. 29–36, 2011.

[64] S. Daugaard, J. Markvart, J. P. Bonde, J. Christoffersen, A. H. Garde, Å. M. Hansen, V. Schlünssen, J. M. Vestergaard, H. T. Vistisen, and H. A. Kolstad, "Light exposure during days with night, outdoor, and indoor work," *Annals of work exposures and health*, vol. 63, no. 6, pp. 651–665, 2019.

[65] K. Tsuzuki, I. Mori, T. Sakoi, and Y. Kurokawa, "Effects of seasonal illumination and thermal environments on sleep in elderly men," *Building and Environment*, vol. 88, pp. 82–88, 2015.

[66] M. Figueiro and M. Rea, "Office lighting and personal light exposures in two seasons: Impact on sleep and mood," *Lighting Research & Technology*, vol. 48, no. 3, pp. 352–364, 2016.

[67] K. Smolders, Y. De Kort, and S. M. van den Berg, "Daytime light exposure and feelings of vitality: Results of a field study during regular weekdays," *Journal of environmental psychology*, vol. 36, pp. 270–279, 2013.

[68] T. Roenneberg and R. G. Foster, "Twilight times: light and the circadian system," *Photochemistry and photobiology*, vol. 66, no. 5, pp. 549–561, 1997.

[69] J. K. Day, B. Futrell, R. Cox, S. N. Ruiz, A. Amirazar, A. H. Zarrabi, and M. Azarbayjani, "Blinded by the light: Occupant perceptions and visual comfort assessments of three dynamic daylight control systems and shading strategies," *Building and Environment*, vol. 154, pp. 107–121, 2019.

[70] J. van Duijnhoven, M. P. Aarts, and H. S. Kort, "The importance of including position and viewing direction when measuring and assessing the lighting conditions of office workers," *Work*, vol. 64, no. 4, pp. 877–895, 2019.

[71] P. Kar, A. Shareef, A. Kumar, K. T. Harn, B. Kalluri, and S. K. Panda, "Revicee: A recommendation based approach for personalized control, visual comfort & energy efficiency in buildings," *Building and Environment*, vol. 152, pp. 135–144, 2019.

[72] J. Van Duijnhoven, M. Burgmans, M. Aarts, A. Rosemann, and H. Kort, "Personal lighting conditions to obtain more evidence in light effect studies," in *Congress of the International Ergonomics Association*, pp. 110–121, Springer, 2018.

[73] K. Houser, P. Boyce, J. Zeitzer, and M. Herf, "Human-centric lighting: Myth, magic or metaphor?," *Lighting Research & Technology*, vol. 53, no. 2, pp. 97–118, 2021.

[74] C. Papatsimpa, J. H. Bonarius, and J.-P. M. Linnartz, "Human centric iot lighting control based on personalized biological clock estimations," in *2020 IEEE 6th World Forum on Internet of Things (WF-IoT)*, pp. 1–6, IEEE, 2020.

[75] A. R. Webb, "Considerations for lighting in the built environment: Non-visual effects of light," *Energy and Buildings*, vol. 38, no. 7, pp. 721–727, 2006.

[76] C. Fournier and A. Wirz-Justice, "Light, health and wellbeing: Implications from chronobiology for architectural design," *World Health Design: Architecture, Culture, Technology*, vol. 3, no. 1, pp. 44–49, 2010.

[77] M. H. Crawford, "Leds for solid-state lighting: performance challenges and recent advances," *IEEE Journal of Selected Topics in Quantum Electronics*, vol. 15, no. 4, pp. 1028–1040, 2009.

[78] E. F. Schubert and J. K. Kim, "Solid-state light sources getting smart," *Science*, vol. 308, no. 5726, pp. 1274–1278, 2005.

[79] J.-C. Marquié, P. Tucker, S. Folkard, C. Gentil, and D. Ansiau, "Chronic effects of shift work on cognition: findings from the visat longitudinal study," *Occupational and environmental medicine*, vol. 72, no. 4, pp. 258–264, 2015.

[80] J. Bowler and P. Bourke, "Facebook use and sleep quality: Light interacts with socially induced alertness," *British Journal of Psychology*, vol. 110, no. 3, pp. 519–529, 2019.

[81] J. K. Martino, C. B. Freelance, and G. L. Willis, "The effect of light exposure on insomnia and nocturnal movement in parkinson's disease: an open label, retrospective, longitudinal study," *Sleep medicine*, vol. 44, pp. 24–31, 2018.

[82] I. Rouch, P. Wild, D. Ansiau, and J.-C. Marquié, "Shiftwork experience, age and cognitive performance," *Ergonomics*, vol. 48, no. 10, pp. 1282–1293, 2005.

[83] B. Jung and M. Inanici, "Measuring circadian lighting through high dynamic range photography," *Lighting Research & Technology*, vol. 51, no. 5, pp. 742–763, 2019.

[84] A. Borisuit, L. Deschamps, J. Kämpf, J.-L. Scartezzini, and M. Münch, "Assessment of circadian weighted radiance distribution using a camera-like light sensor," tech. rep., EPFL Solar Energy and Building Physics Laboratory (LESO-PB), 2013.

[85] P. Khademagha, M. Aries, A. Rosemann, and E. van Loenen, "New method for analyzing a luminous environment considering non-image-forming effects of light," in *Proceedings of the PLEA 2017 Conference: Design to thrive*, vol. 2, pp. 3245–3252, 2017.

[86] P. Khademagha, M. Aries, A. L. Rosemann, and E. Van Loenen, "A multidirectional spectral measurement method and instrument to investigate non-image-forming effects of light," *Measurement science and technology*, vol. 29, no. 8, p. 085902, 2018.

[87] B. Y. Jung, *Measuring circadian light through High Dynamic Range (HDR) photography*. PhD thesis, 2017.

[88] C. DeCusatis, *Handbook of applied photometry*. American Inst. of Physics, 1997.

[89] D. Pavanello, R. Galleano, and R. P. Kenny, "Uncertainty propagation of spectral matching ratios measured using a calibrated spectroradiometer," *Applied Sciences*, vol. 8, no. 2, p. 186, 2018.

[90] M. Mansoor, I. Haneef, S. Akhtar, A. De Luca, and F. Udrea, "Silicon diode temperature sensorsâa review of applications," *Sensors and Actuators A: Physical*, vol. 232, pp. 63–74, 2015.

[91] G.-S. Jeong, W. Bae, and D.-K. Jeong, "Review of cmos integrated circuit technologies for high-speed photo-detection," *Sensors*, vol. 17, no. 9, p. 1962, 2017.

[92] M. Bigas, E. Cabruja, J. Forest, and J. Salvi, "Review of cmos image sensors," *Microelectronics journal*, vol. 37, no. 5, pp. 433–451, 2006.

[93] J. G. Casey, A. Collier-Oxandale, and M. Hannigan, "Performance of artificial neural networks and linear models to quantify 4 trace gas species in an oil and gas production region with low-cost sensors," *Sensors and Actuators B: Chemical*, vol. 283, pp. 504–514, 2019.

[94] S. Malagón Fernández, "Artificial neural networks applied to improve low-cost air quality monitoring precision," B.S. thesis, Universitat Politècnica de Catalunya, 2018.

[95] I. Zaman, N. Jain, and A. Förster, "Artificial neural network based soil vwc and field capacity estimation using low cost sensors," in *2018 IFIP/IEEE International Conference on Performance Evaluation and Modeling in Wired and Wireless Networks (PEMWN)*, pp. 1–6, IEEE, 2018.

[96] I. R. de Sousa, R. V. de Oliveira Segundo, C. M. de Sá Medeiros, and E. T. Silva, "Estimation of global solar irradiance with ldr sensor and artificial neural network embedded in an 8-bit microcontroller," in *2018 International Joint Conference on Neural Networks (IJCNN)*, pp. 1–8, IEEE, 2018.

[97] F. Mancilla-David, F. Riganti-Fulginei, A. Laudani, and A. Salvini, "A neural network-based low-cost solar irradiance sensor," *IEEE Transactions on Instrumentation and Measurement*, vol. 63, no. 3, pp. 583–591, 2013.

[98] J. Coronel-Reyes, I. Ramirez-Morales, E. Fernandez-Blanco, D. Rivero, and A. Pazos, "Determination of egg storage time at room temperature using a low-cost nir spectrometer and machine learning techniques," *Computers and Electronics in Agriculture*, vol. 145, pp. 1–10, 2018.

[99] B. Dong, B. Andrews, K. P. Lam, M. Höynck, R. Zhang, Y.-S. Chiou, and D. Benitez, "An information technology enabled sustainability test-bed (itest) for occupancy detection through an environmental sensing network," *Energy and Buildings*, vol. 42, no. 7, pp. 1038–1046, 2010.

[100] R. Hecht-Nielsen, "Kolmogorovâs mapping neural network existence theorem," in *Proceedings of the international conference on Neural Networks*, vol. 3, pp. 11–14, IEEE Press New York, 1987.

[101] A. K. Mikkilineni, J. Dong, T. Kuruganti, and D. Fugate, "A novel occupancy detection solution using low-power ir-fpa based wireless occupancy sensor," *Energy and Buildings*, vol. 192, pp. 63–74, 2019.

[102] A. Carre and T. Williamson, "Design and validation of a low cost indoor environment quality data logger," *Energy and Buildings*, vol. 158, pp. 1751–1761, 2018.

[103] K. Han and J. Zhang, "Energy-saving building system integration with a smart and low-cost sensing/control network for sustainable and healthy living environments: Demonstration case study," *Energy and Buildings*, vol. 214, p. 109861, 2020.

[104] E. Arens, A. Ghahramani, R. Przybyla, M. Andersen, S. Min, T. Peffer, P. Raftery, M. Zhu, V. Luu, and H. Zhang, "Measuring 3d indoor air velocity via an inexpensive low-power ultrasonic anemometer," *Energy and Buildings*, vol. 211, p. 109805, 2020.

[105] "Lighting passport." http://www.asensetek.com/lighting-passport/. Accessed: 2019-11-08.

[106] "Wavego." https://waveillumination.com/our-solutions/wavego/. Accessed: 2019-11-08.

[107] M. Canazei, W. Pohl, J. Weninger, H. Bliem, E. M. Weiss, C. Koch, A. Berger, B. Firulovic, and C. Marth, "Effects of adjustable dynamic bedroom lighting in a maternity ward," *Journal of Environmental Psychology*, vol. 62, pp. 59–66, 2019.

[108] J. G. Jetcheva, M. Majidpour, and W.-P. Chen, "Neural network model ensembles for building-level electricity load forecasts," *Energy and Buildings*, vol. 84, pp. 214–223, 2014.

[109] J. De Oña and C. Garrido, "Extracting the contribution of independent variables in neural network models: a new approach to handle instability," *Neural Computing and Applications*, vol. 25, no. 3, pp. 859–869, 2014.

[110] J. Amita, J. S. Singh, and G. P. Kumar, "Prediction of bus travel time using artificial neural network," *International Journal for Traffic and Transport Engineering*, vol. 5, no. 4, pp. 410–424, 2015.

[111] H. Yin, J. A. Costa, and G. Barreto, *Intelligent Data Engineering and Automated Learning–IDEAL 2012: 13th International Conference, Natal, Brazil, August 29-31, 2012, Proceedings*, vol. 7435. Springer, 2012.

[112] Z. Zeng, T. Huang, and W. X. Zheng, "Multistability of recurrent neural networks with time-varying delays and the piecewise linear activation function," *IEEE Transactions on Neural Networks*, vol. 21, no. 8, pp. 1371–1377, 2010.

[113] J. Han and C. Moraga, "The influence of the sigmoid function parameters on the speed of backpropagation learning," in *International workshop on artificial neural networks*, pp. 195–201, Springer, 1995.

[114] C.-W. Lin and J.-S. Wang, "A digital circuit design of hyperbolic tangent sigmoid function for neural networks," in *2008 IEEE International Symposium on Circuits and Systems*, pp. 856–859, IEEE, 2008.

[115] M. Dorofki, A. H. Elshafie, O. Jaafar, O. A. Karim, and S. Mastura, "Comparison of artificial neural network transfer functions abilities to simulate extreme runoff data," *International Proceedings of Chemical, Biological and Environmental Engineering*, vol. 33, pp. 39–44, 2012.

[116] C.-C. Yu and B.-D. Liu, "A backpropagation algorithm with adaptive learning rate and momentum coefficient," in *Proceedings of the 2002 International Joint Conference on Neural Networks. IJCNN'02 (Cat. No. 02CH37290)*, vol. 2, pp. 1218–1223, IEEE, 2002.

[117] C. Kanzow, N. Yamashita, and M. Fukushima, "Withdrawn: Levenberg–marquardt methods with strong local convergence properties for solving nonlinear equations with convex constraints," *Journal of Computational and Applied Mathematics*, vol. 173, no. 2, pp. 321–343, 2005.

[118] L. Scales, *Introduction to non-linear optimization*. Macmillan International Higher Education, 1985.

[119] A. Al-Bayati, I. A Saleh, and K. K Abbo, "Conjugate gradient back-propagation with modified polack–rebier updates for training feed forward neural network," *IRAQI JOURNAL OF STATISTICAL SCIENCES*, vol. 11, no. 20, pp. 164–173, 2011.

[120] M. J. D. Powell, "Restart procedures for the conjugate gradient method," *Mathematical programming*, vol. 12, no. 1, pp. 241–254, 1977.

[121] R. Battiti, "First-and second-order methods for learning: between steepest descent and newton's method," *Neural computation*, vol. 4, no. 2, pp. 141–166, 1992.

[122] P. E. Gill, W. Murray, and M. H. Wright, *Practical optimization*. SIAM, 2019.

[123] D. E. Rumelhart, G. E. Hinton, and R. J. Williams, "Learning representations by back-propagating errors," *nature*, vol. 323, no. 6088, pp. 533–536, 1986.

[124] Z. Zhao, H. Xin, Y. Ren, and X. Guo, "Application and comparison of bp neural network algorithm in matlab," in *2010 International Conference on Measuring Technology and Mechatronics Automation*, vol. 1, pp. 590–593, IEEE, 2010.

[125] S. Chatterjee, "Learning and memorization," in *International Conference on Machine Learning*, pp. 755–763, PMLR, 2018.

[126] B. Sharma and K. Venugopalan, "Comparison of neural network training functions for hematoma classification in brain ct images," *IOSR J. Comput. Eng*, vol. 16, no. 1, pp. 31–35, 2014.

[127] F. D. Baptista, S. Rodrigues, and F. Morgado-Dias, "Performance comparison of ann training algorithms for classification," in *2013 IEEE 8th International Symposium on Intelligent Signal Processing*, pp. 115–120, IEEE, 2013.

[128] Y. Bengio, A. Courville, and P. Vincent, "Representation learning: A review and new perspectives," *IEEE transactions on pattern analysis and machine intelligence*, vol. 35, no. 8, pp. 1798–1828, 2013.

[129] F. Cordoni, "A comparison of modern deep neural network architectures for energy spot price forecasting," *Digital Finance*, vol. 2, pp. 189–210, 2020.

[130] S. B. Driss, M. Soua, R. Kachouri, and M. Akil, "A comparison study between mlp and convolutional neural network models for character recognition," in *Real-Time Image and Video Processing 2017*, vol. 10223, p. 1022306, International Society for Optics and Photonics, 2017.

[131] M. Figueiro, R. Hamner, A. Bierman, and M. Rea, "Comparisons of three practical field devices used to measure personal light exposures and activity levels," *Lighting Research & Technology*, vol. 45, no. 4, pp. 421–434, 2013.

[132] M. Moeck, "Accuracy of luminance maps obtained from high dynamic range images," *Leukos*, vol. 4, no. 2, pp. 99–112, 2007.

[133] T. Kruisselbrink, M. Aries, and A. Rosemann, "A practical device for measuring the luminance distribution," *International Journal of Sustainable Lighting*, vol. 19, no. 1, pp. 75–90, 2017.

[134] T. W. Kruisselbrink, R. Dangol, and E. J. van Loenen, "Feasibility of ceiling-based luminance distribution measurements," *Building and Environment*, vol. 172, p. 106699, 2020.

[135] M. M. Mallis and C. DeRoshia, "Circadian rhythms, sleep, and performance in space," *Aviation, space, and environmental medicine*, vol. 76, no. 6, pp. B94–B107, 2005.

[136] M. Knoop, O. Stefani, B. Bueno, B. Matusiak, R. Hobday, A. Wirz-Justice, K. Martiny, T. Kantermann, M. Aarts, N. Zemmouri, *et al.*, "Daylight: What makes the difference?," *Lighting Research & Technology*, vol. 52, no. 3, pp. 423–442, 2020.

[137] C. C. Kyba, T. Kuester, A. S. De Miguel, K. Baugh, A. Jechow, F. Hölker, J. Bennie, C. D. Elvidge, K. J. Gaston, and L. Guanter, "Artificially lit surface of earth at night increasing in radiance and extent," *Science advances*, vol. 3, no. 11, p. e1701528, 2017.

[138] J. C. Messenger, *Telework in the 21st century: An evolutionary perspective*. Edward Elgar Publishing, 2019.

[139] M. G. Figueiro, "Disruption of circadian rhythms by light during day and night," *Current sleep medicine reports*, vol. 3, no. 2, pp. 76–84, 2017.

[140] M. Ruger, M. C. Gordijn, D. G. Beersma, B. de Vries, and S. Daan, "Time-of-day-dependent effects of bright light exposure on human psychophysiology: comparison of daytime and nighttime exposure," *American Journal of Physiology-regulatory, integrative and comparative physiology*, vol. 290, no. 5, pp. R1413–R1420, 2006.

[141] M. Münch and V. Bromundt, "Light and chronobiology: implications for health and disease," *Dialogues in clinical neuroscience*, vol. 14, no. 4, p. 448, 2012.

[142] L. Walker, *Choosing a sustainable future: Ideas and inspiration from Ithaca, NY*. New Society Publishers, 2010.

[143] "Ilumi." https://ilumi.co/. Accessed: 2021-02-20.

[144] M. S. Rea, M. G. Figueiro, J. D. Bullough, and A. Bierman, "A model of phototransduction by the human circadian system," *Brain Research Reviews*, vol. 50, no. 2, pp. 213–228, 2005.

[145] M. Boubekri, I. N. Cheung, K. J. Reid, C.-H. Wang, and P. C. Zee, "Impact of windows and daylight exposure on overall health and sleep quality of office workers: a case-control pilot study," *Journal of clinical sleep medicine*, vol. 10, no. 6, pp. 603–611, 2014.

[146] A. Iversen, N. Roy, M. Hvass, M. Jørgensen, J. Christoffersen, W. Osterhaus, and K. Johnsen, "Daylight calculations in practice: An investigation of the ability of nine daylight simulation programs to calculate the daylight factor in five typical rooms," 2013.

[147] D. H. Avery, D. N. Eder, M. A. Bolte, C. J. Hellekson, D. L. Dunner, M. V. Vitiello, and P. N. Prinz, "Dawn simulation and bright light in the treatment of sad: a controlled study," *Biological psychiatry*, vol. 50, no. 3, pp. 205–216, 2001.

[148] A. Birchler-Pedross, C. M. Schröder, M. Münch, V. Knoblauch, K. Blatter, C. Schnitzler-Sack, A. Wirz-Justice, and C. Cajochen, "Subjective well-being is modulated by circadian phase, sleep pressure, age, and gender," *Journal of biological rhythms*, vol. 24, no. 3, pp. 232–242, 2009.

[149] M. S. Rea and M. Figueiro, "Light as a circadian stimulus for architectural lighting," *Lighting research & technology*, vol. 50, no. 4, pp. 497–510, 2018.

[150] S. M. Rajaratnam and J. Arendt, "Health in a 24-h society," *The Lancet*, vol. 358, no. 9286, pp. 999–1005, 2001.

[151] S. Banks and D. F. Dinges, "Behavioral and physiological consequences of sleep restriction," *Journal of clinical sleep medicine*, vol. 3, no. 5, pp. 519–528, 2007.

[152] S. Kumar, W. J. Nilsen, A. Abernethy, A. Atienza, K. Patrick, M. Pavel, W. T. Riley, A. Shar, B. Spring, D. Spruijt-Metz, *et al.*, "Mobile health technology evaluation: the mhealth evidence workshop," *American journal of preventive medicine*, vol. 45, no. 2, pp. 228–236, 2013.

[153] W. T. Riley, D. E. Rivera, A. A. Atienza, W. Nilsen, S. M. Allison, and R. Mermelstein, "Health behavior models in the age of mobile interventions: are our theories up to the task?," *Translational behavioral medicine*, vol. 1, no. 1, pp. 53–71, 2011.

[154] S. Krishna, S. A. Boren, and E. A. Balas, "Healthcare via cell phones: a systematic review," *Telemedicine and e-Health*, vol. 15, no. 3, pp. 231–240, 2009.

[155] A. R. Hevner, "A three cycle view of design science research," *Scandinavian journal of information systems*, vol. 19, no. 2, p. 4, 2007.

[156] R. Schnall, M. Rojas, S. Bakken, W. Brown, A. Carballo-Dieguez, M. Carry, D. Gelaude, J. P. Mosley, and J. Travers, "A user-centered model for designing consumer mobile health (mhealth) applications (apps)," *Journal of biomedical informatics*, vol. 60, pp. 243–251, 2016.

[157] P. C. Dykes, D. Stade, F. Chang, A. Dalal, G. Getty, R. Kandala, J. Lee, L. Lehman, K. Leone, A. F. Massaro, *et al.*, "Participatory design and development of a patient-centered toolkit to engage hospitalized patients and care partners in their plan of care," in *AMIA Annual Symposium Proceedings*, vol. 2014, p. 486, American Medical Informatics Association, 2014.

[158] R. A. Virzi, "Refining the test phase of usability evaluation: How many subjects is enough?," *Human factors*, vol. 34, no. 4, pp. 457–468, 1992.

[159] J. Nielsen, "How many test users in a usability study," *Nielsen Norman Group*, vol. 4, no. 06, 2012.

[160] F. Design, "Figma: the collaborative interface design tool," 2020.

[161] "Otter voice notes." https://otter.ai/login. Accessed: 2021-08-07.

[162] A. Bangor, P. T. Kortum, and J. T. Miller, "An empirical evaluation of the system usability scale," *Intl. Journal of Human–Computer Interaction*, vol. 24, no. 6, pp. 574–594, 2008.

[163] A. Bangor, P. Kortum, and J. Miller, "Determining what individual sus scores mean: Adding an adjective rating scale," *Journal of usability studies*, vol. 4, no. 3, pp. 114–123, 2009.

[164] J. Brooke, "Sus: a retrospective," *Journal of usability studies*, vol. 8, no. 2, pp. 29–40, 2013.

[165] J. R. Lewis and J. Sauro, "The factor structure of the system usability scale," in *International conference on human centered design*, pp. 94–103, Springer, 2009.

[166] J. Sauro and J. R. Lewis, "When designing usability questionnaires, does it hurt to be positive?," in *Proceedings of the SIGCHI conference on human factors in computing systems*, pp. 2215–2224, 2011.

[167] T. S. Tullis and J. N. Stetson, "A comparison of questionnaires for assessing website usability," in *Usability professional association conference*, vol. 1, pp. 1–12, Minneapolis, USA, 2004.

[168] H.-F. Hsieh and S. E. Shannon, "Three approaches to qualitative content analysis," *Qualitative health research*, vol. 15, no. 9, pp. 1277–1288, 2005.

[169] T. Sharon, "The rainbow spreadsheet: A collaborative lean ux research." https://www.smashingmagazine.com/2013/04/rainbow-spreadsheet-collaborative-ux-research-tool/. Accessed: 2021-07-02.

[170] T. Sharon, *It's our research: getting stakeholder buy-in for user experience research projects*. Elsevier, 2012.

[171] Ãcole Polytechnique FÃ©dÃ©rale de Lausanne (EPFL), "Spektro, interactive dashboard for exploring nonvisual spectrum lighting." https://spektro.epfl.ch/about. Accessed: 2021-08-06.

[172] M. Spitschan, J. Mead, C. Roos, C. Lowis, B. Griffiths, P. Mucur, and M. Herf, "luox: novel open-access and open-source web platform for calculating and sharing physiologically relevant quantities for light and lighting," *Wellcome Open Research*, vol. 6, 2021.

[173] D. Chrimes, N. R. Kitos, A. Kushniruk, and D. M. Mann, "Usability testing of avoiding diabetes thru action plan targeting (adapt) decision support for integrating care-based counseling of pre-diabetes in an electronic health record," *International journal of medical informatics*, vol. 83, no. 9, pp. 636–647, 2014.

[174] S. Marien, D. Legrand, R. Ramdoyal, J. Nsenga, G. Ospina, V. Ramon, and A. Spinewine, "A user-centered design and usability testing of a web-based medication reconciliation application integrated in an ehealth network," *International journal of medical informatics*, vol. 126, pp. 138–146, 2019.

[175] L. C. Li, P. M. Adam, A. F. Townsend, D. Lacaille, C. Yousefi, D. Stacey, D. Gromala, C. D. Shaw, P. Tugwell, and C. L. Backman, "Usability testing of answer: a web-based methotrexate decision aid for patients with rheumatoid arthritis," *BMC medical informatics and decision making*, vol. 13, no. 1, pp. 1–12, 2013.

[176] J. Brooke *et al.*, "Sus-a quick and dirty usability scale," *Usability evaluation in industry*, vol. 189, no. 194, pp. 4–7, 1996.

[177] S. Hubalek, D. Zöschg, and C. Schierz, "Ambulant recording of light for vision and non-visual biological effects," *Lighting Research & Technology*, vol. 38, no. 4, pp. 314–321, 2006.

[178] Hamamatsu, "Mini-spectrometer." https://www.hamamatsu.com/resources/pdf. Accessed: 2019-11-08.

[179] K. van Creveld and K. Mansfield, "Lit environments that promote health and well-being," *Building Services Engineering Research and Technology*, vol. 41, no. 2, pp. 193–209, 2020.

[180] K. Konis, "A circadian design assist tool to evaluate daylight access in buildings for human biological lighting needs," *Solar Energy*, vol. 191, pp. 449–458, 2019.

[181] C. S. Pechacek, M. Andersen, and S. W. Lockley, "Preliminary method for prospective analysis of the circadian efficacy of (day) light with applications to healthcare architecture," *Leukos*, vol. 5, no. 1, pp. 1–26, 2008.

[182] M. Andersen, J. Mardaljevic, and S. W. Lockley, "A framework for predicting the non-visual effects of daylight–part i: photobiology-based model," *Lighting research & technology*, vol. 44, no. 1, pp. 37–53, 2012.

[183] K. Konis, "A novel circadian daylight metric for building design and evaluation," *Building and Environment*, vol. 113, pp. 22–38, 2017.

[184] M. Inanici, M. Brennan, and E. Clark, "Spectral daylighting simulations: Computing circadian light," in *Proceedings of BS2015: 14th Conference of International Building Performance Simulation Association, Hyderabad, India*, pp. 1245–1252, 2015.